3. Beyond Canonical Flows

Alexander J. Smits

Department of Mechanical and Aerospace Engineering
Princeton University

Lecture 3, 24 August 2023
Les Houches School of Physics

ÉCOLE DE
PHYSIQUE
DES HOUCHES

Non-canonical flows

- Roughness
- Pressure gradients
- Streamline curvature
- 3D effects in nominally 2D flows
- Flow control
- Compressible flows

Trygve - stock.adobe.com

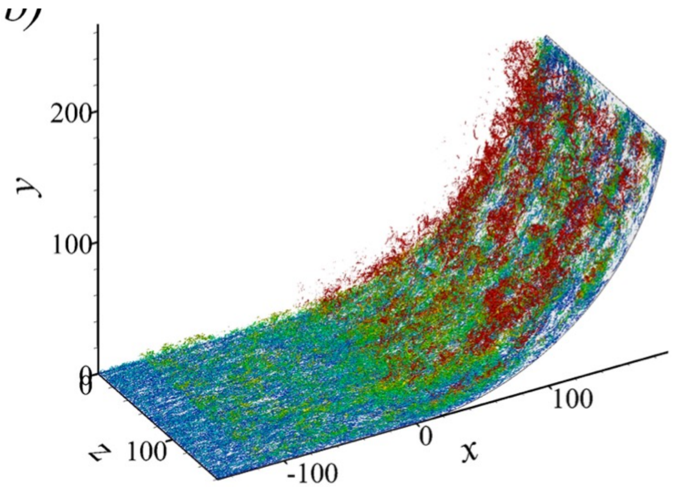

You et al. (2021)

Head (1982)

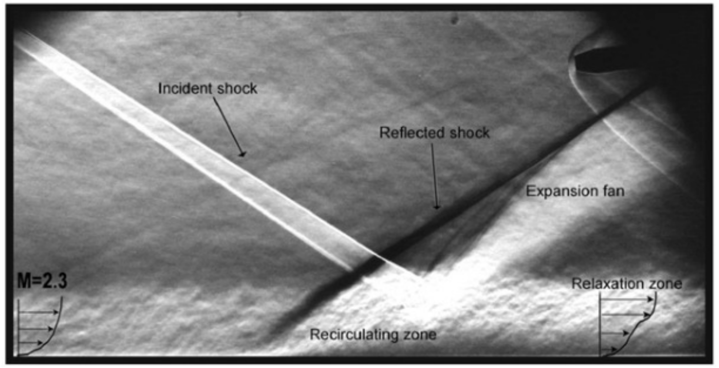

Dupont et al. (2005)

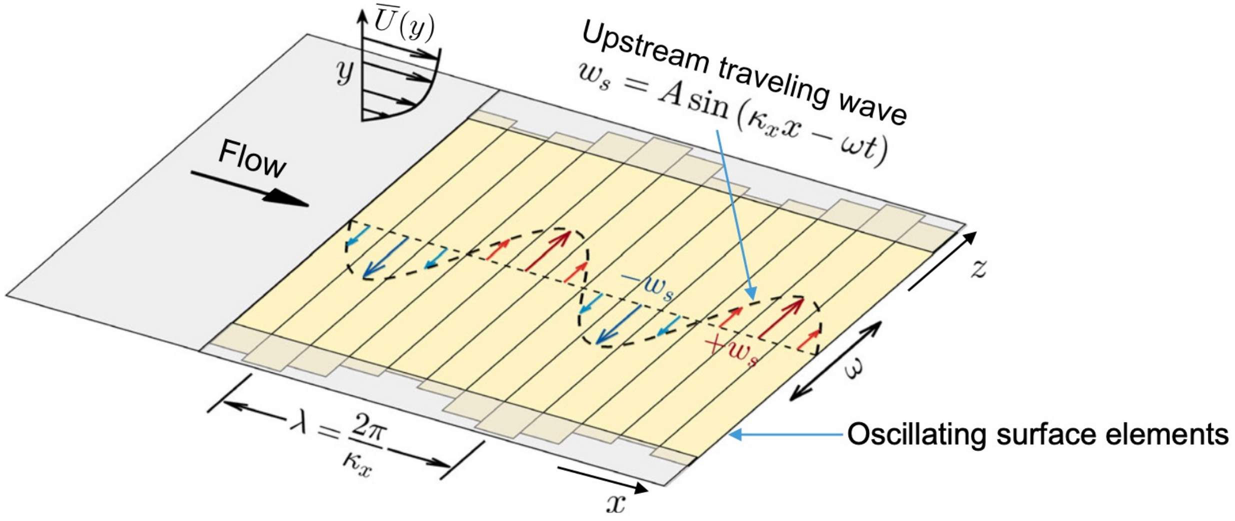

Marusic et al. (2021)

Types of roughness

- Large industrial roughness
- Sandgrain roughness
- Sparse vs. dense distribution
- Grooves vs. grains
- k-type vs. d-type (relative magnitudes of the frictional and pressure drags)
- $k/\delta << 1$
- Multiple length scales
- No ab initio prediction

- Townsend's Reynolds number similarity hypothesis
  - The turbulence beyond a few roughness heights from the wall is independent of the surface condition

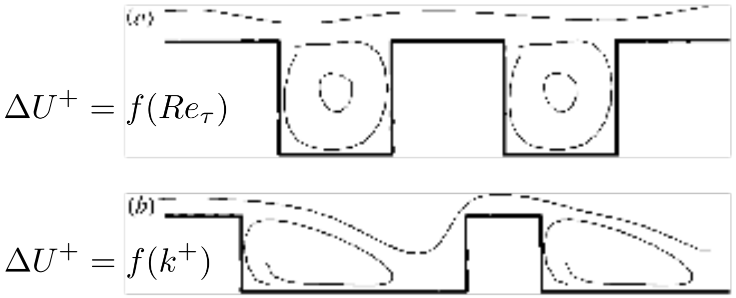

Figure 2 Geometry of (*a*) *d*-type, and (*b*) *k*-type slotted walls. Flow is from left to right.

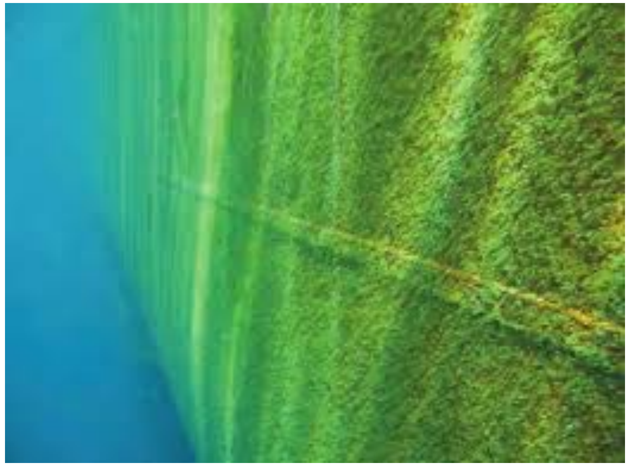

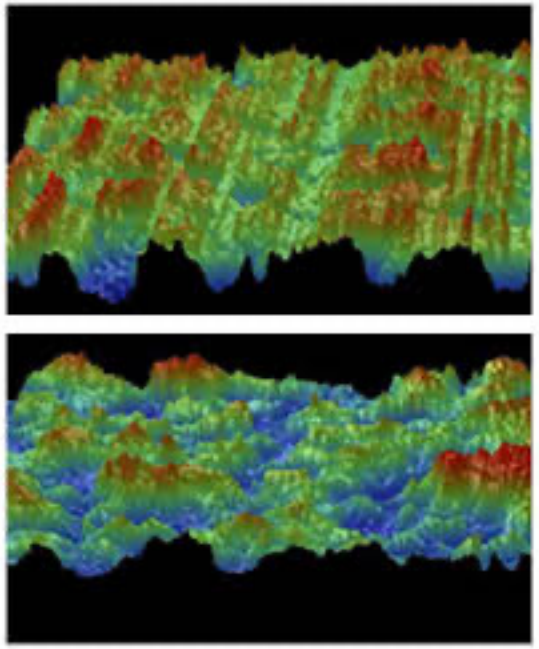

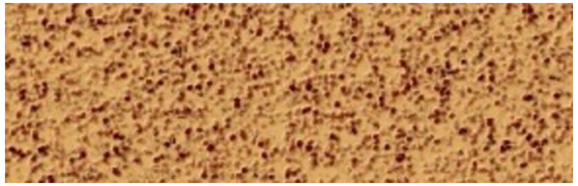

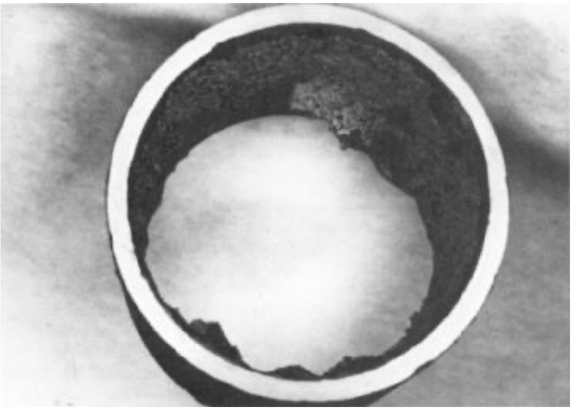

Pipe flow friction: the Moody Diagram

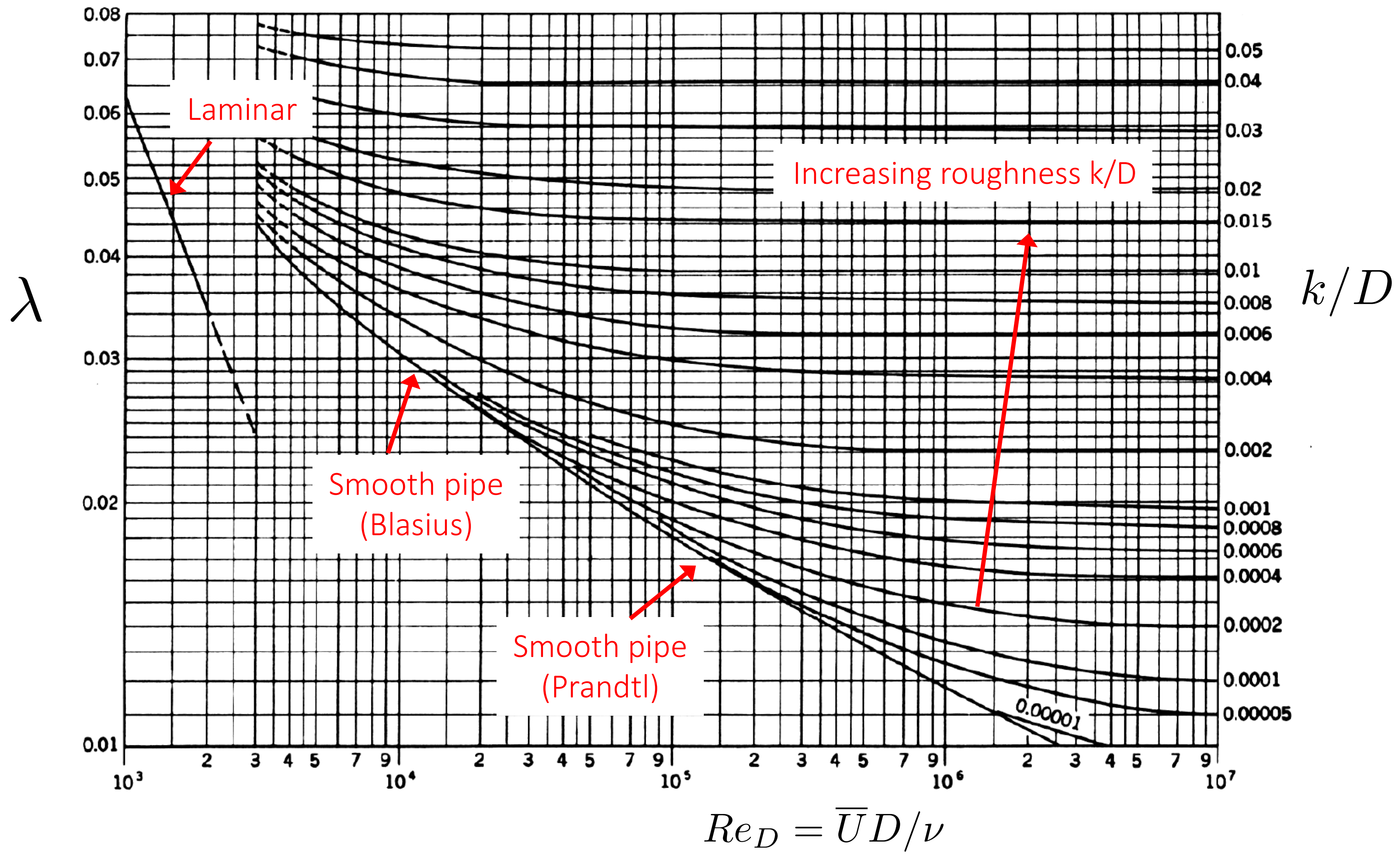

Nikuradse’s sandgrain experiments

- What is k?
  - rms roughness height: k_{rms}
  - equivalent sandgrain roughness: k_s

- $k_s^+ < 5$, smooth
- $5 < k_s^+ < 70$, transitionally rough
- $k_s^+ > 70$, fully rough

$$k_s^+ = k_s u_\tau / \nu$$

- Moody diagram gives l in terms of k/D not k^+

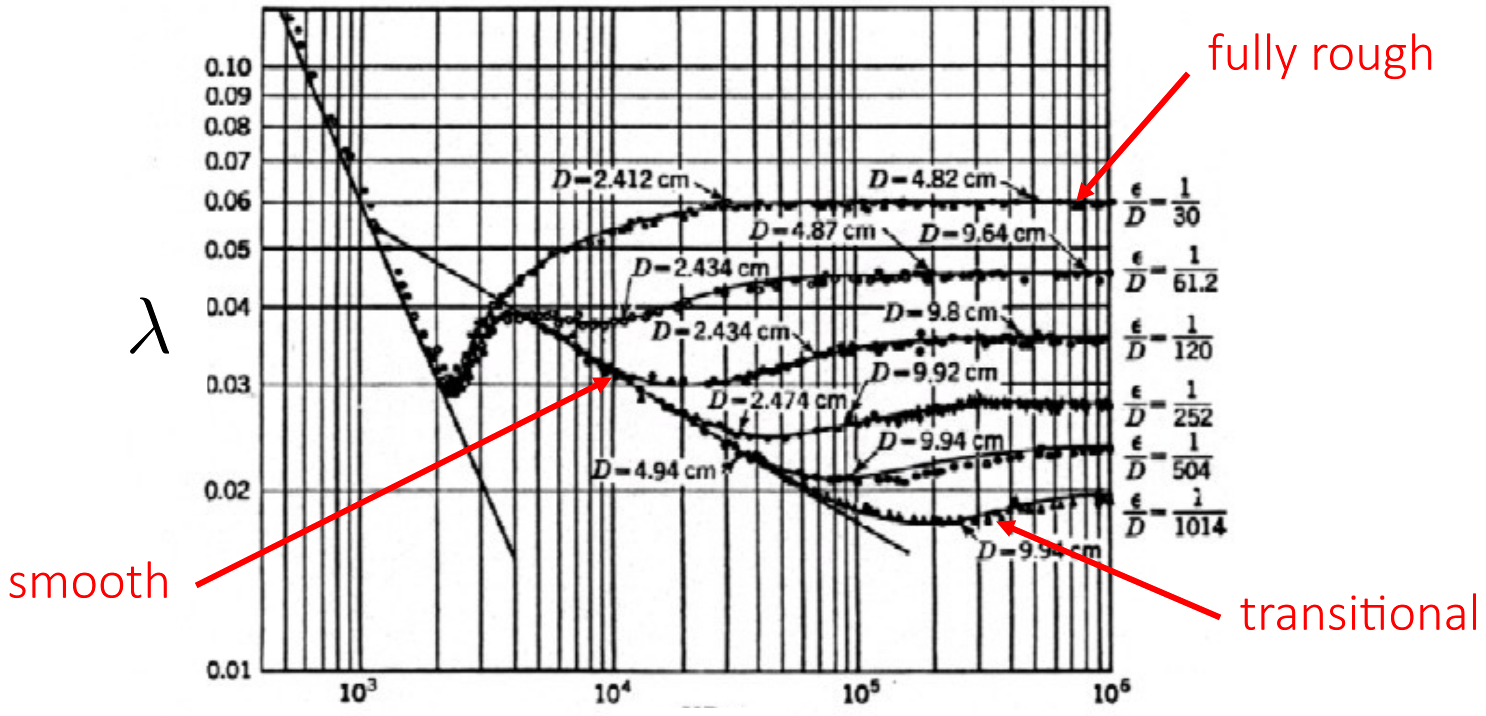

λ

$$Re_D = \overline{U} D / \nu$$

“Quadratic resistance" in fully rough regime: Reynolds number independence

Fully rough: equivalent sand grain roughness

Description of surface	k_s, mm	k_s/k_{rms}
Uniform sand with 0.35 mm diam. small grains in 2 in. pipe ([11] Surface I)	0.48	1.36
Uniform sand with large 3.5 mm grains covering 2.5% of area ([11] Surface II)	0.73	—
Uniform sand with large 3.5 mm grains covering 5% of area ([11] Surface III)	0.93	—
48% area smooth, 47% area uniformly covered fine grains, 5% area covered large grains ([11] Surface IV)	0.66	—
95% area smooth, 5% area covered large grains ([11] Surface V)	0.38	0.11
Hamburg sand $k = 1.35$ mm radius [20]	2.22	1.64
Cup-head rivets touching 2.6 mm radius [20]	3.65	1.40
polished spheres touching 4.1 mm radius [20]	2.57	0.63
Cup-head rivets, 5 diam. apart, 2.6 mm radius [20]	0.31	0.12
Galvanized-iron pipes [12]	0.15	—
Asphalted cast-iron pipes [12]	0.13	—
Uncoated cast-iron pipes [12]	0.25	—
Wrought-iron pipes [12]	0.043	—
Wire mesh, various [19]	—	≈ 1
Heterogeneous glass beads, Gaussian distribution [19]	—	5

Transitional roughness

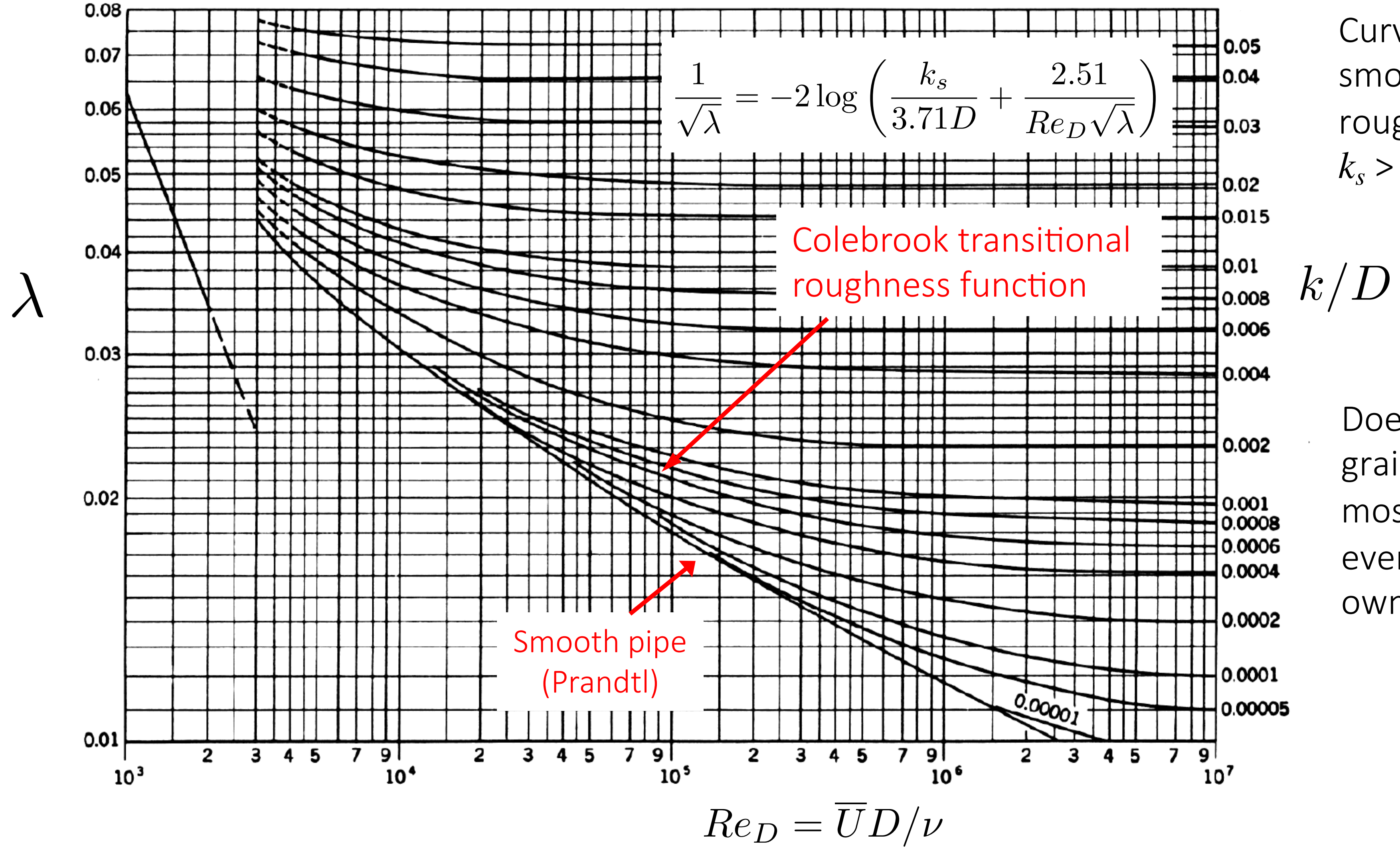

Curve fit to join smooth and fully rough regime for $k_s > 100$

Does not fit sand grain roughness, nor most other types, not even Colebrook's own data

Superpipe experiments on honed roughness

Smooth pipe, 6µin

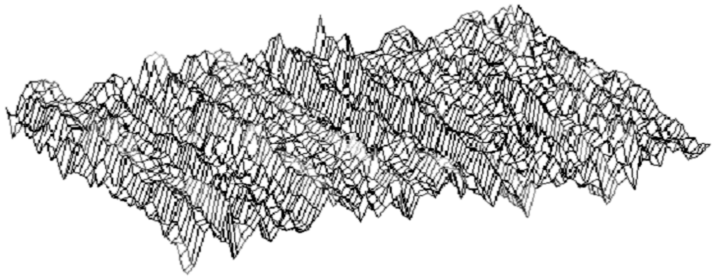

$$\frac{k_{RMS}}{D} = 1.16 \times 10^{-6} \quad k_{RMS} = 0.15\mu m$$

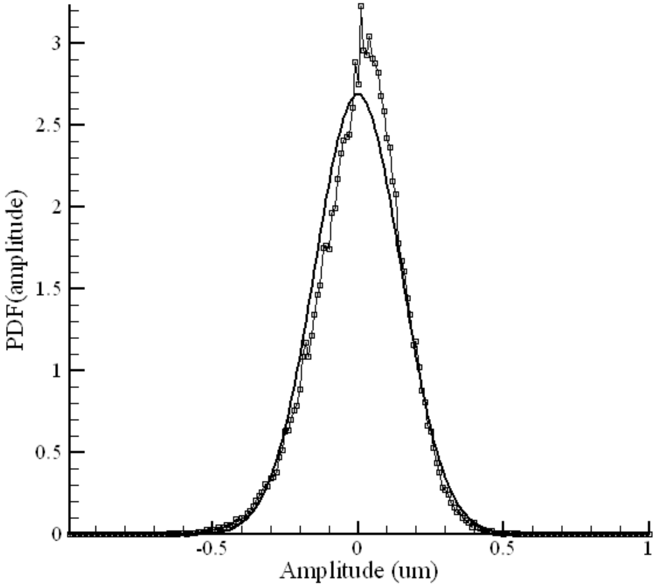

Zagarola & Smits (1998); McKeon & Smits (2004)

Honed rough pipe, 98µin

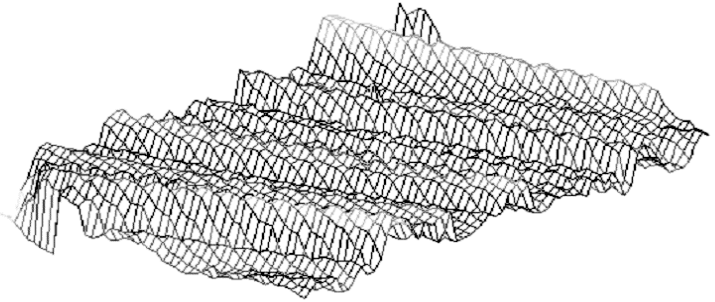

$$\frac{k_{RMS}}{D} = 1.94 \times 10^{-5} \quad k_{RMS} = 2.5\mu m$$

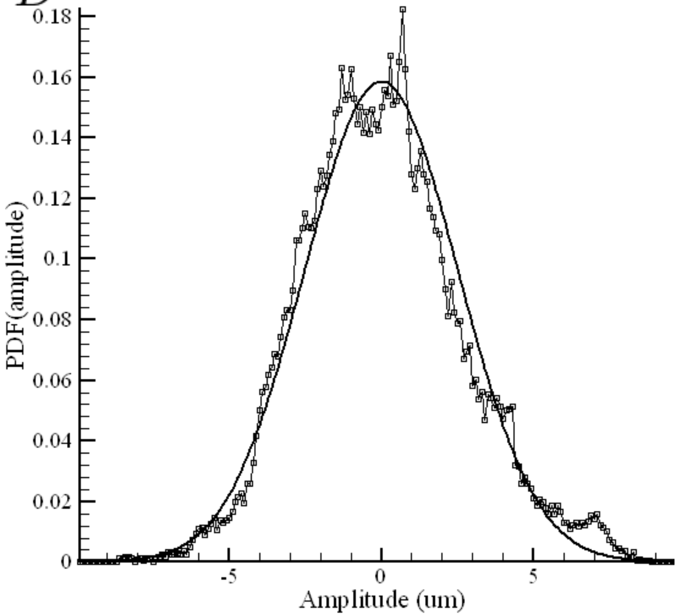

Shockling, Allen & Smits (2006)

Velocity profiles in smooth regime

honed pipe

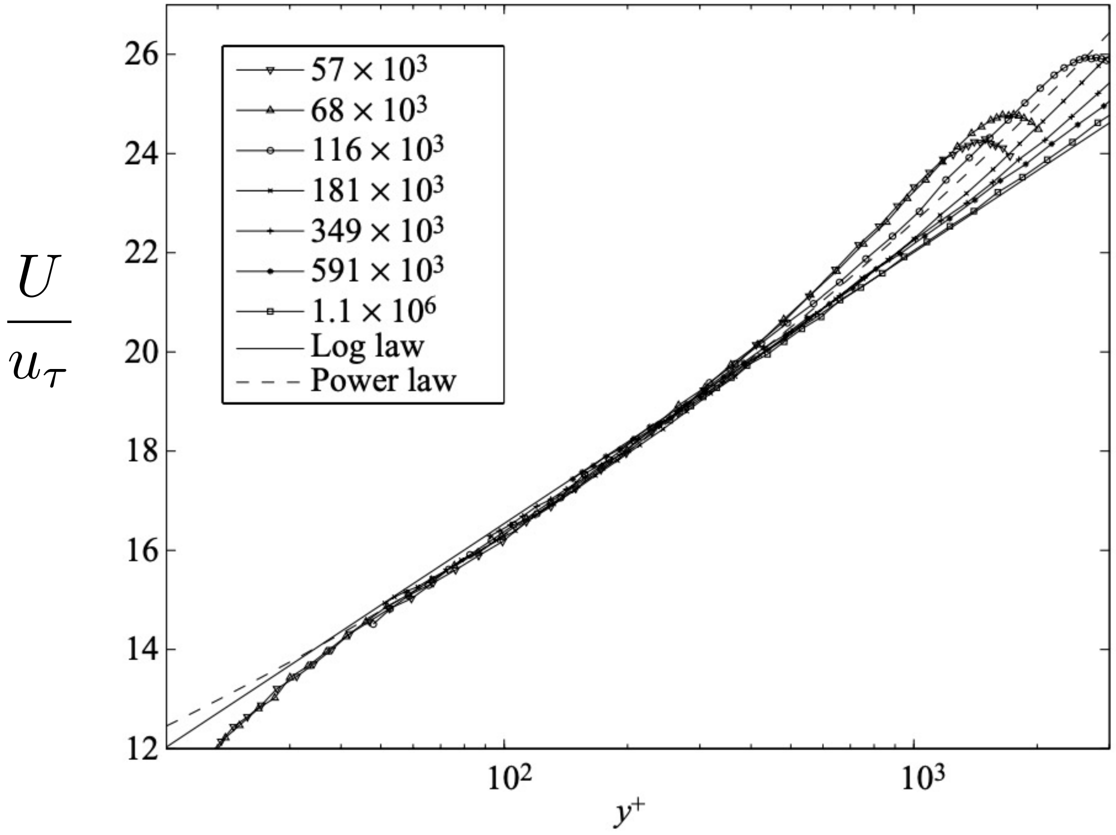

Profiles in smooth regime

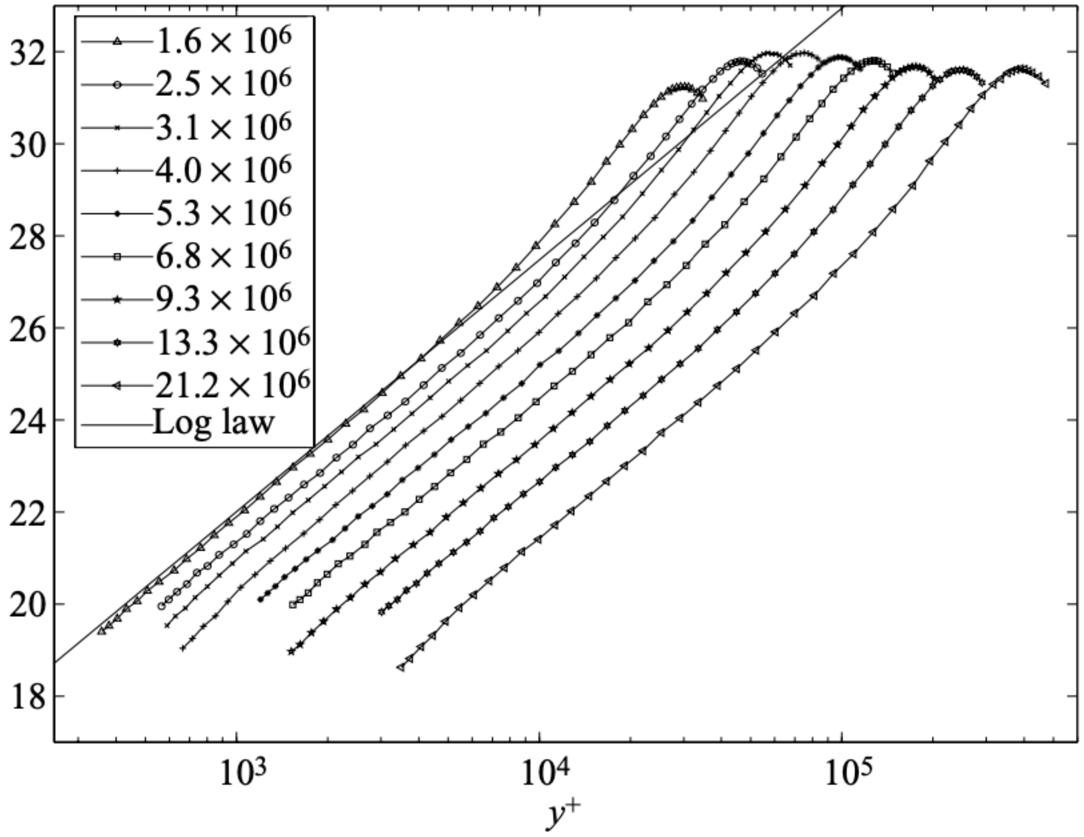

Profiles in rough regime

Inner scaling - all profiles

honed pipe

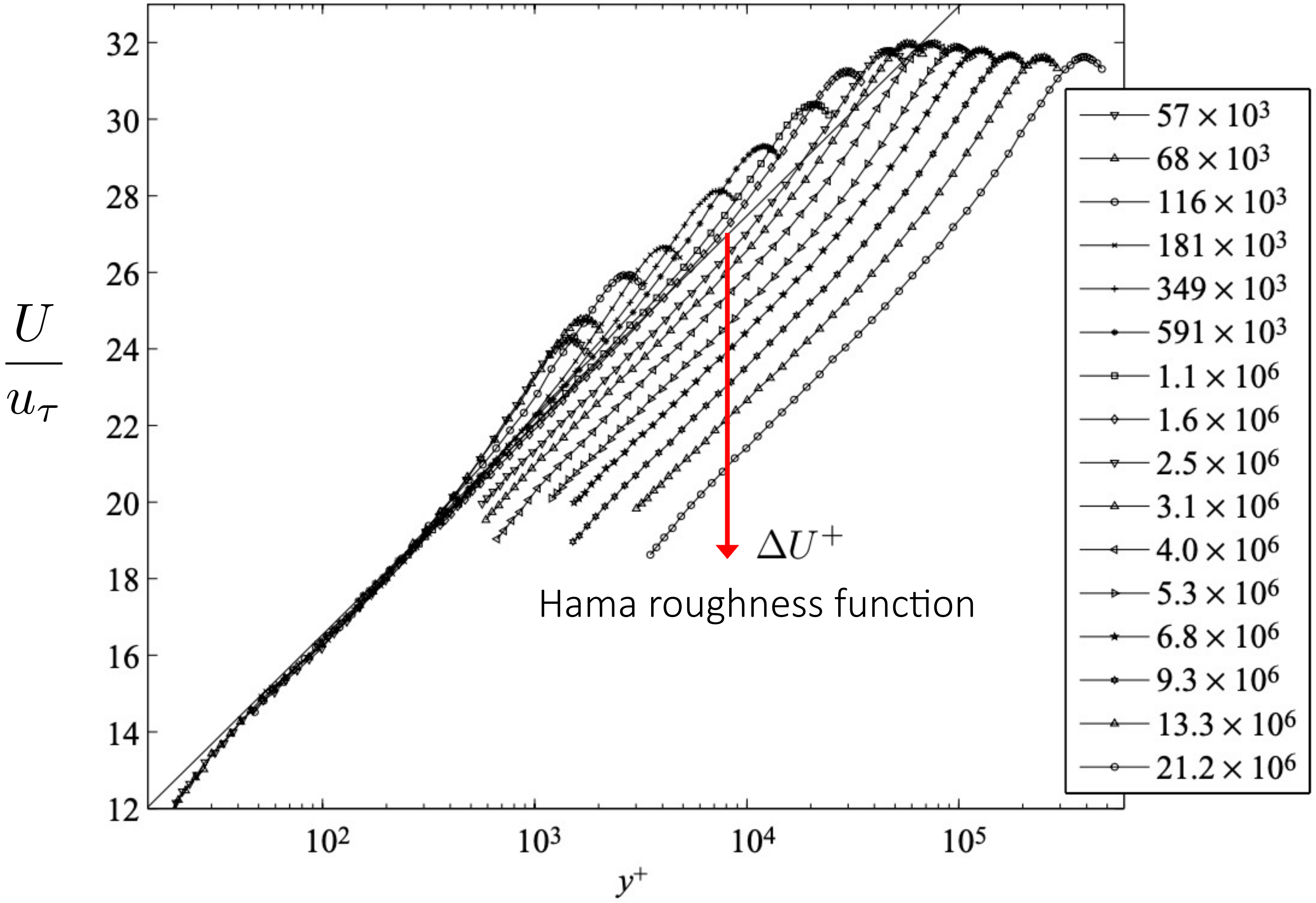

Velocity profiles in transitional/rough regime

$$\frac{U}{u_\tau} = \frac{1}{\kappa} \ln \frac{y u_\tau}{\nu} + B - \frac{\Delta U}{u_\tau}$$

That is, $$U^+ = \frac{1}{\kappa} \ln y^+ + B - \Delta U^+$$

Nikuradse's roughness function (relating Hama to sand grain roughness):

$$\Delta U^+ = \frac{1}{\kappa} \ln \left(k_s^+ \right) + B - 8.5$$

Roughness height (atmospheric boundary layer):

$$z_0^+ = \exp[\kappa(\Delta U^+ - B)]$$

Honed pipe: inner scaling

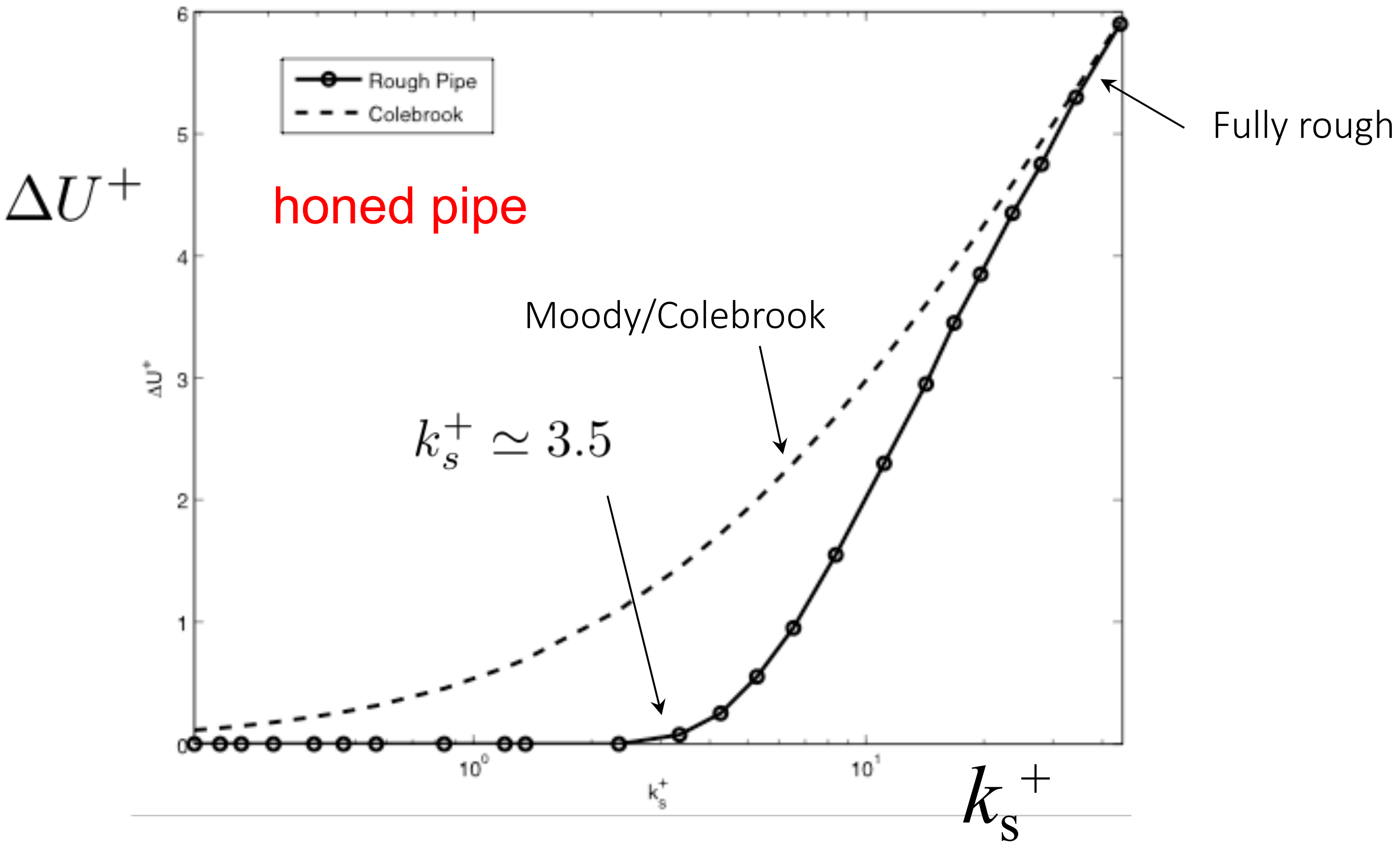

Honed surfaces do not follow Colebrook

Friction factor results for honed pipe

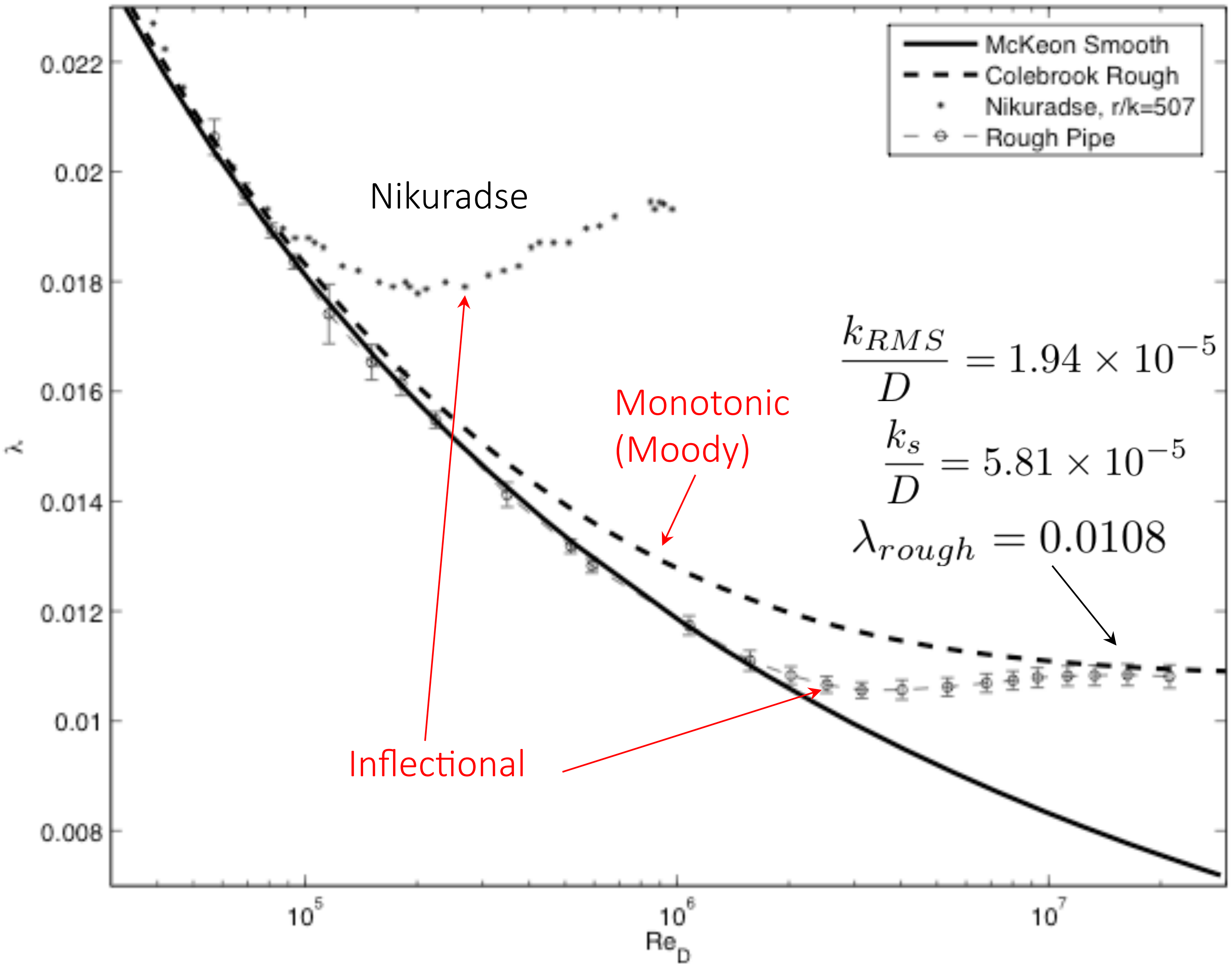

Honed pipe velocity profiles: outer scaling

- Collapse for smooth, transitional, and fully rough flows
  - Townsend's hypothesis supported

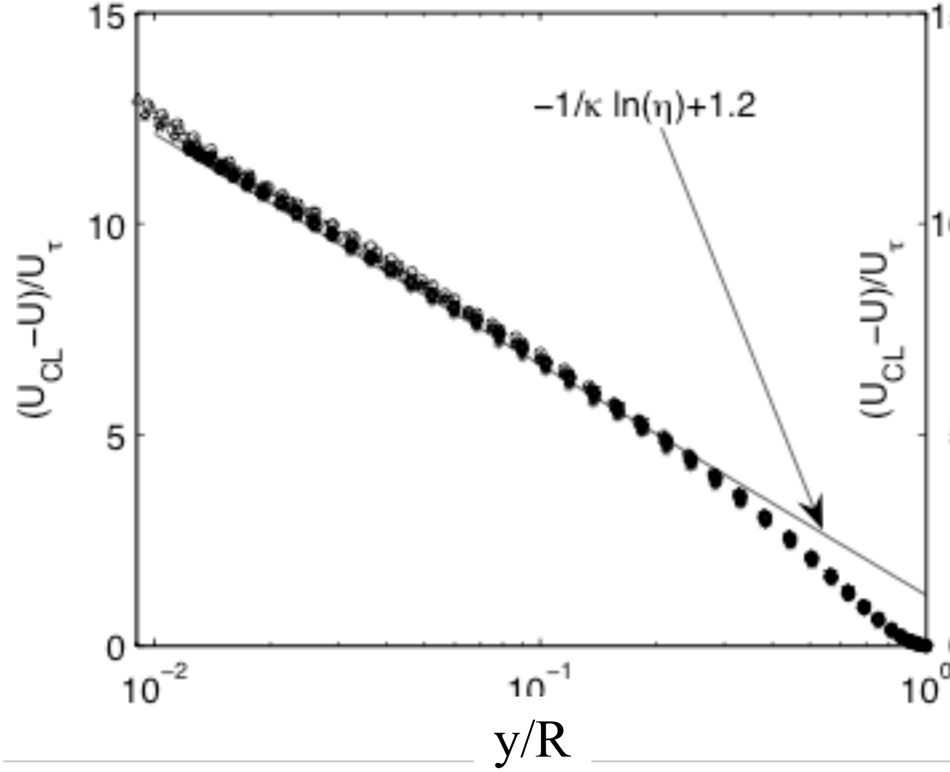

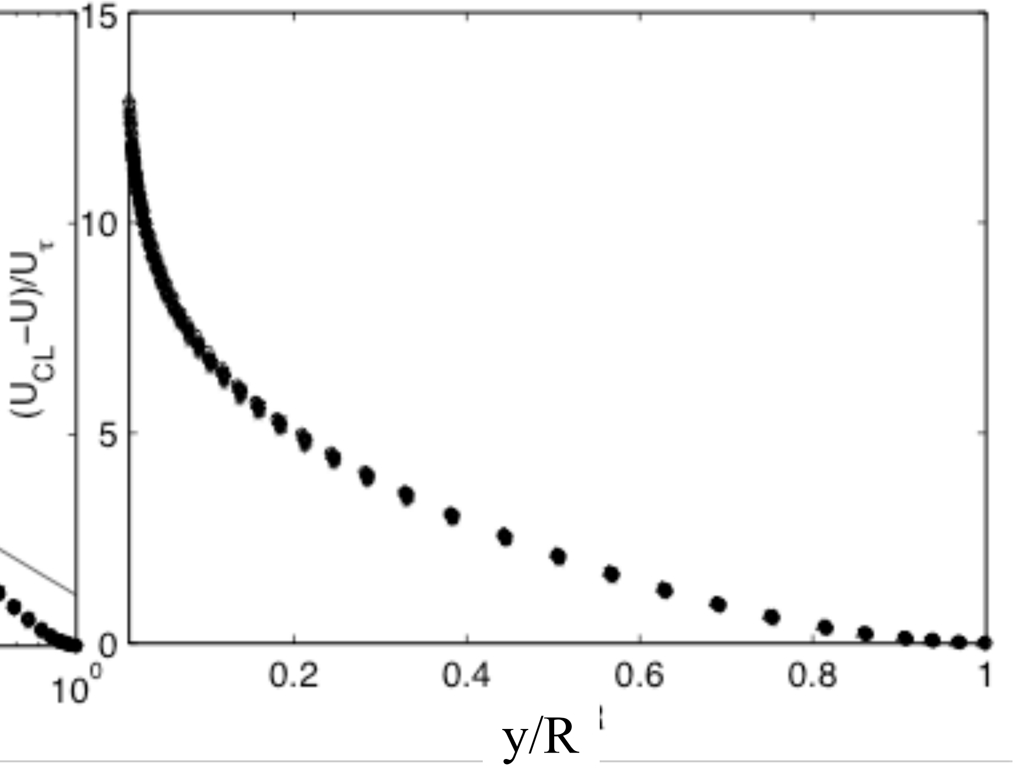

$$300 \times 10^3 \leq Re_D \leq 21.2 \times 10^6$$

Honed pipe turbulence results

- Collapse for smooth, transitional, and fully rough flows
  - Townsend's hypothesis supported

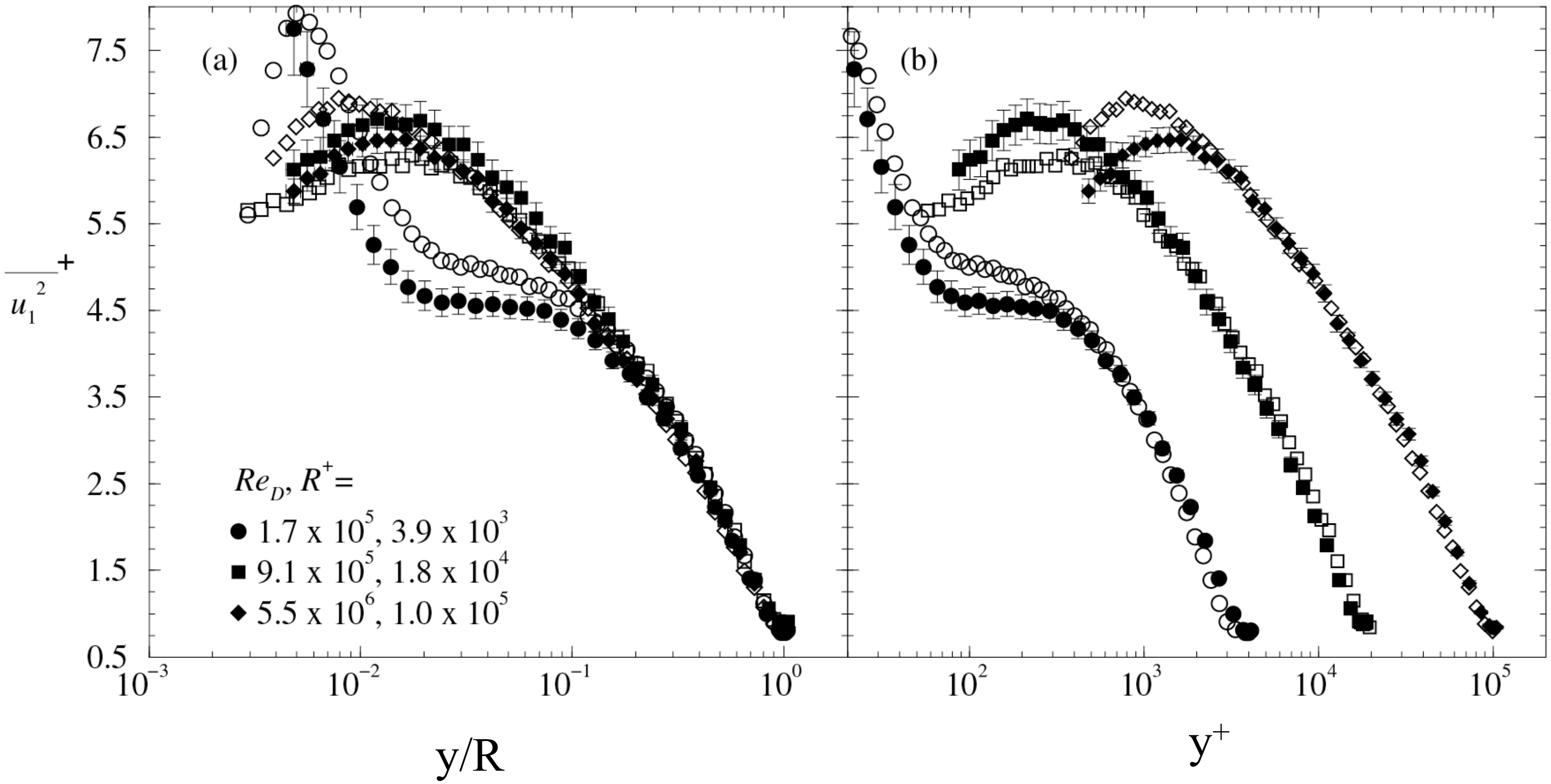

Kunkel, Allen & Smits (2007)

Honed pipe turbulence results

- Collapse for smooth, transitional, and fully rough flows
  - Townsend's hypothesis supported

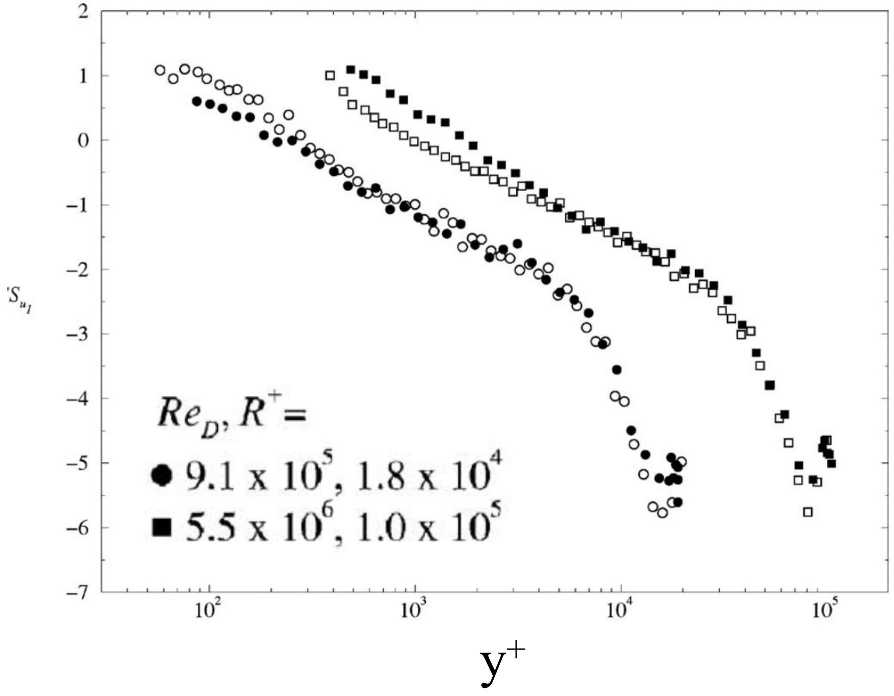

Skewness

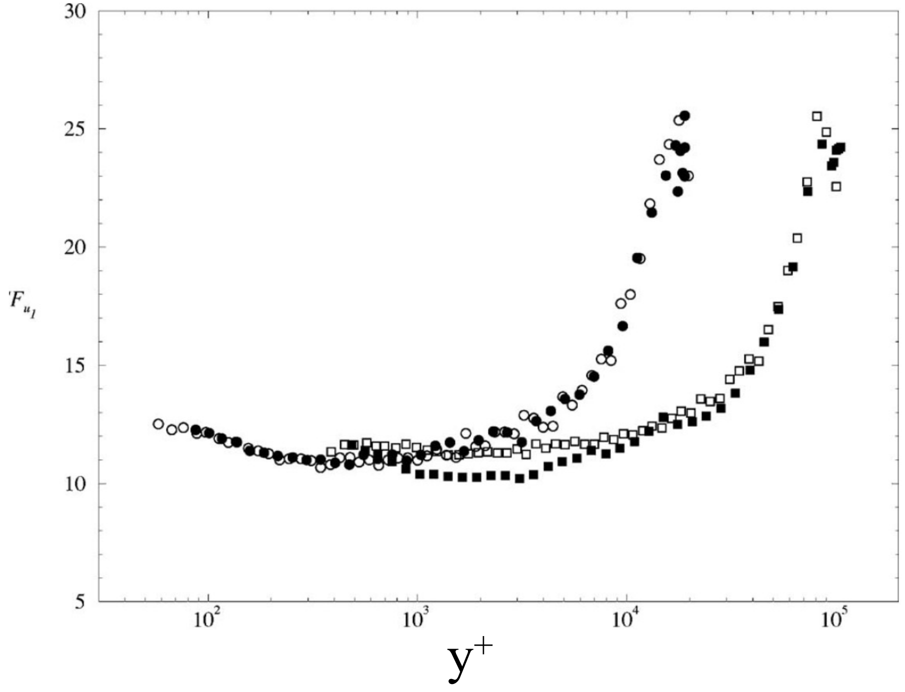

Flatness

Honed pipe turbulence results

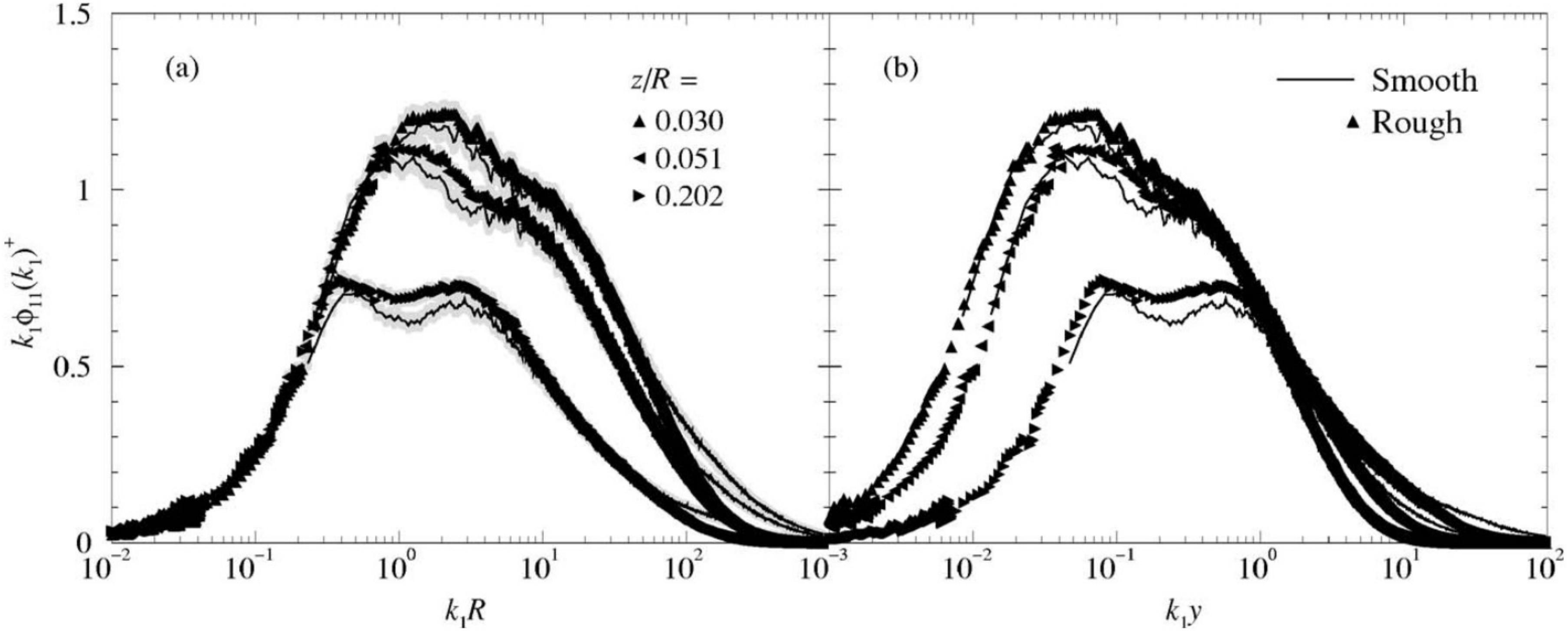

Premultiplied spectra, $Re_\tau = 10^5$

$$\overline{u^2} = \int_0^\infty E(k)dk = \int_0^\infty kE(k)d\log k$$

Commercial steel surface roughness

Honed rough pipe, 98μin

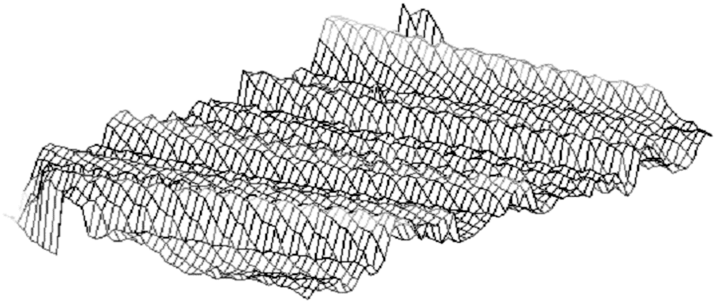

$$\frac{k_{RMS}}{D} = 1.94 \times 10^{-5} \quad k_{RMS} = 2.5\mu m$$

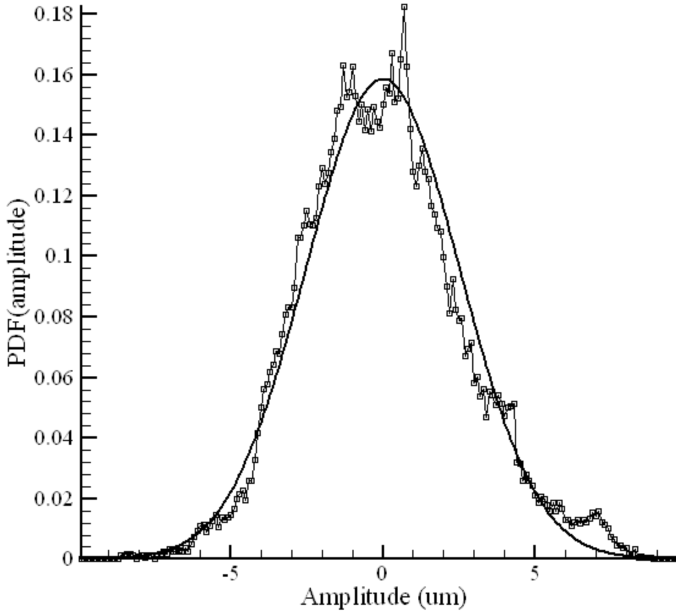

Shockling, Allen & Smits (2006)

Commercial steel rough pipe, 195μin

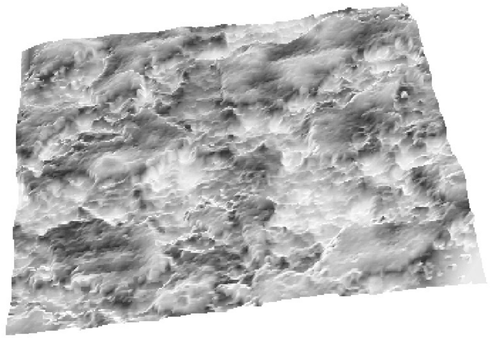

$$\frac{k_{RMS}}{D} = 3.82 \times 10^{-5} \quad k_{RMS} = 5.0\mu m$$

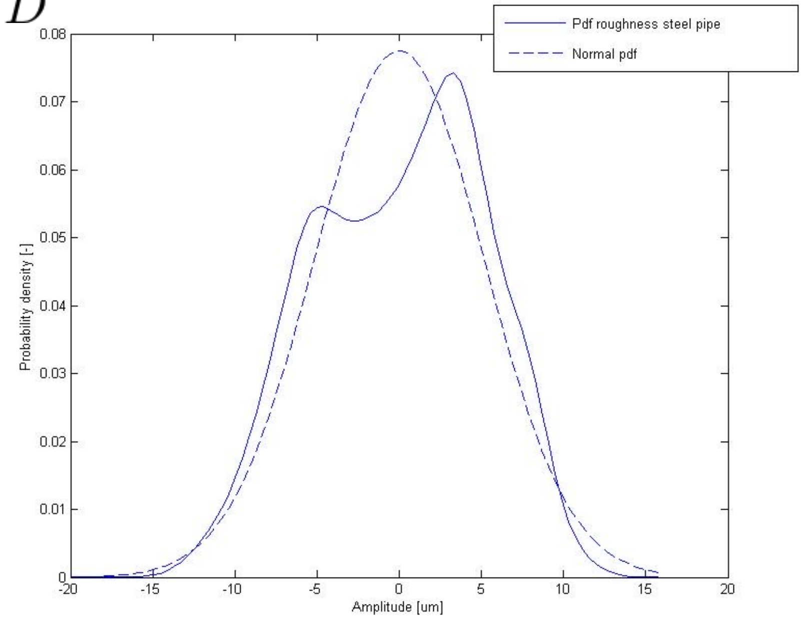

Langelandsvik, Kunkel & Smits (2008)

Commercial steel pipe friction factor

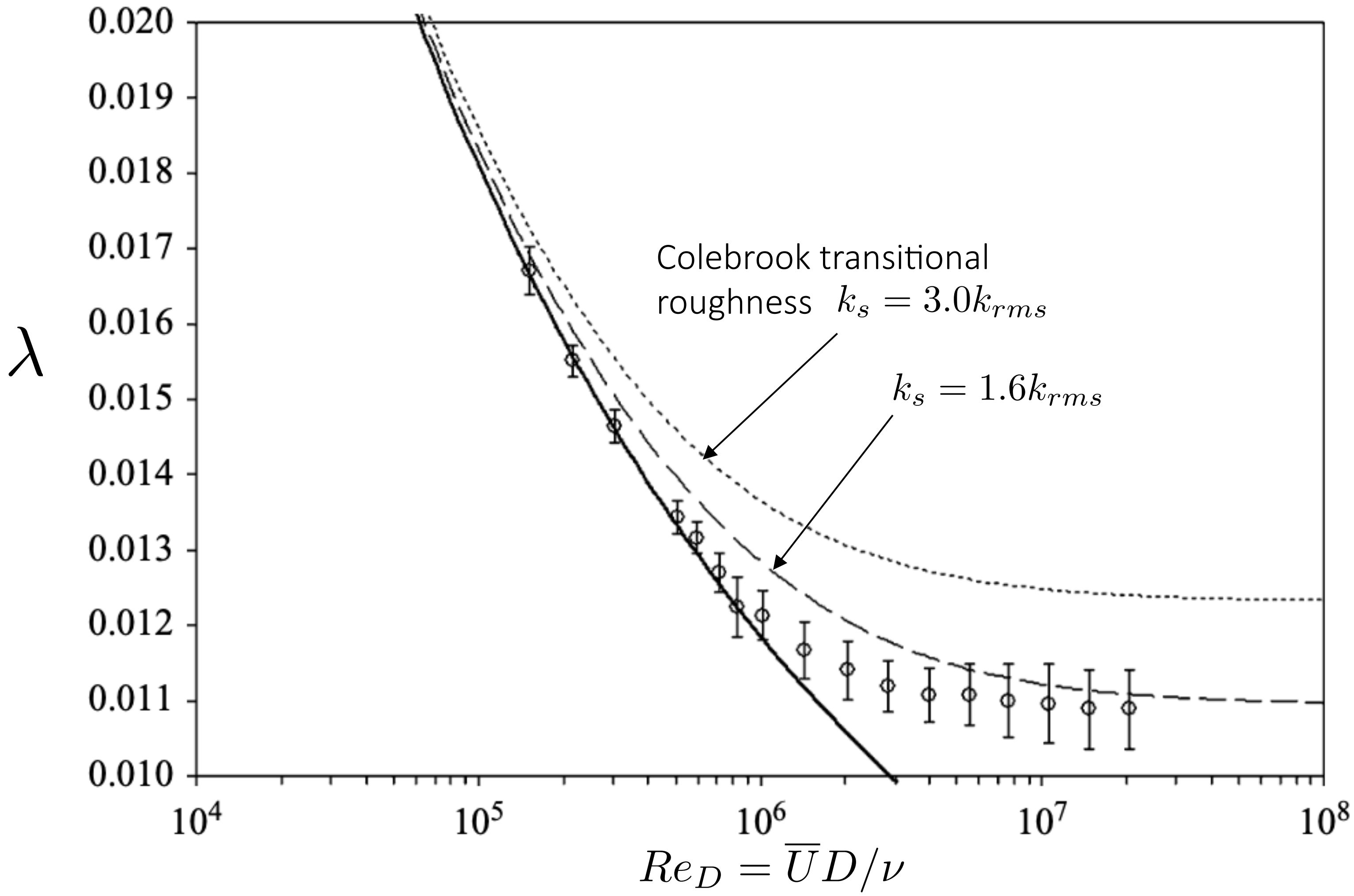

Commercial steel pipe does not follow Colebrook

Hama roughness function

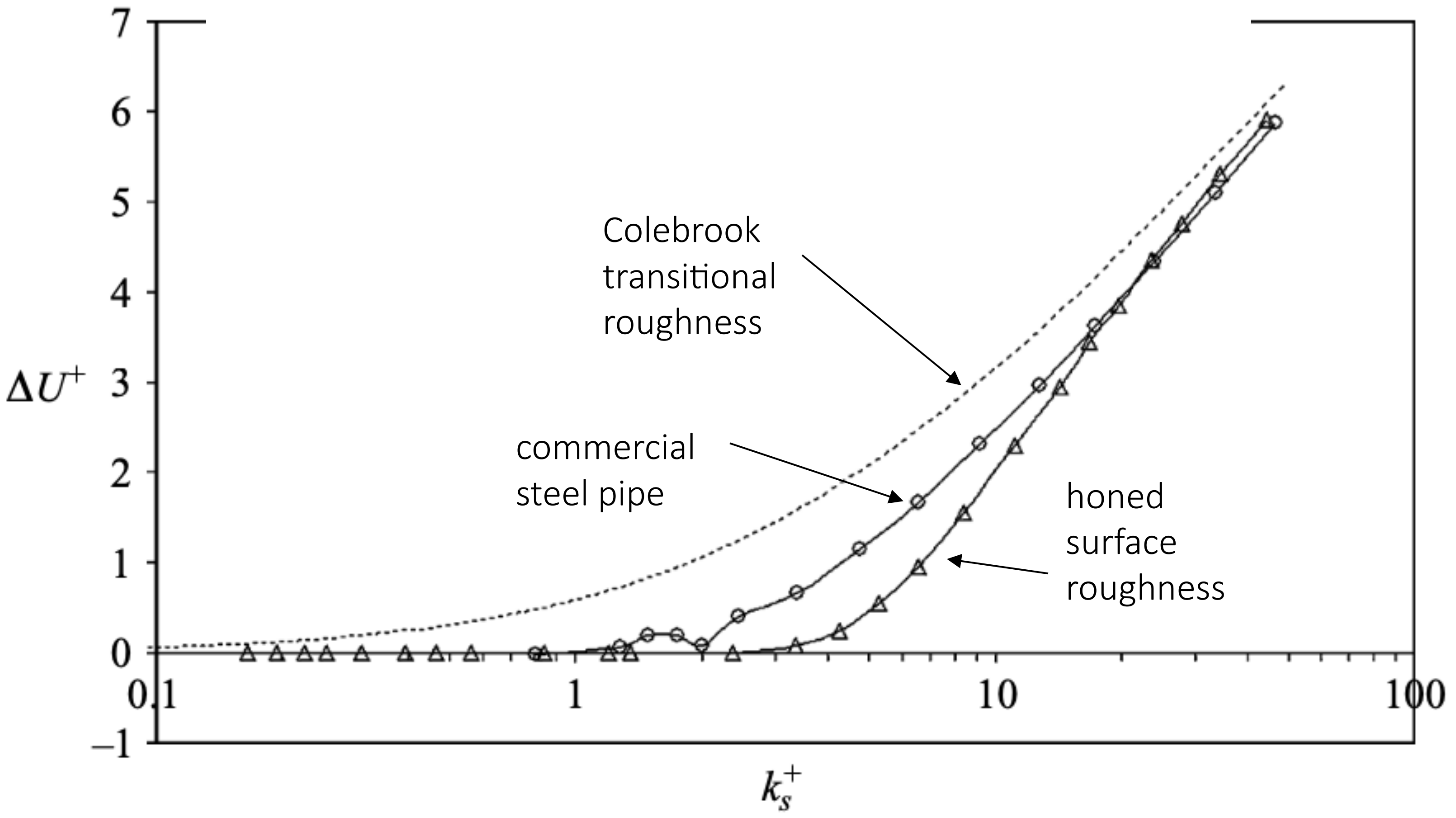

Commercial steel pipe does not follow Colebrook

Rough pipe summary

- Honed surface roughness
- Smooth $\longrightarrow$ transitional $\longrightarrow$ fully rough
- $k_{rms}/D = 19 \times 10^{-6}$
- Smooth for $k_s^+ < 3.5$
- Fully rough for $k_s^+ > 30$
- $k_s = 3.0k_{rms}$

- Inflectional friction factor not monotonic (Nikuradse not Colebrook)

- Commercial steel pipe roughness
- Smooth $\longrightarrow$ transitional $\longrightarrow$ fully rough
- $k_{rms}/D = 38 \times 10^{-6}$
- Smooth for $k_s^+ < 3.1$
- Fully rough for $k_s^+ > 50$
- $k_s = 1.5k_{rms}$ (instead of $3.5k_{rms}$)!

- Friction factor monotonic (but not Colebrook)

- Townsend's hypothesis confirmed for mean flow and turbulence (even for $y/\delta \sim 0.01$, $k/\delta \ll 1$)
- Connection between k and roughness type remains elusive

Adverse pressure gradients

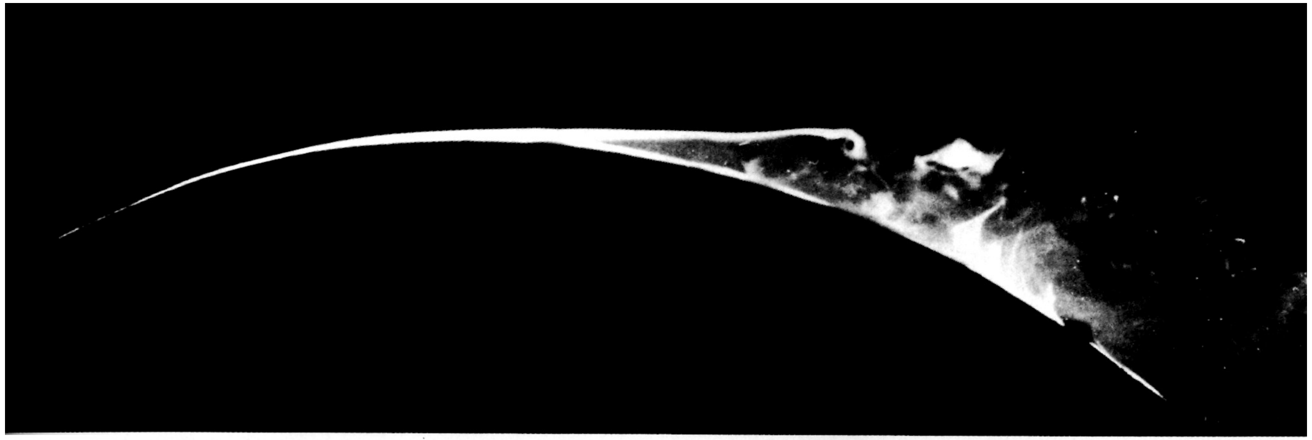

Laminar separation

Turbulent separation

Head (1982)

Adverse pressure gradients

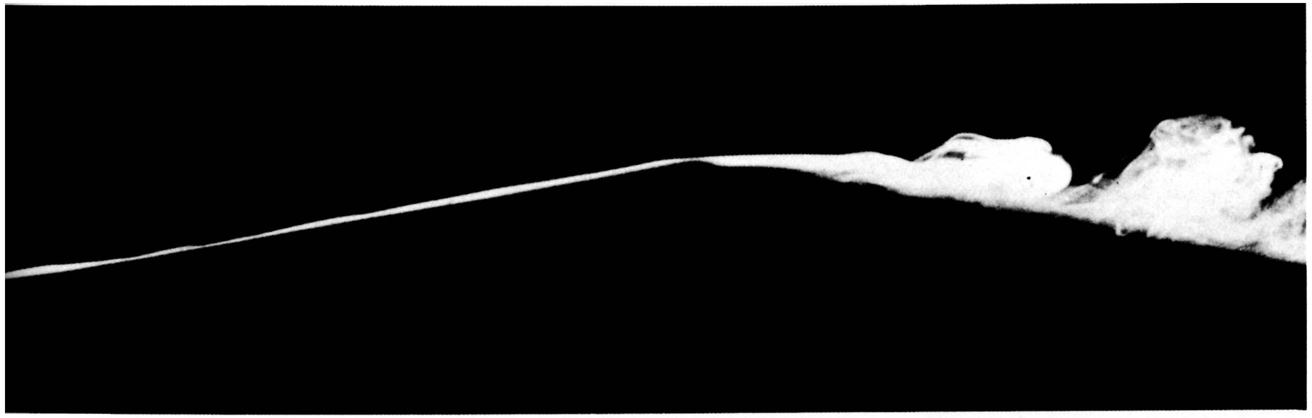

Laminar separation

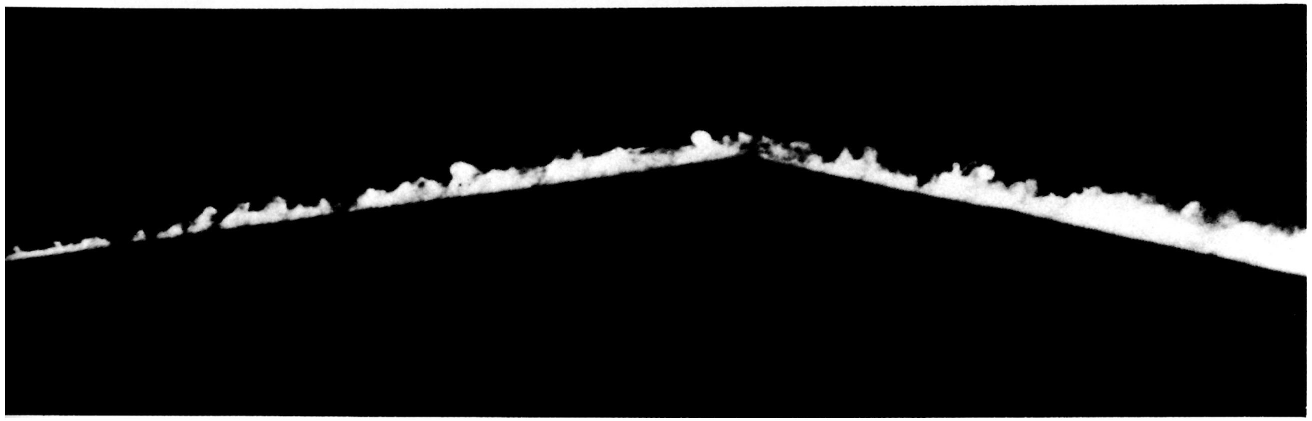

Turbulent no separation

Head (1982)

Pressure gradient

- Externally-imposed pressure gradient
- S/L curvature set by pressure gradient
- Blockage effects

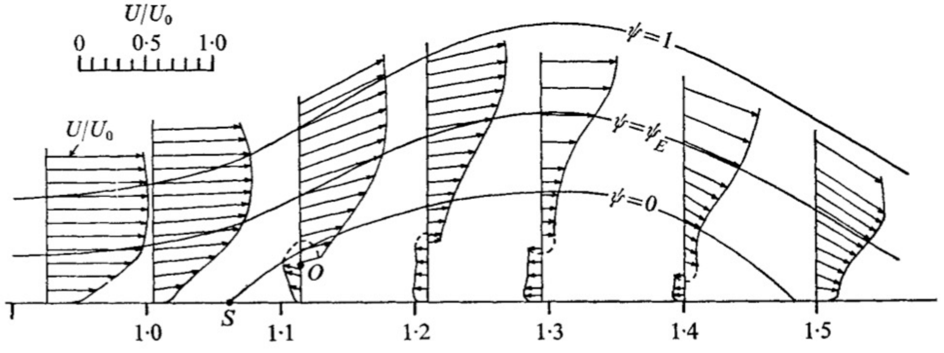

Perry & Fairlie (1969)

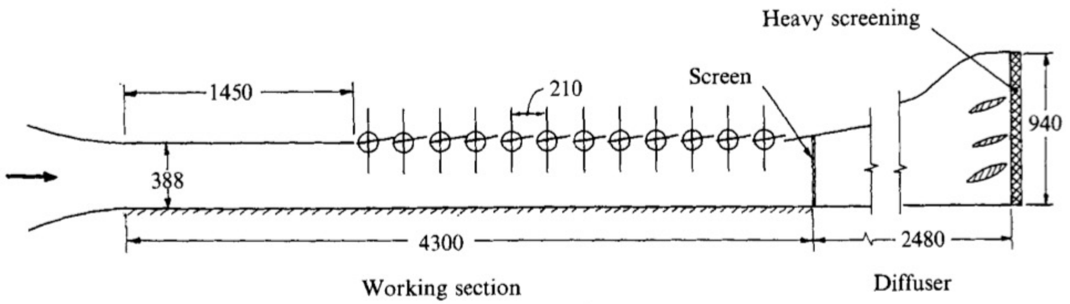

Marusic & Perry (1995)

- Body-generated pressure gradient
- S/L curvature and divergence set by body <u>and</u> PG
- Blockage effects

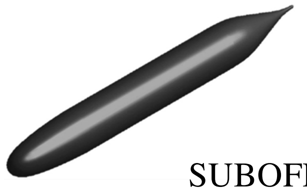

SUBOFF

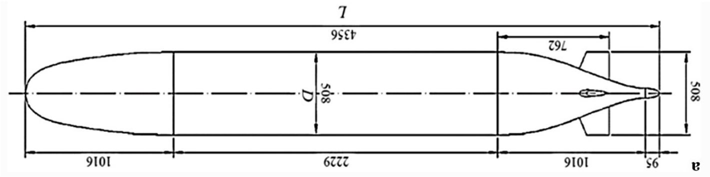

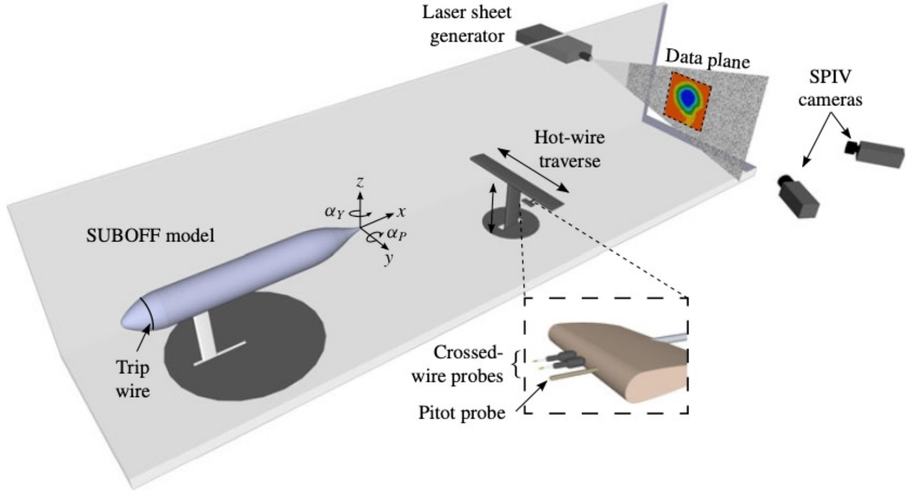

Jimenez, Hultmark & Smits (2010)

Adverse pressure gradients

- How do you measure pg?
- What effect does pg have on the mean flow and the turbulence?

$$K = \frac{\nu}{U_\infty^2}\frac{dU_\infty}{dx} \qquad P^+ = \frac{\nu}{\rho u_\tau^3}\frac{dp}{dx}$$

$$\beta = \frac{\delta^*}{\tau_w}\frac{dp}{dx}$$ Clauser pg parameter

$$\Lambda = \frac{\delta}{\rho U_\infty^2 dp/dx}\frac{dp}{dx}$$ Castillo & George (2001)

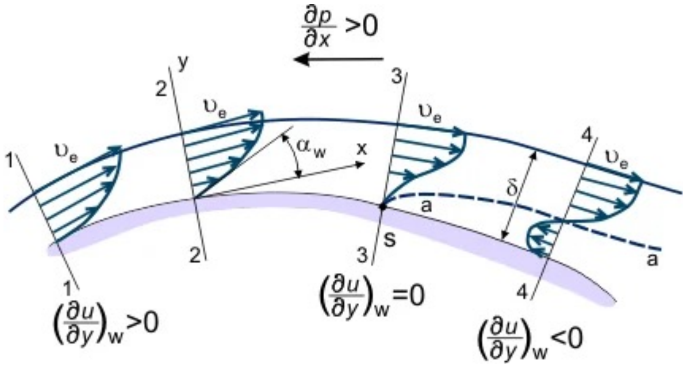

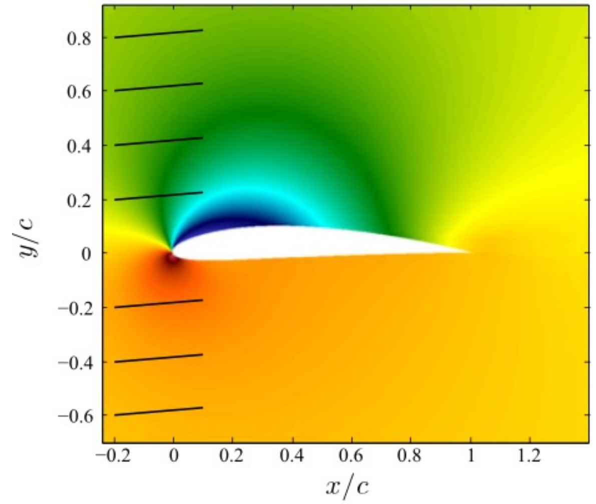

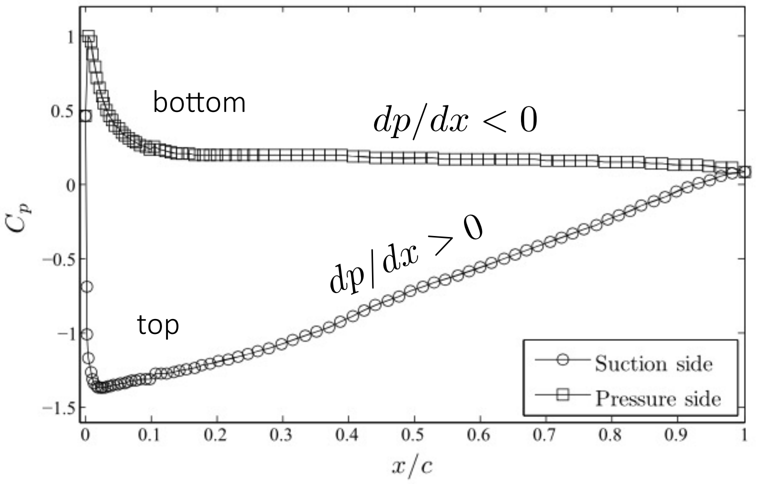

Vinuesa et al. (2017)

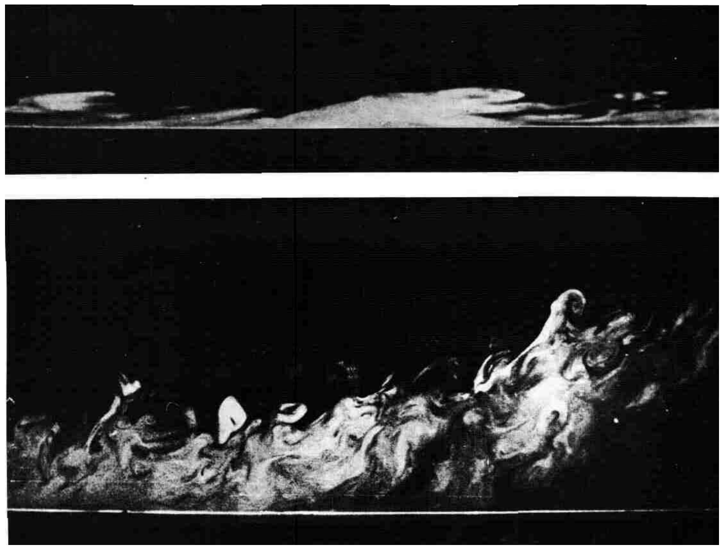

Falco in Head (1982)

Behavior near the wall

- Very near the wall, the viscous effects dominate, and 2D boundary layer equations give

$$\frac{dp_w}{dx} = \frac{\partial}{\partial y}\left(\mu \frac{\partial U}{\partial y}\right)\bigg|_0$$

- That is, for favorable pressure gradients, the gradient of the total stress is negative

- For adverse pressure gradients it is positive, and we expect to see a peak in the shear stress profile

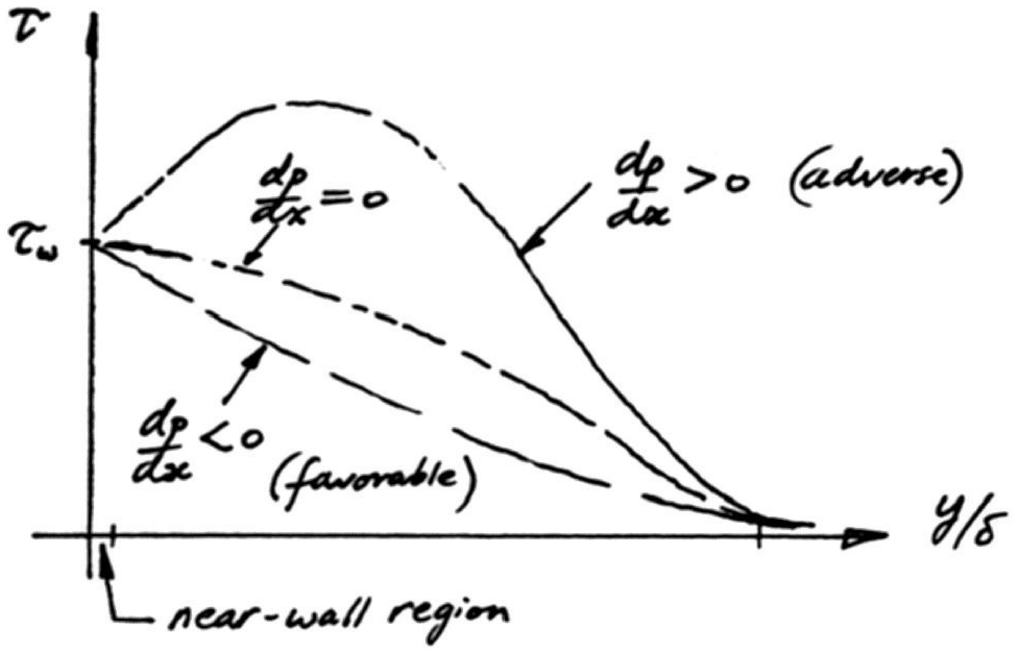

Favorable pressure gradient ($dp/dx < 0$)

Relaminarization $K > 3 \times 10^{-6}$

$$K = \frac{\nu}{U_\infty^2}\frac{dU_\infty}{dx}$$

$K < 2 \times 10^{-6}$

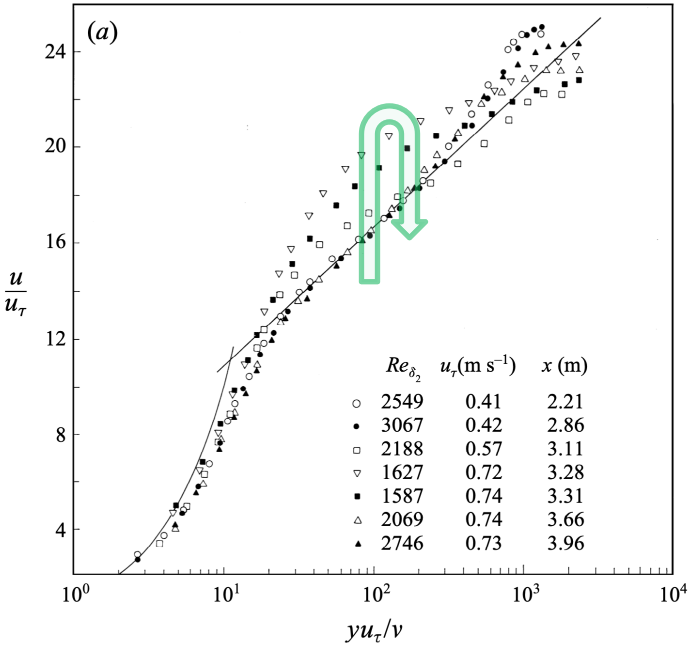

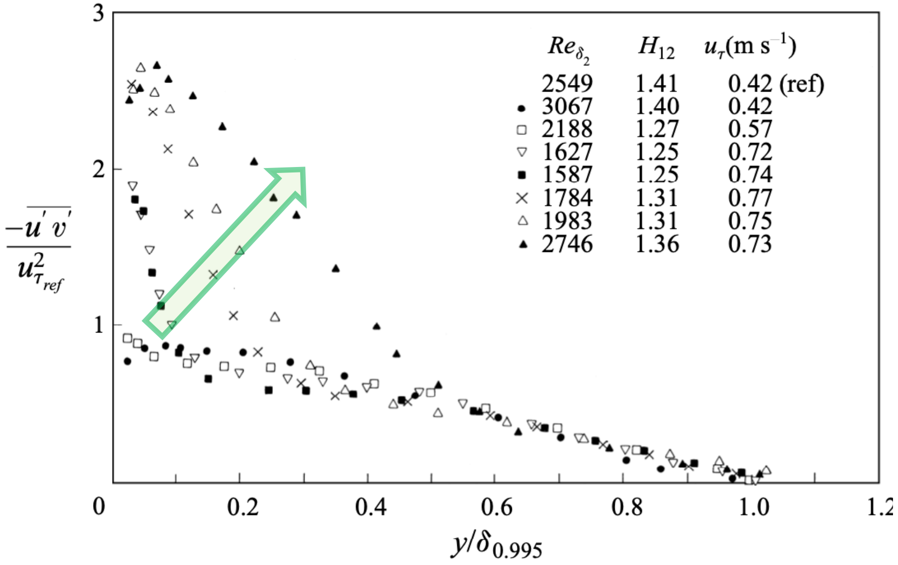

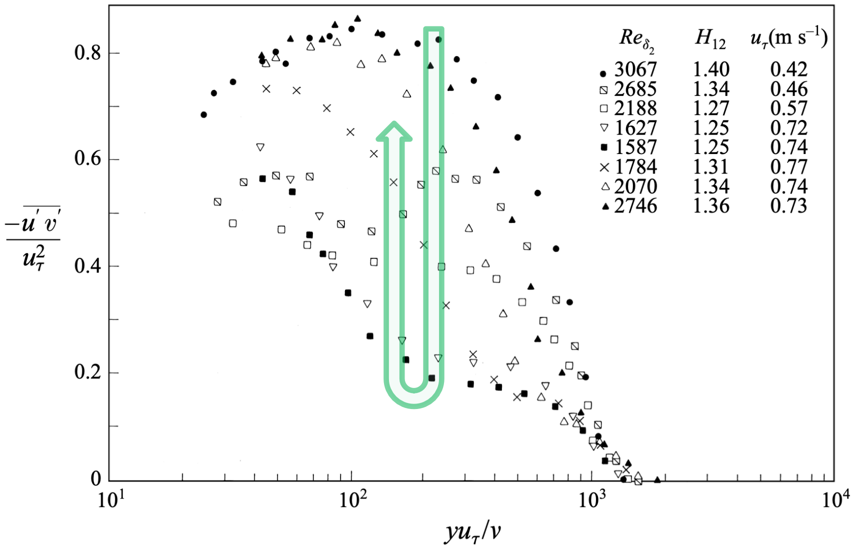

Fernholz & Warnack Part 1 (1998)

Adverse pressure gradient ($dp/dx > 0$)

$$0 \leq K \leq -2.82 \times 10^{-7}$$

$$K = \frac{\nu}{U_\infty^2}\frac{dU_\infty}{dx} \qquad \beta = \frac{\delta^*}{\tau_w}\frac{dp}{dx}$$

$$0 \leq \beta \leq 4.74$$

$$-0.17 \leq \beta \leq 2.31$$

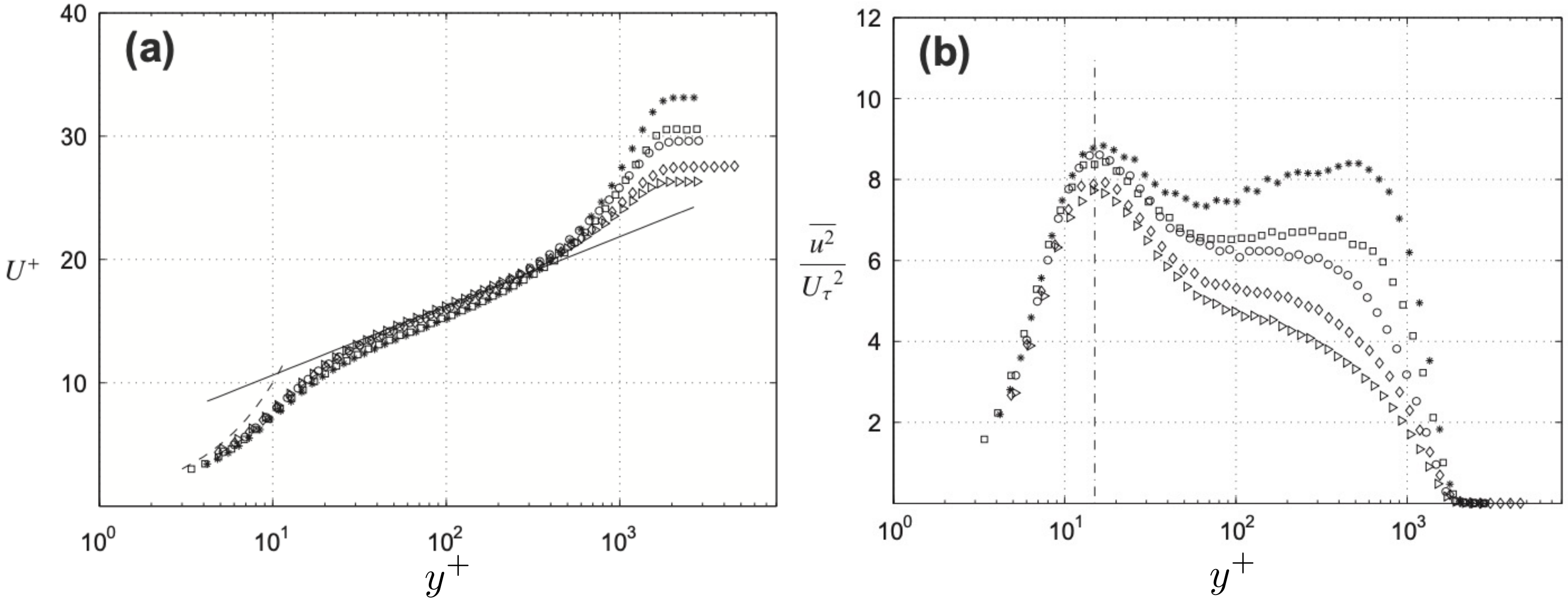

Monty et al. (2011)

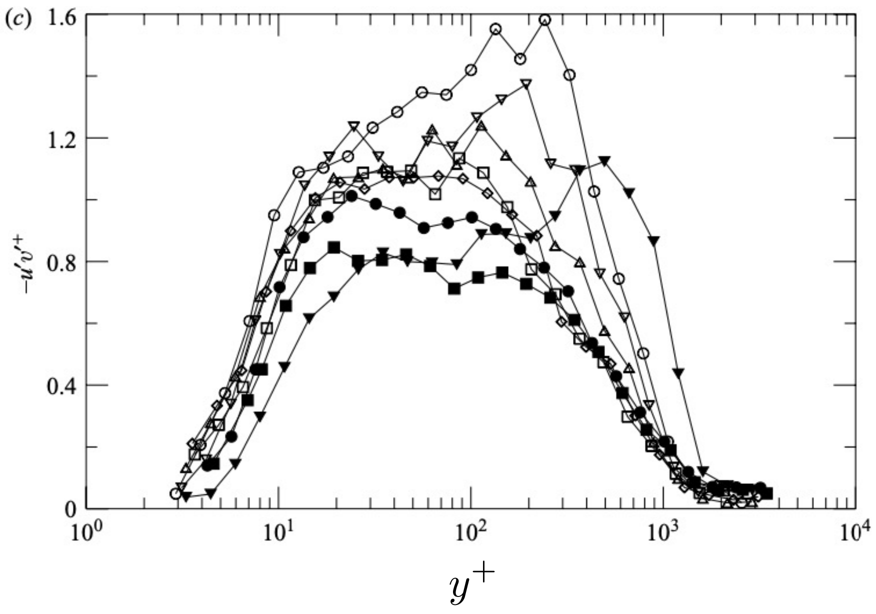

Aubertine & Eaton (2005)

Scaling pressure gradient boundary layers

Favorable pg

$$\frac{U_\infty - \bar{U}}{u_{ZS}}$$

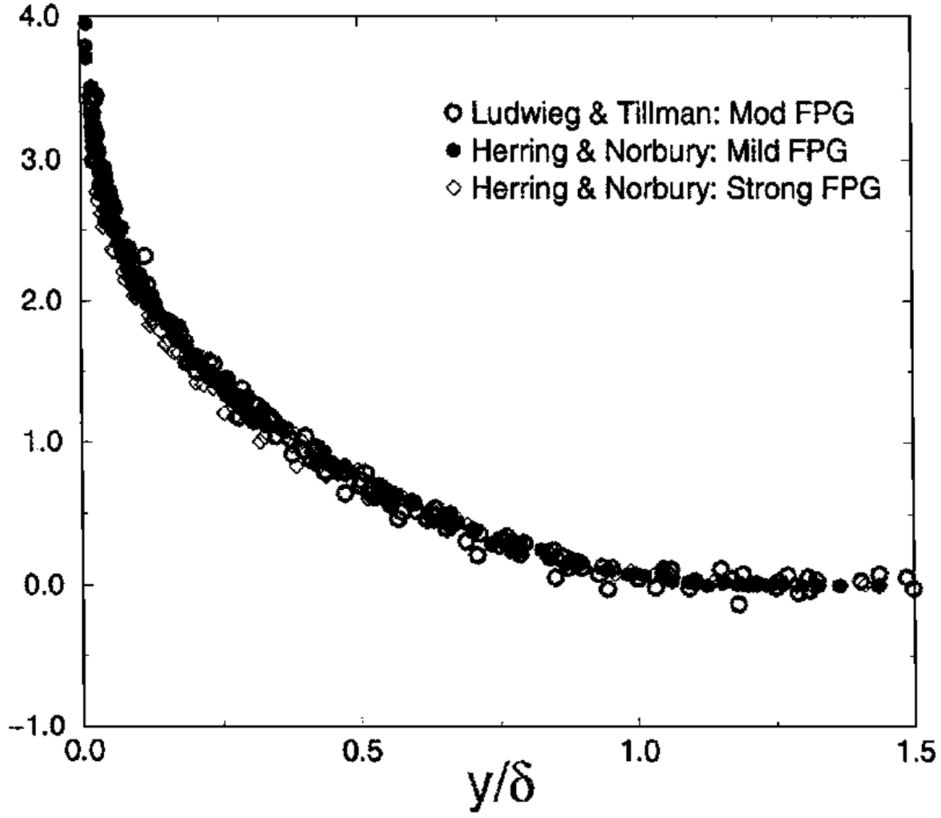

Adverse pg

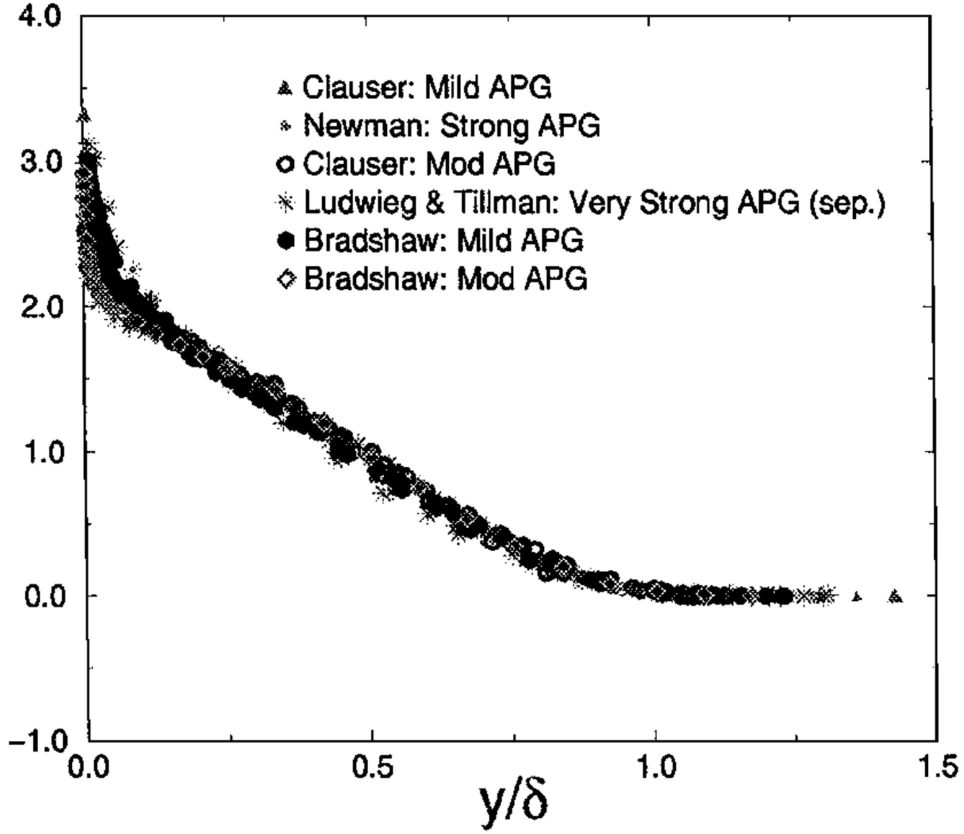

$$u_{ZS} = (\delta^*/\delta)U_\infty$$

Castillo & George (2001)

Streamline curvature

Effect of short regions of curvature on turbulent boundary layers

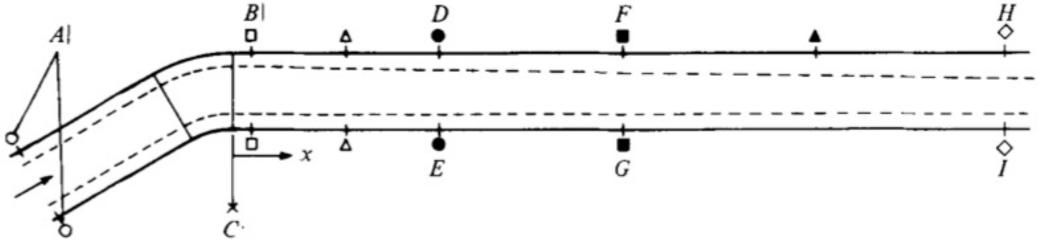

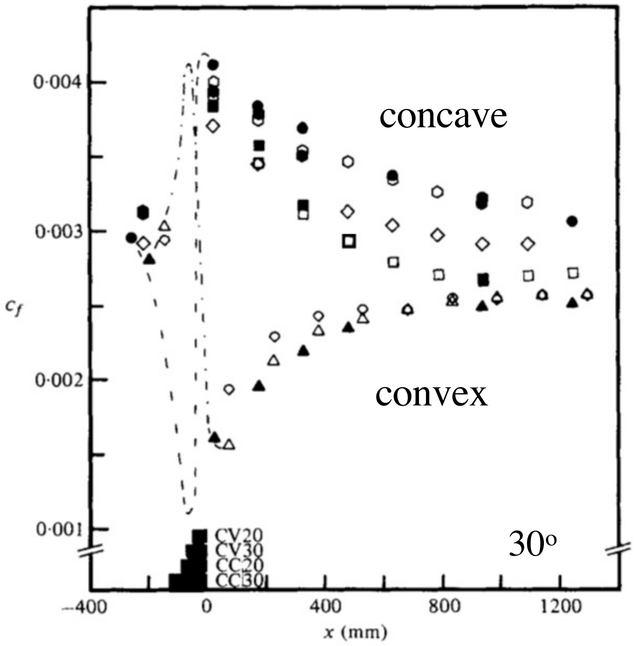

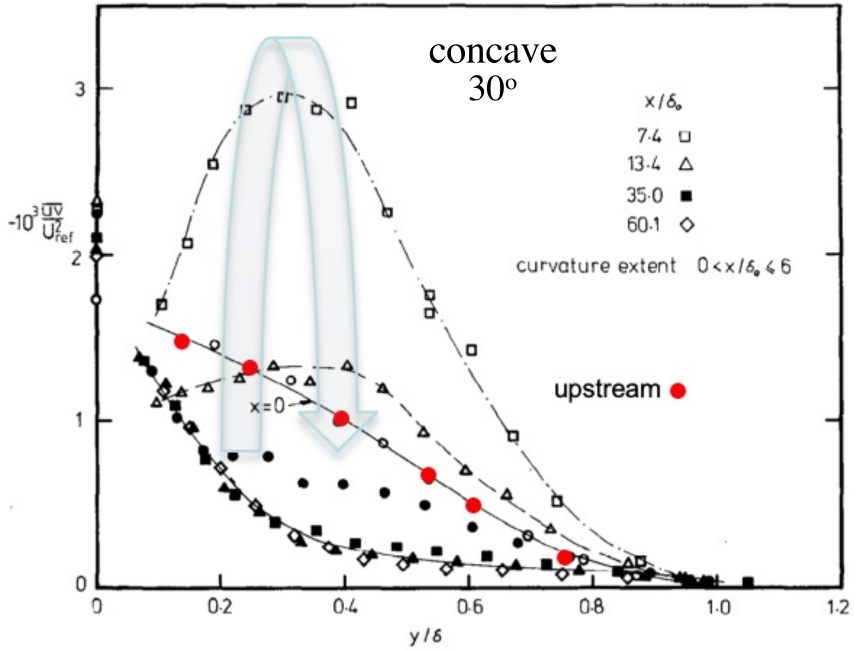

- Convex curvature is stabilizing
  - Expected to promote separation
  - Slow recovery
- Concave curvature is destabilizing
  - Expected to delay separation
  - Non-monotonic flow recovery
  - Appearance of TG vortices

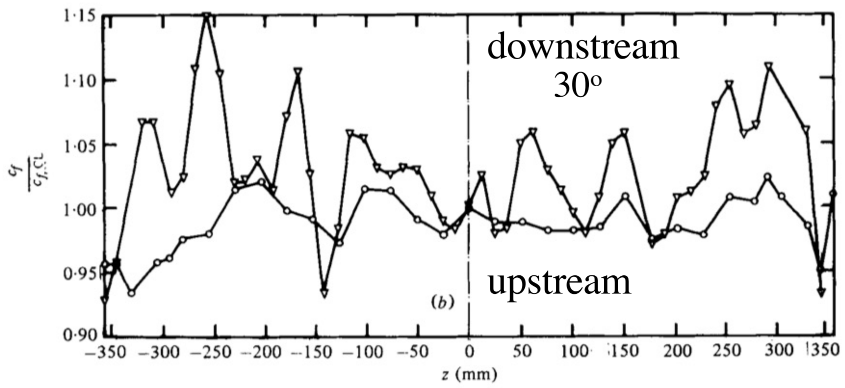

Smits, Young & Bradshaw (1979)

Upstream history effects, initial conditions

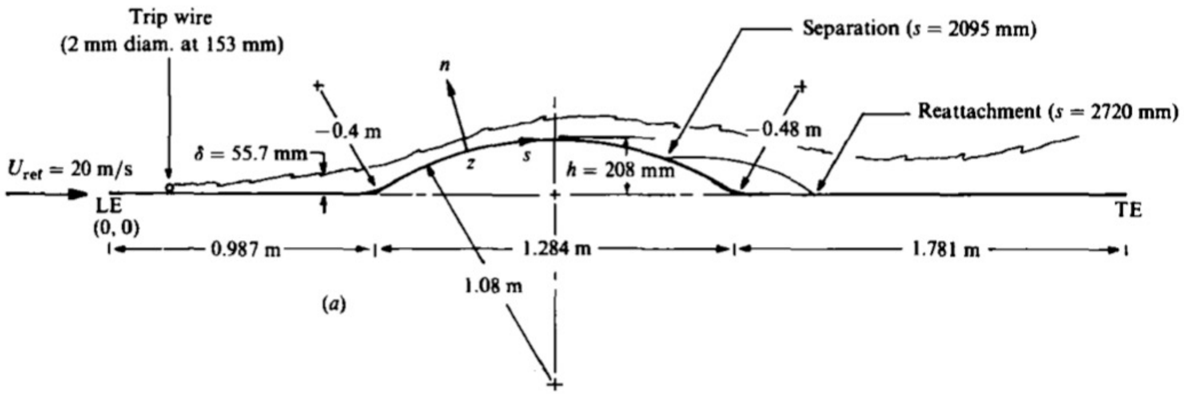

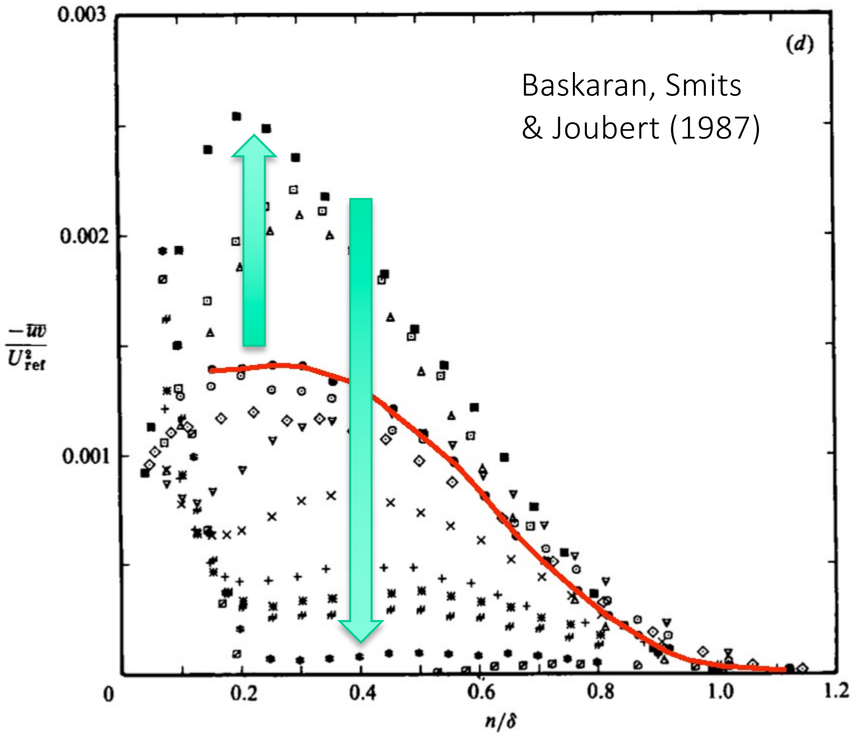

- Reynolds number
- Tripping conditions
- Roughness
- Incoming flow uniformity (2D, 3D)
- Freestream turbulence level

- Castillo, L. and Walker, D. J. 1992. Effect of upstream conditions on the outer flow of turbulent boundary layers. AIAA J.
- Devenport, W.J. and Lowe, K.T., 2022. Equilibrium and non-equilibrium turbulent boundary layers. Progr. Aerosp. Sci.
- Vishwanathan, V., Fritsch, D.J., Lowe, K.T. and Devenport, W.J., 2022. History effects and wall similarity of non-equilibrium turbulent boundary layers in varying pressure gradient over rough and smooth surfaces. TSFP12.

- Slow recovery from upstream disturbances (sometimes very slow)
- Successive pressure gradients do not add linearly

Reynolds number effects

Song & Eaton (2004)

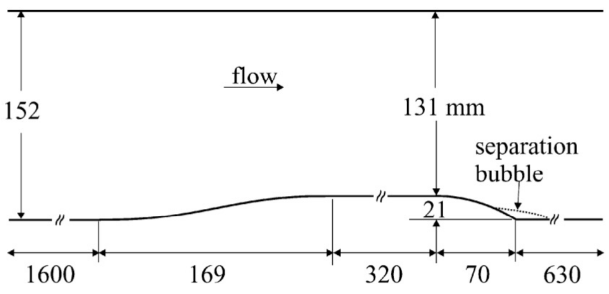

$$Re_{\tau,\text{ref}} = 525,\ 1410,\ 2686,\ 4621,\ 6676$$

Drozdz et al. (2021)

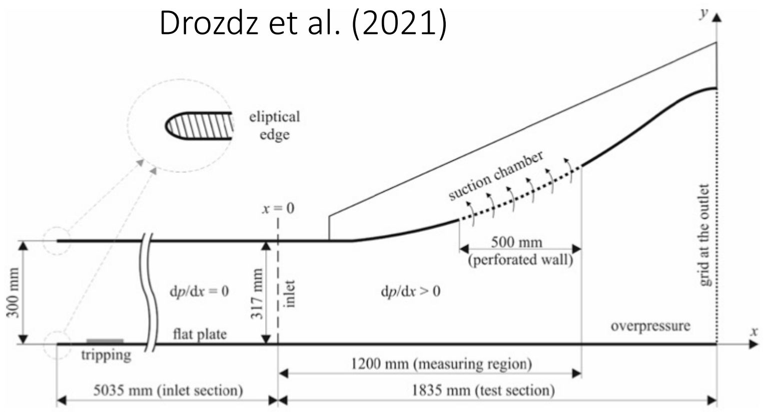

$$Re_{\tau,\text{ref}} = 1350,\ 2700,\ 4000$$

- Expect separation to be delayed with increasing Reynolds number due to enhanced mixing: only true for low Reynolds number
- For Re_τ >1000, little effect on location of separation and reattachment
- Mean flow generally only a weak (or no) function of Reynolds number
- u^2 in separated shear layer strongly increases with Re_τ, but relaxes relatively quickly, followed by –uv and then v^2
- Stress equilibrium (internal) layer observed to grow downstream of reattachment.
- Pressure recovery increases with Re_τ

Unsteadiness with steady freestream

Unsteady motions in the turbulent separation bubble
Wang & Ghaemi (2022)

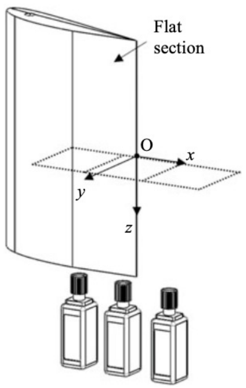

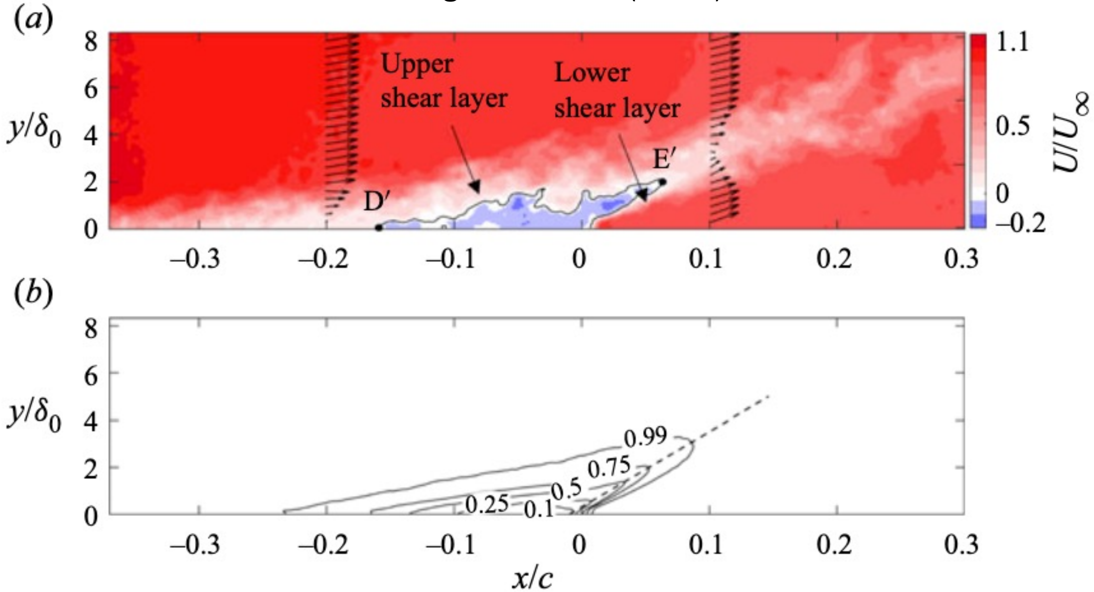

- Separation bubble on NACA 4418 airfoil at 9.7^{o}
- Unsteady separation and reattachment

Falco in Head (1982)

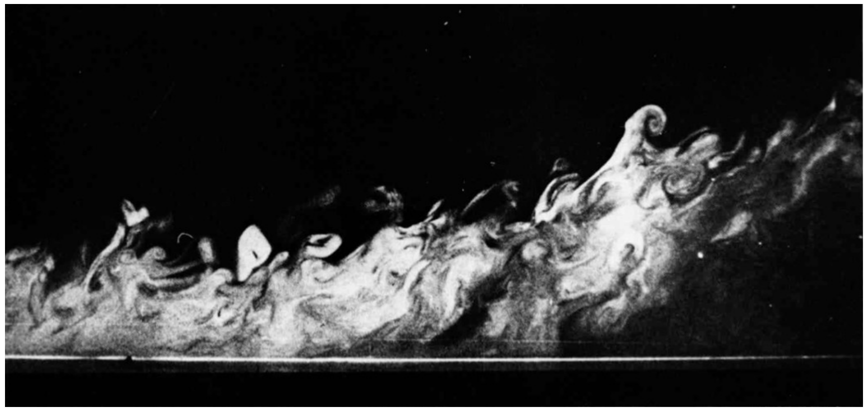

- Unsteadiness well documented in SWBLI
- Increases with shock strength
- Unsteady pressure and heat loadings
- VLSM + shear layer instability + TG vortices

3D effects in nominally 2D flows

Wang & Ghaemi (2022)

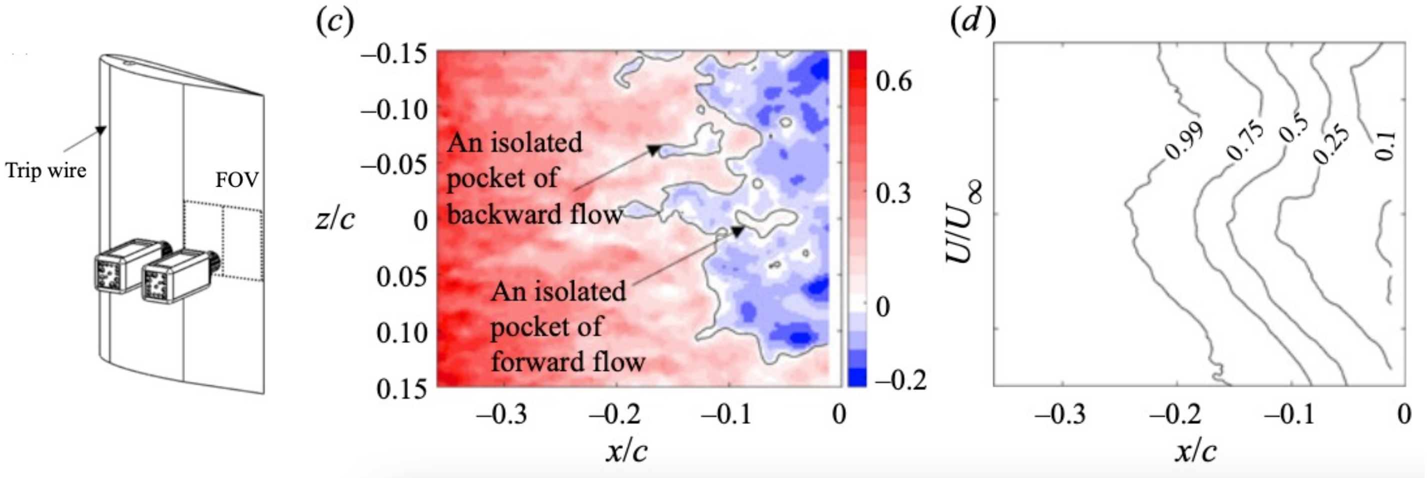

- Significant spanwise variation (TG vortices, stall cells)

- Well documented in SWBLI
- Increases with shock strength
- TG vortices

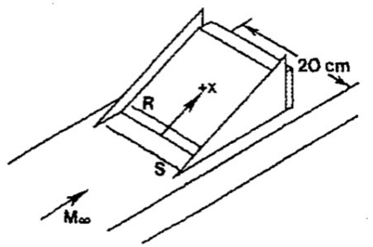

SWBLI Mach 2.9, 8° to 24°
Settles et al. (1979)

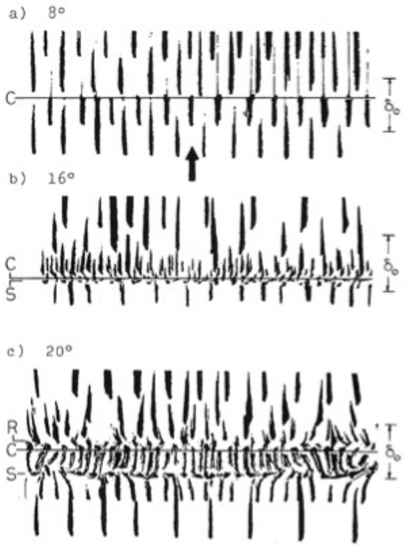

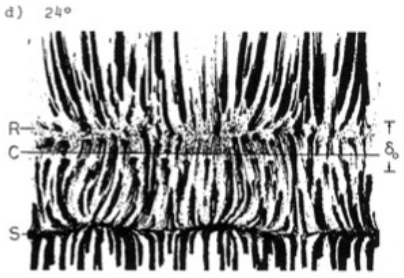

3D symmetric flows

Flowfield for 6:1 Prolate Spheroid at α = 20°

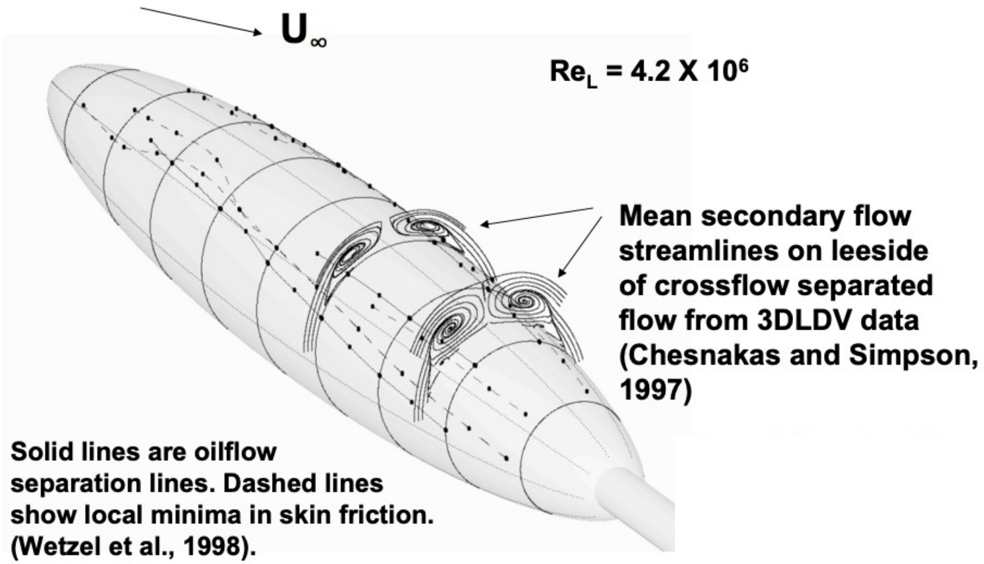

"Open" and "closed" separation
Flow topology, critical points, lines of convergence and divergence, etc.

SUBOFF at α = 40°

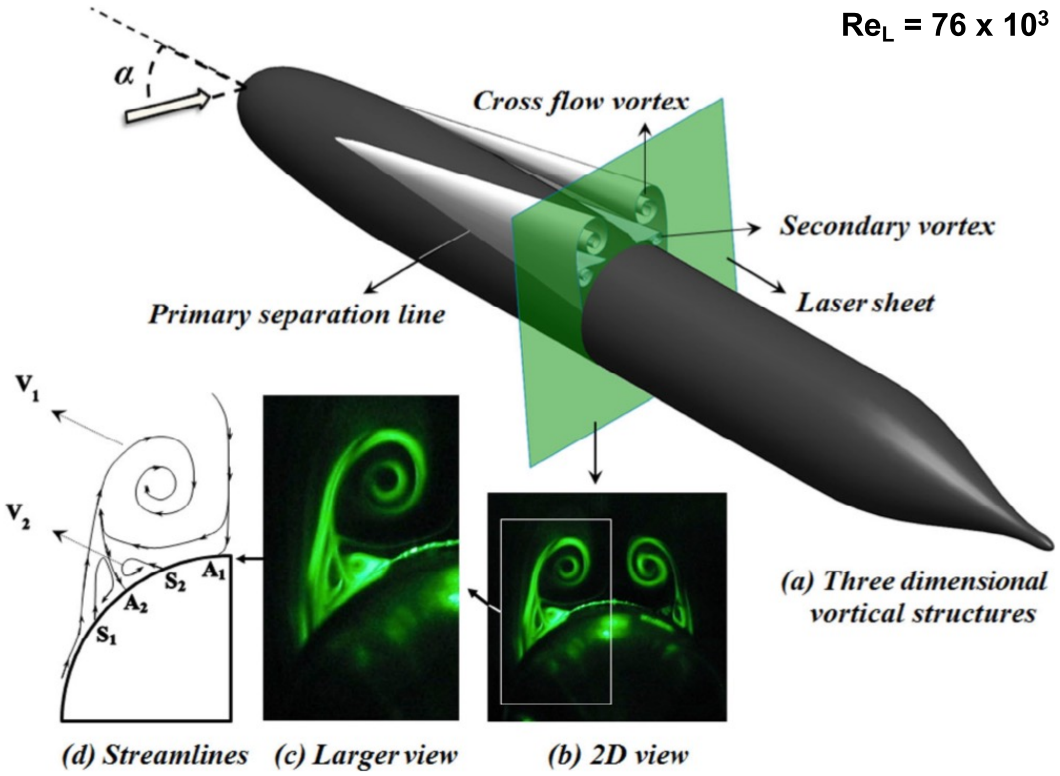

Saeidinezhad et al. (2015)
Fu (2019) AVT-307

Asymmetry in nominally symmetric flows

6:1 prolate spheroid

Re_L = 18,000

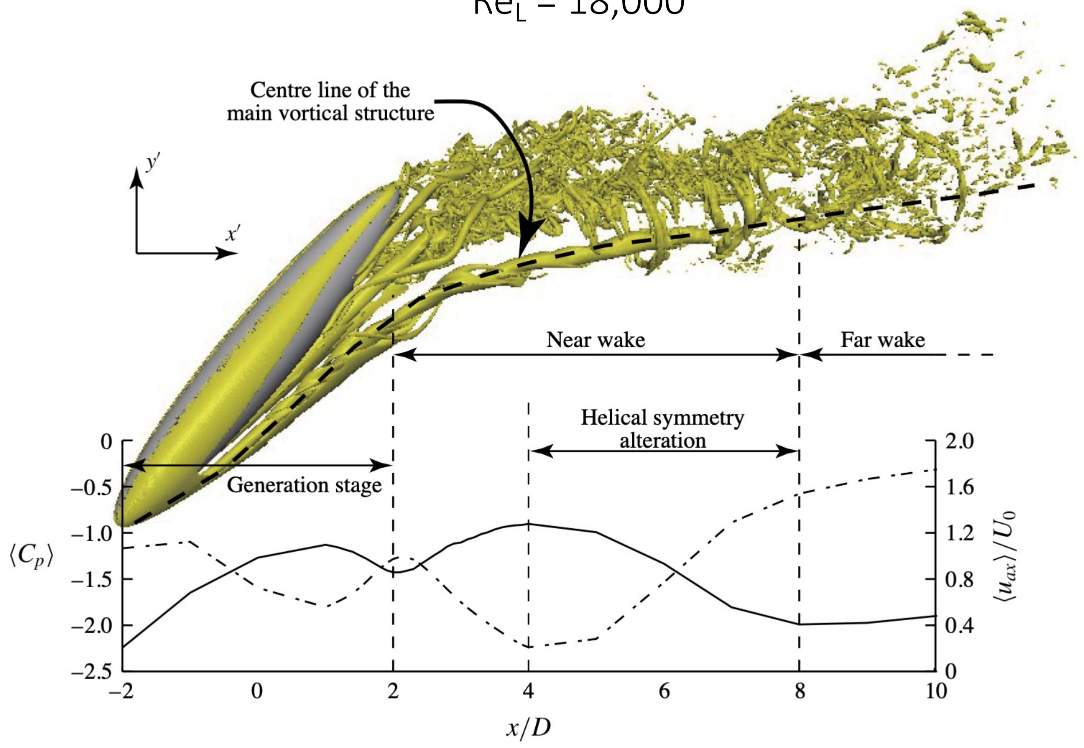

DNS at α = 45°

- For Re_L < 3,000, the wake is symmetrical
- Strong asymmetries appear at higher Reynolds numbers

Jiang et al. (2016)

Asymmetry in nominally symmetric flows

SUBOFF no appendages

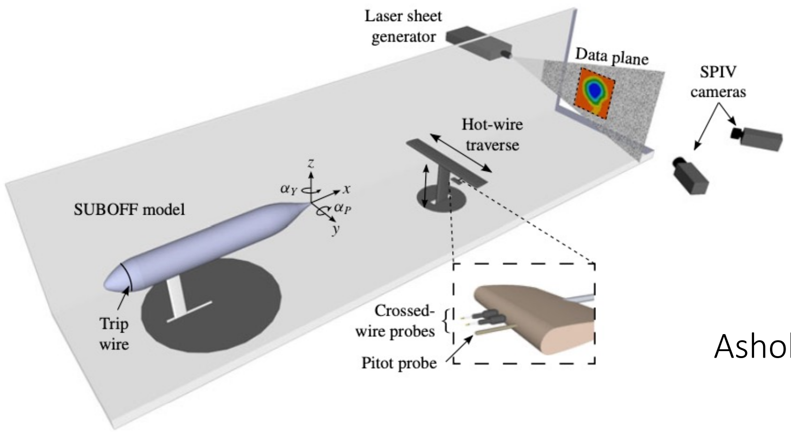

Ashok et al. (2015)

Experiments on SUBOFF model in pitch

$2.4 \times 10^6 < Re_L < 30 \times 10^6$

Persistent tilt in wake, immune to disturbances

0^o pitch

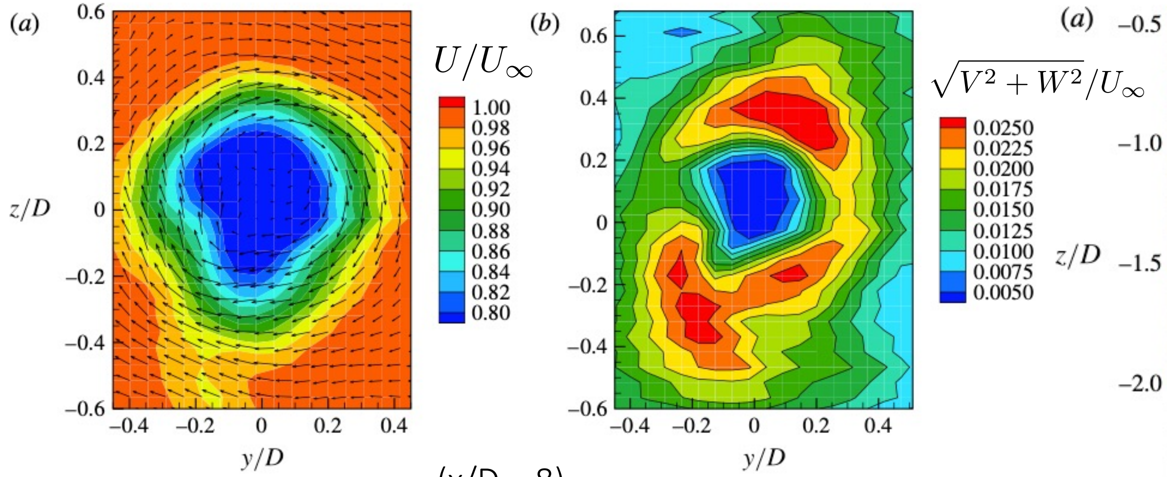

(x/D = 8)

8^o pitch

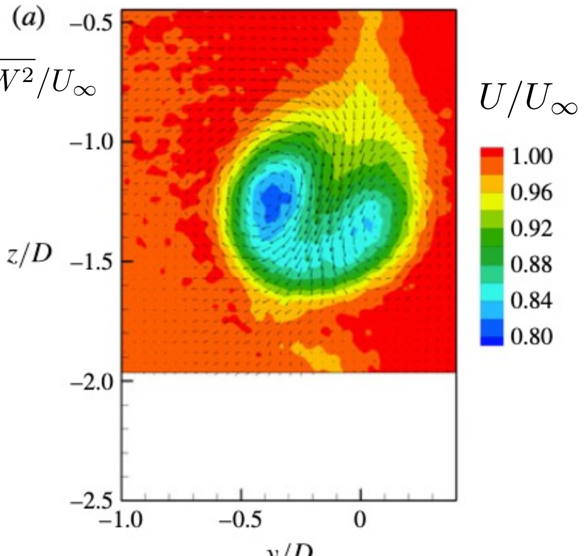

Asymmetry in nominally symmetric flows

Sharp-nosed bodies

α = 40^o (Fiechter, 1966)

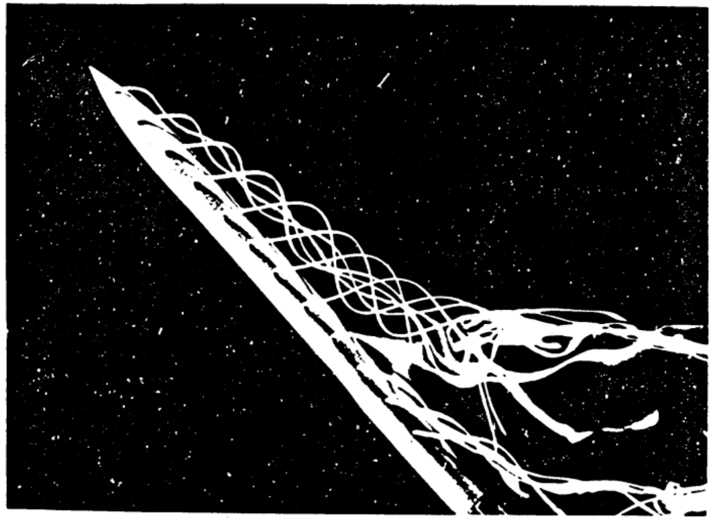

α = 40^o (Luo et al. 1998)

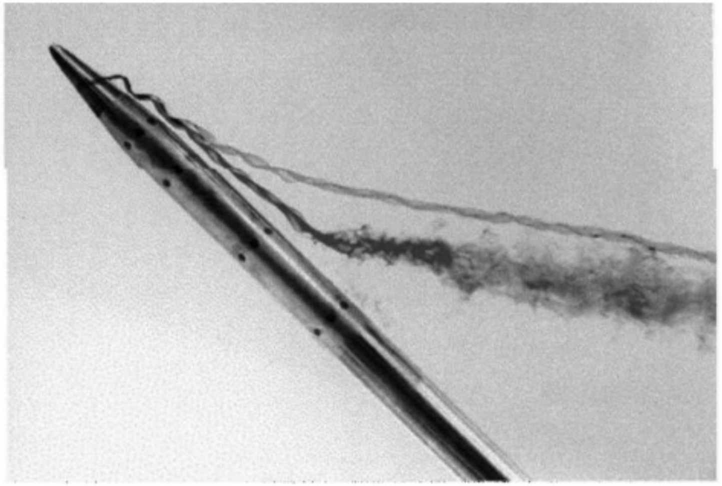

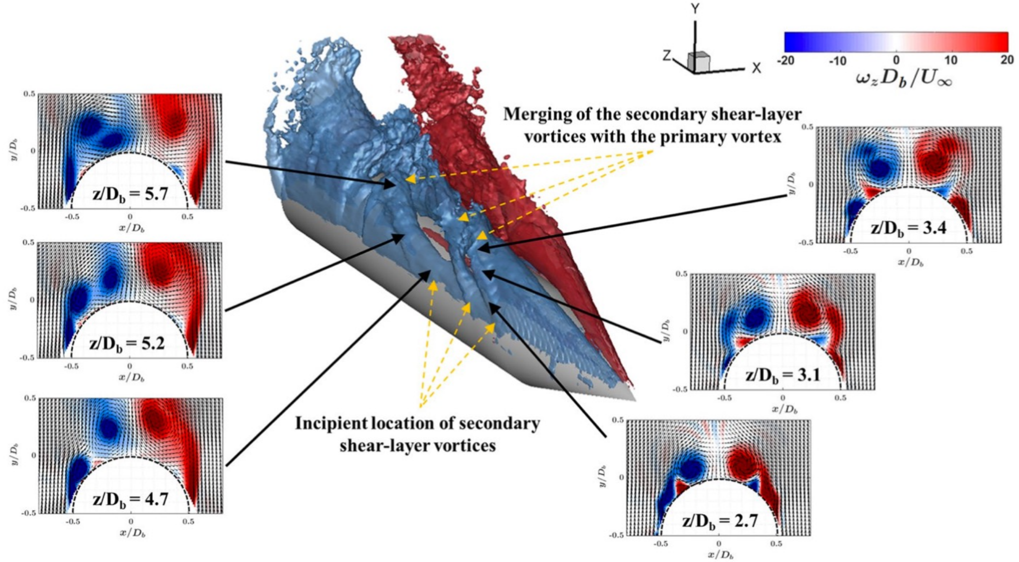

Cone-cylinder body at α = 40^o (Kumar et al. (2020, PIV)

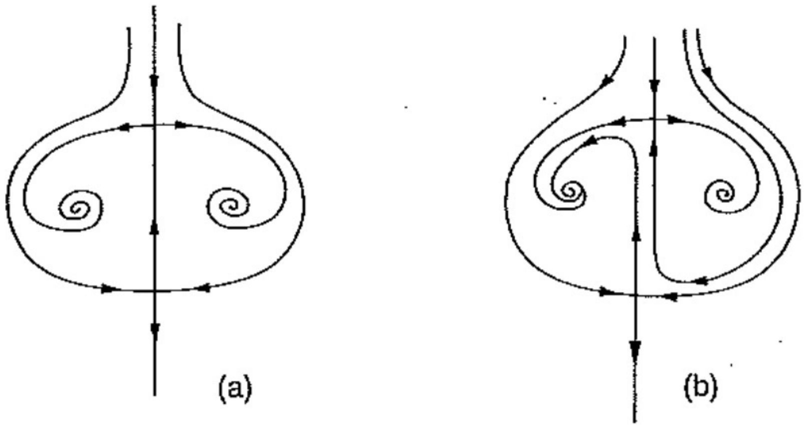

Symmetry is hard (Perry & Hornung, 1984)

Significant, unsteady side forces

Asymmetry in nominally symmetric flows

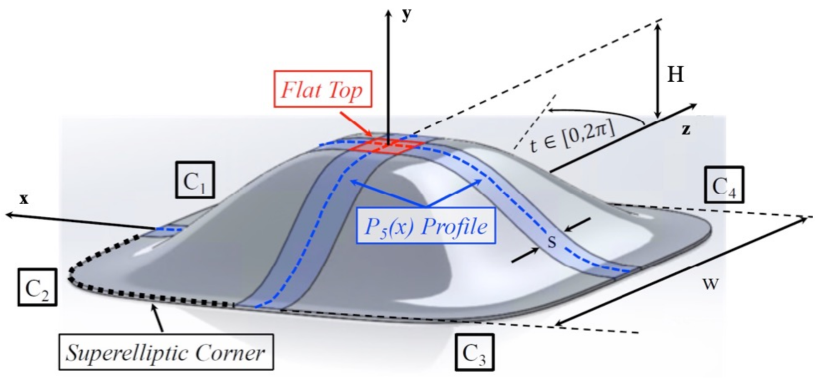

BeVERLI Hill model at 0^o, Re_H = 650,000

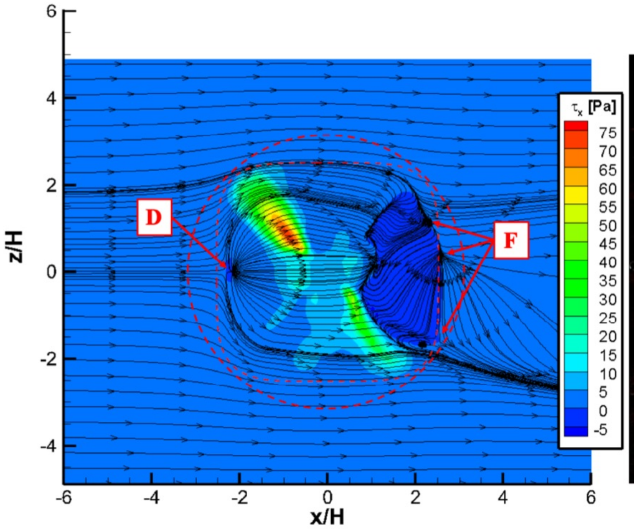

RANS S-A wall shear stress

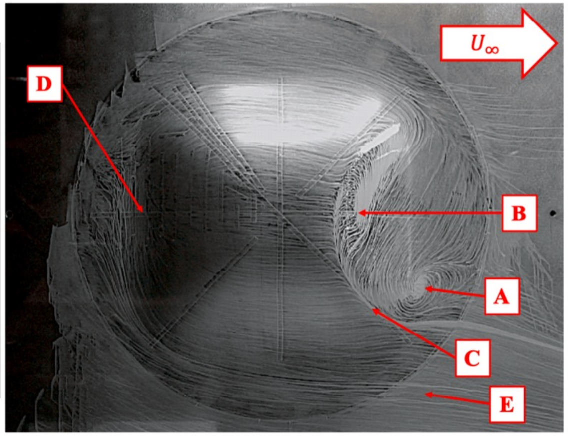

Experiment flow visualization

Gargiulo et al. (2021) AVT-349

Asymmetry in experiment and computation

Response to strong perturbations

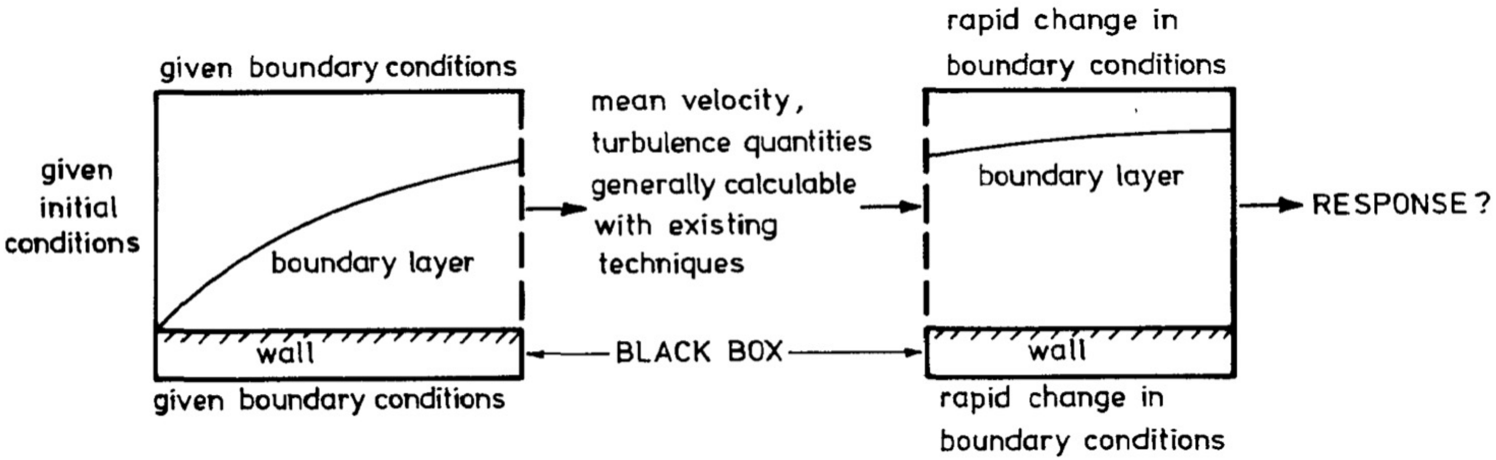

Examples:

- Sudden change in surface roughness
- Rapid changes in pressure gradient
- Rapid changes in surface curvature
- Application of suction or blowing
- Shock-wave boundary layer interaction

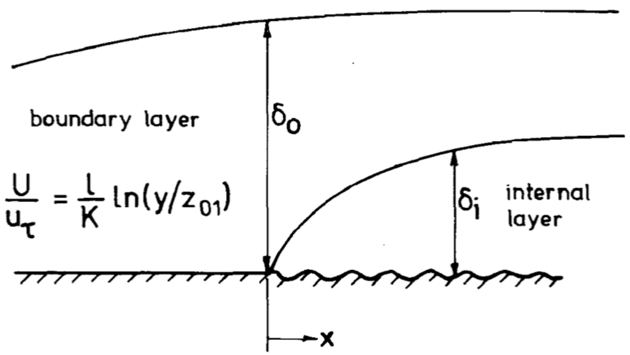

Smits & Wood (1985)

Strongly perturbed turbulent flows

- Boundary layer response to short regions of roughness and heat transfer, with relevance to atmospheric flows
  - Andreopoulos & Wood JFM 1982; Andreopoulos 1983
- Interested in non-equilibrium wall-bounded flows
- Especially impulsive changes:
  - Roughness, wall curvature, pressure gradient, heat transfer, buoyancy, etc.
  - Are there universal features (e.g., overshoots) in the flow response, and what does it say about production, dissipation, transport?
  - Can we use this knowledge for flow control?
- Four new examples
  - Pipe flow response to change in roughness (rough-to-smooth)
  - Pipe flow response to square bar roughness element
  - Pipe flow passive mode control
  - Boundary layer active wall motion control

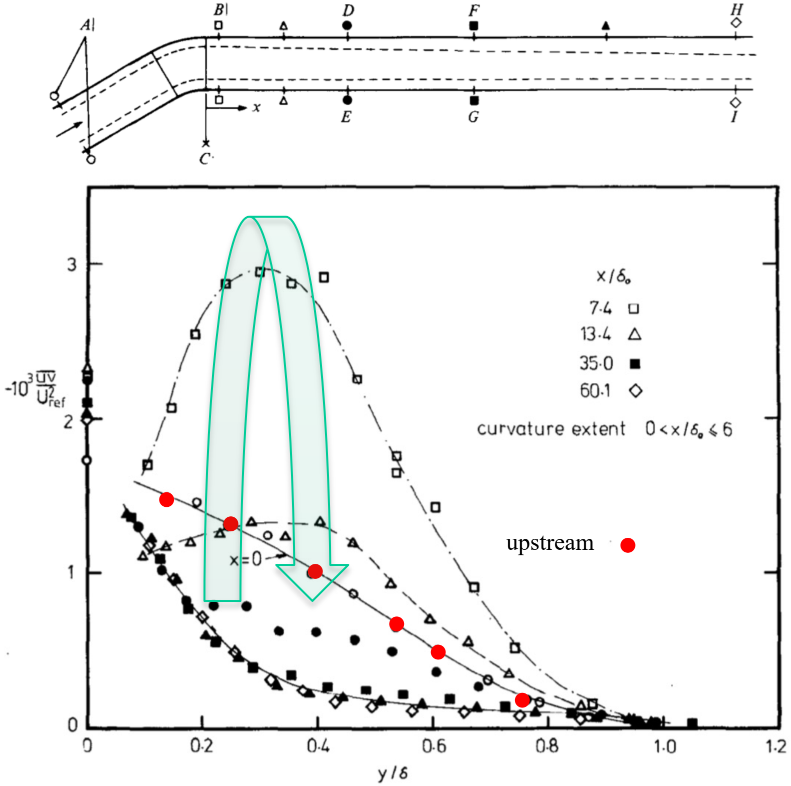

Impulse in concave curvature (taken at a crest in skin friction), with turning angle of 30° (Smits et al., JFM 1979)

Response length scales

Response time for stress-containing eddies: $$t_\tau = \frac{\text{TKE}}{\text{rate of production}} = \frac{k}{-\overline{uv}\,\partial U/\partial y}$$

$$x_\tau = U t_\tau$$

For Re_τ = 5200 (Moser & Lee DNS channel flow):

$x_\tau^+ \approx 50 \;\; (x_\tau/\delta \approx 0.01)$ inner layer response distance at y^+=15

$x_\tau^+ \approx 75{,}000 \; (x_\tau/\delta \approx 15)$ outer layer response distance at y/δ =0.2

How does this relate to perturbations?

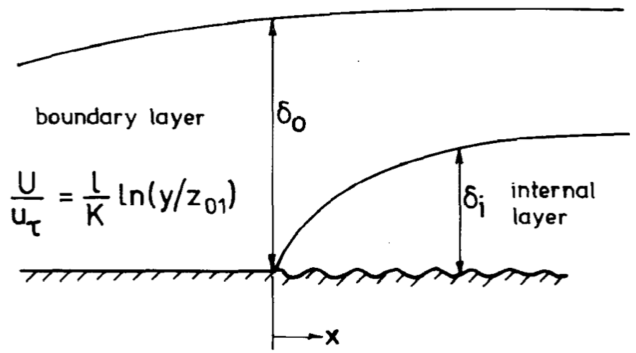

Bradshaw (1973); Smits & Wood (1985)

Step change in roughness

- Antonia & Luxton (1971) Smooth-to-Rough
- Inner region: overshoot of stress levels
- Outer region: stress “bore” moving outwards, reflecting growth of the inner layer

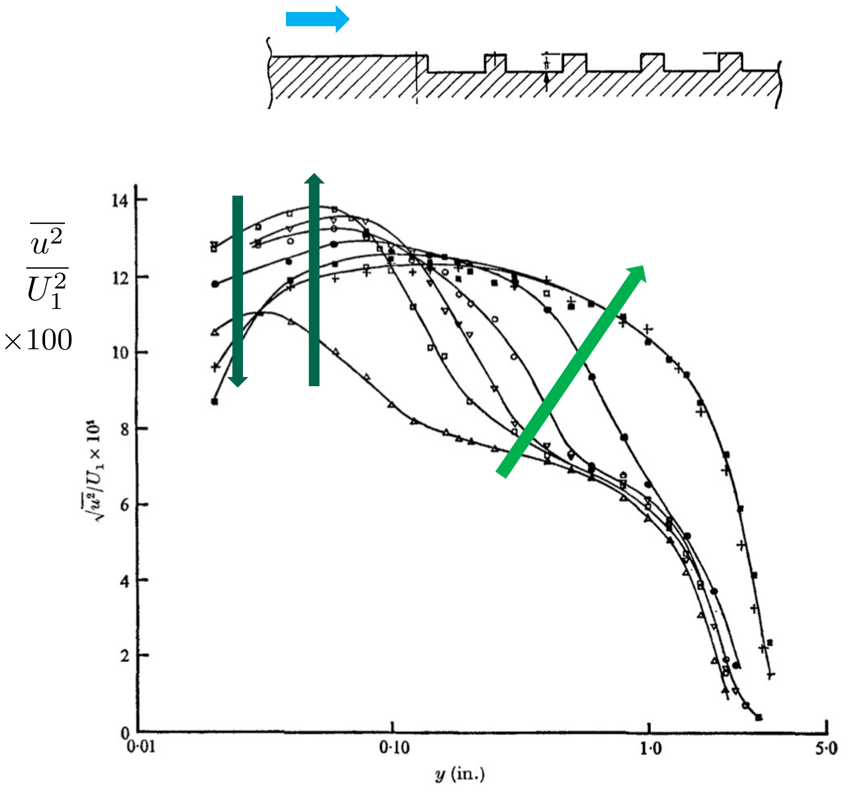

Antonia & Luxton Part I (1971)

- Antonia & Luxton (1971) Rough-to-Smooth
- Inner region: rapid collapse of stress levels
- Outer region: slower collapse of stress levels

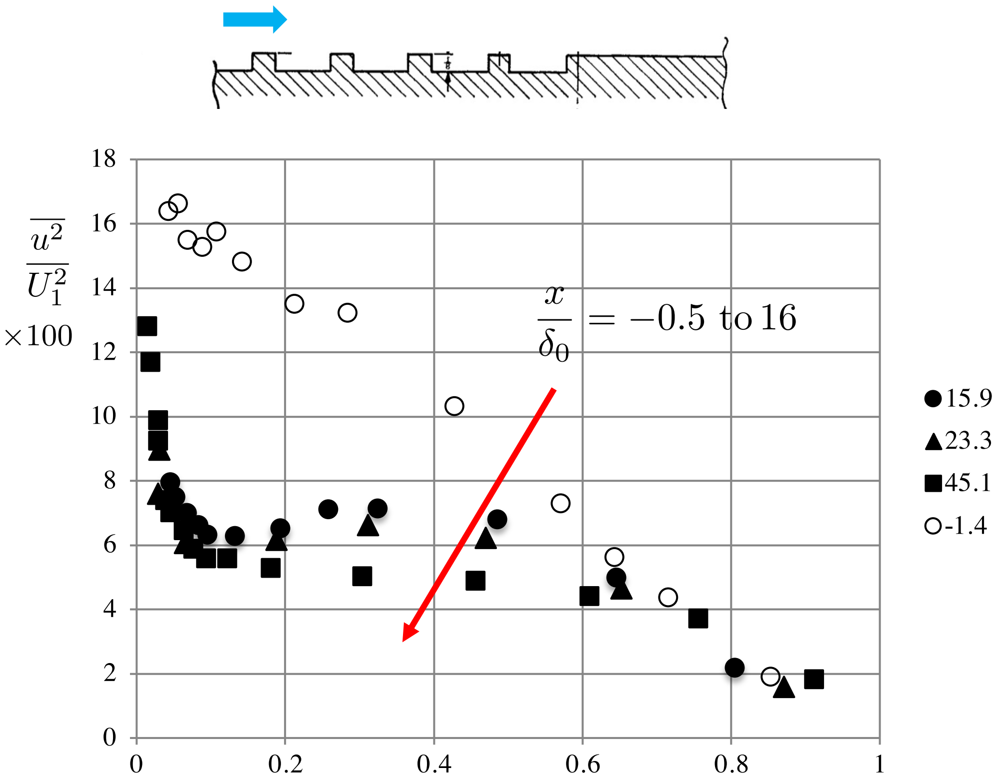

Antonia & Luxton Part II (1971)

Step change in roughness

- Antonia & Luxton (1971) Smooth-to-Rough
- Inner region: overshoot of stress levels
- Outer region: stress “bore” moving outwards, reflecting growth of the inner layer

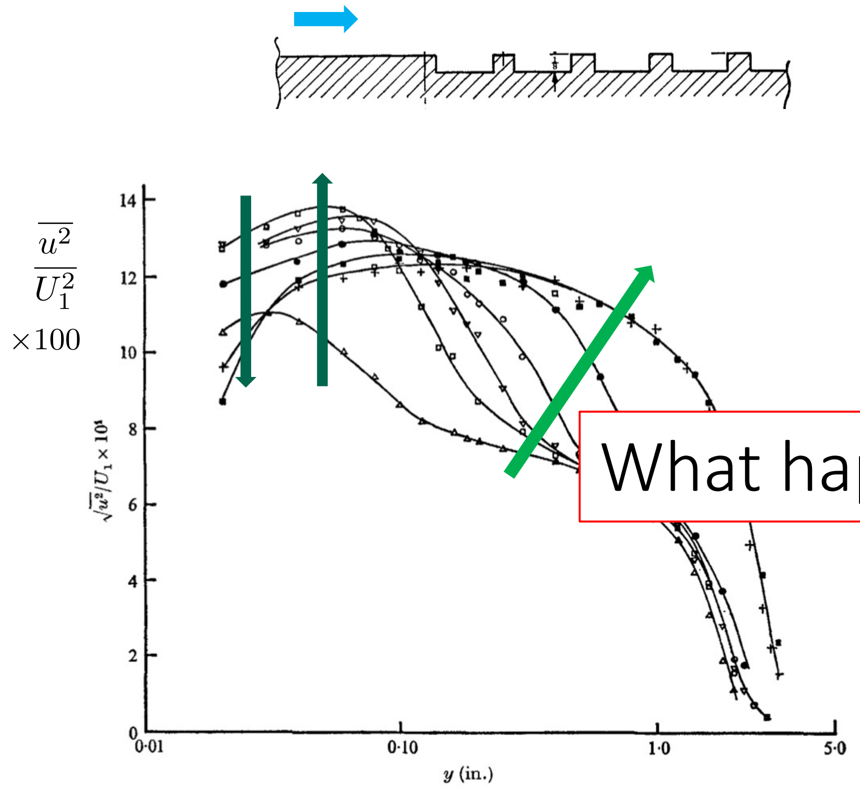

Antonia & Luxton Part I (1971)

- Antonia & Luxton (1971) Rough-to-Smooth
- Inner region: rapid collapse of stress levels
- Outer region: slower collapse of stress levels

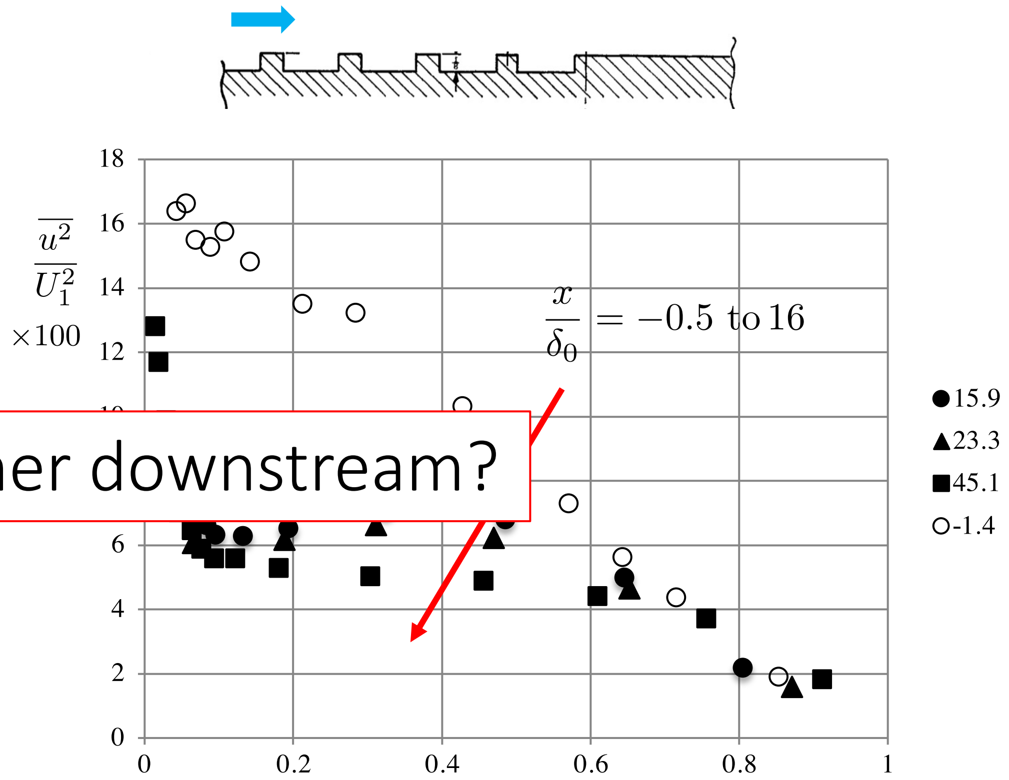

Antonia & Luxton Part II (1971)

What happens further downstream?

1. Step change in roughness $(\lambda_R/\lambda_S = 9.1)$

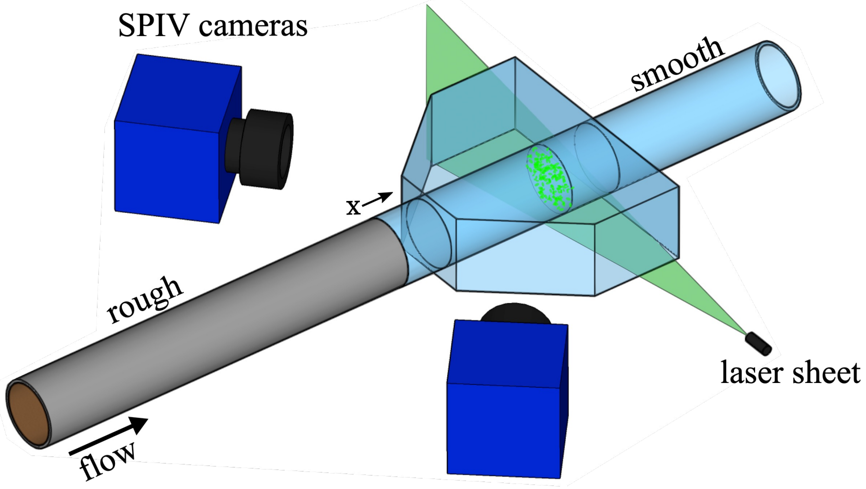

friction factor

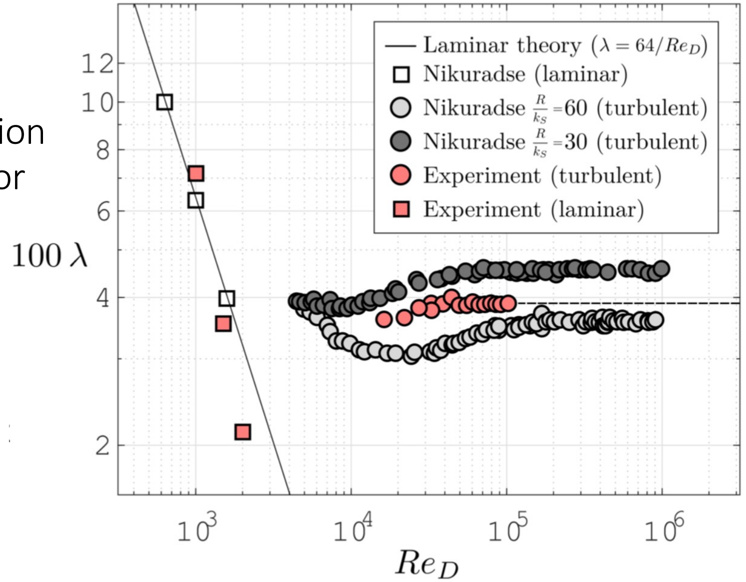

$R/k_s \approx 57$

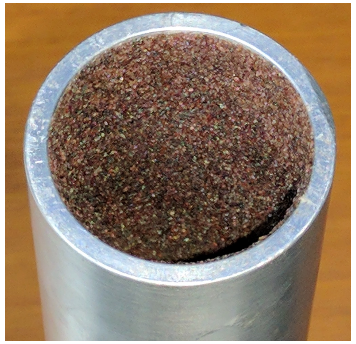

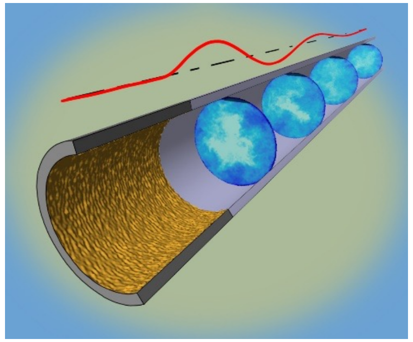

Van Buren et al. (2020)

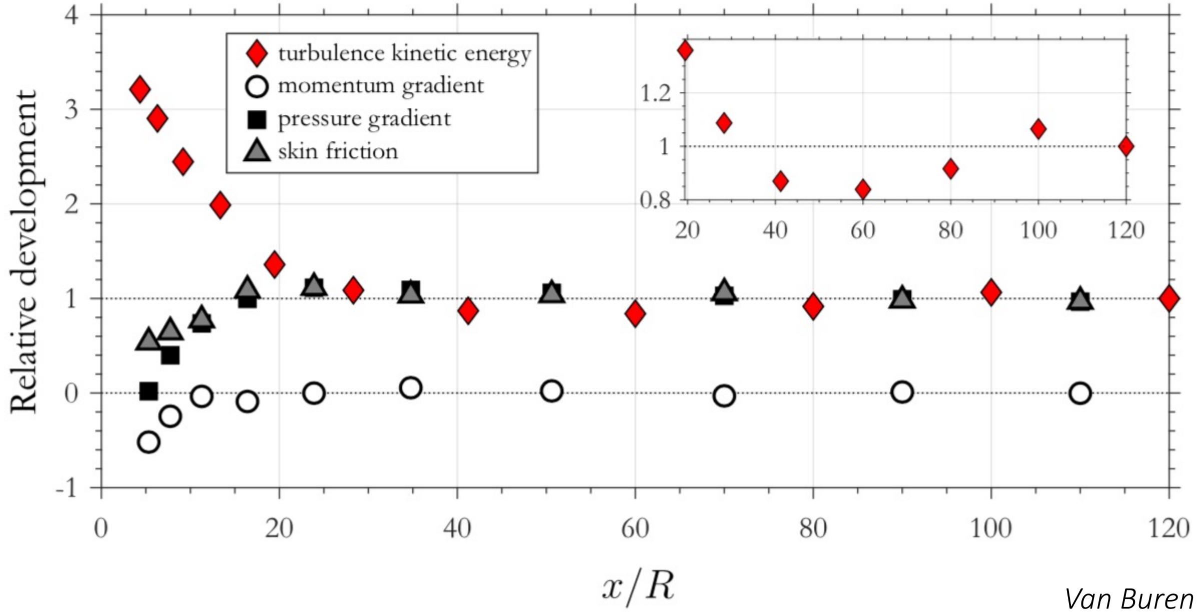

Van Buren et al. (2020)

Step change in roughness: mean flow

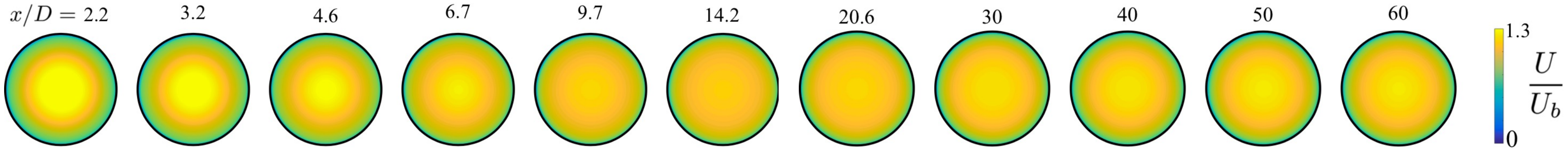

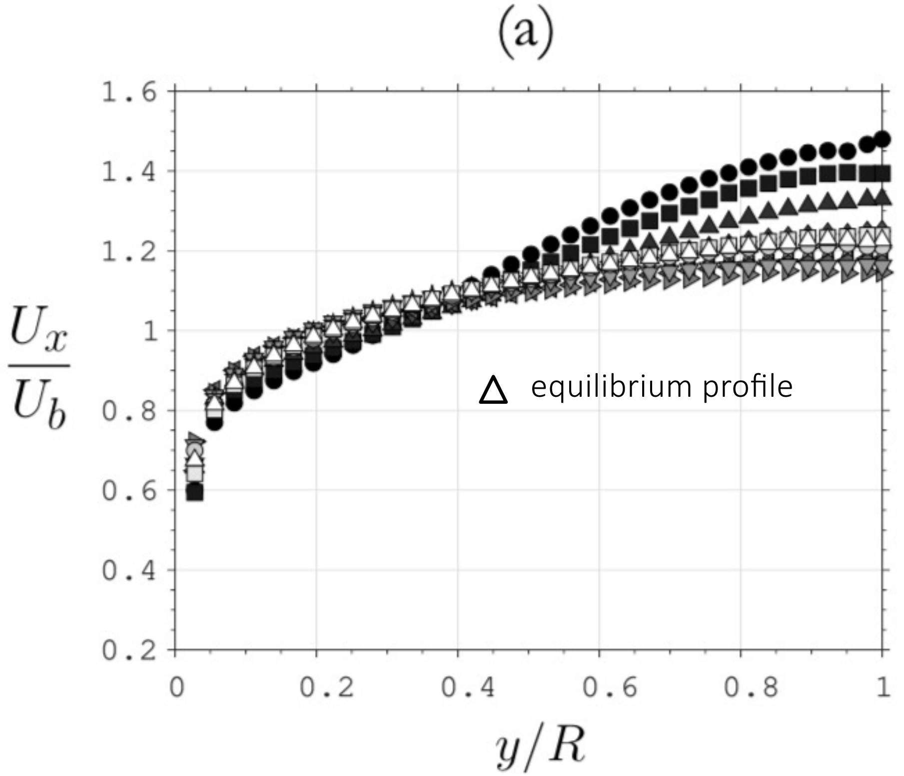

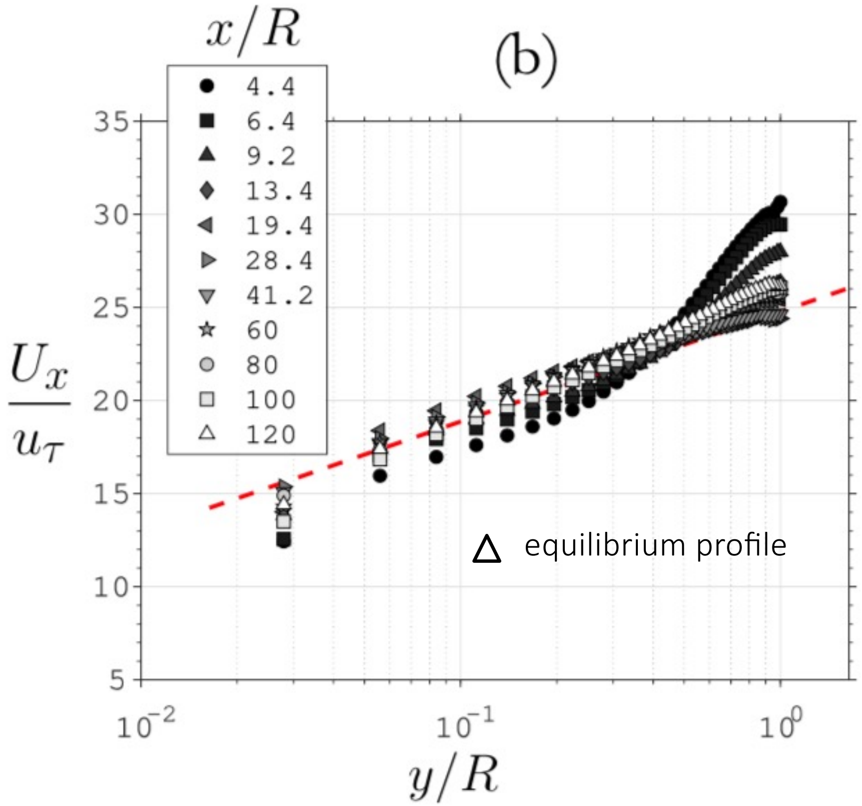

Step change in roughness: shear stress

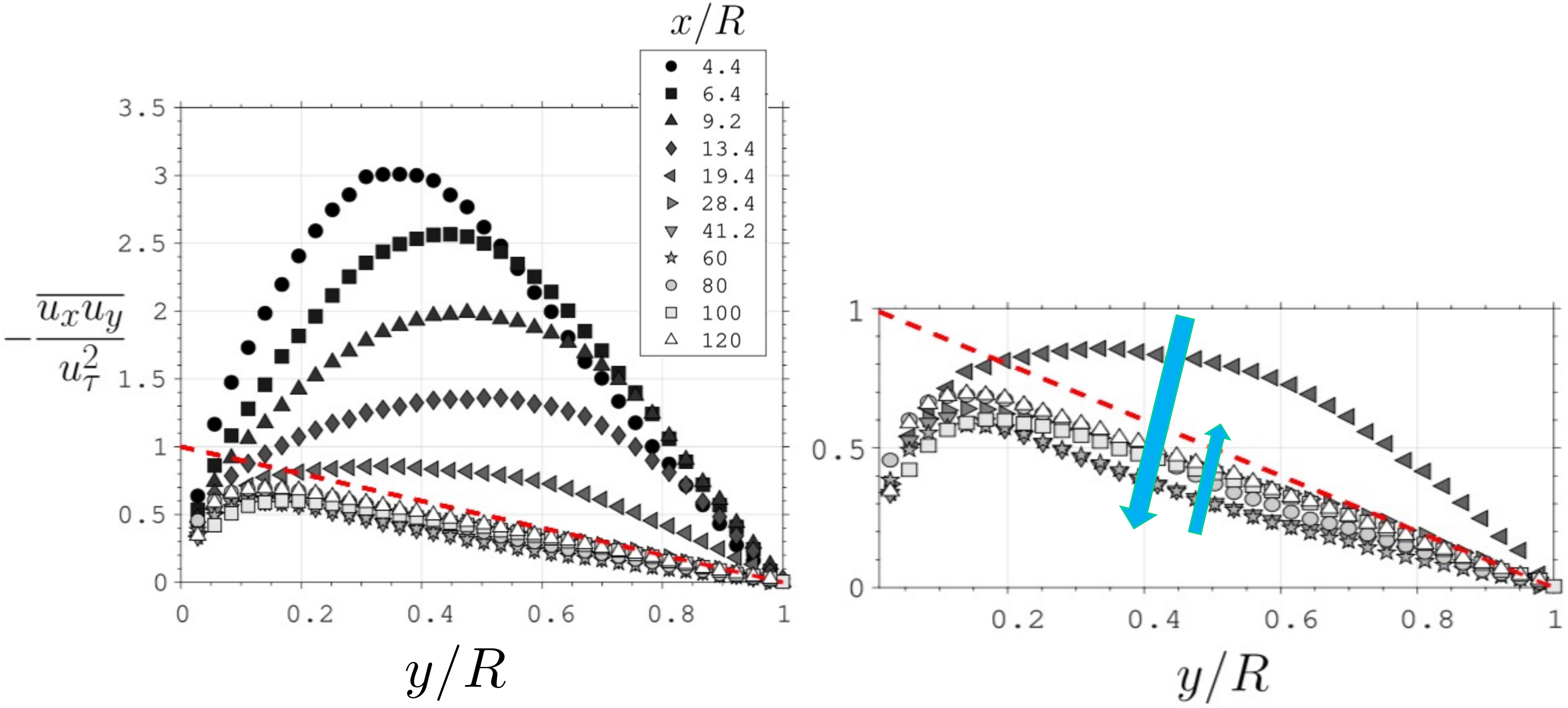

Step change in roughness: turbulence production

$$-\overline{u_x u_r}\frac{\partial U_x}{\partial r}\frac{R}{u_\tau^3}$$

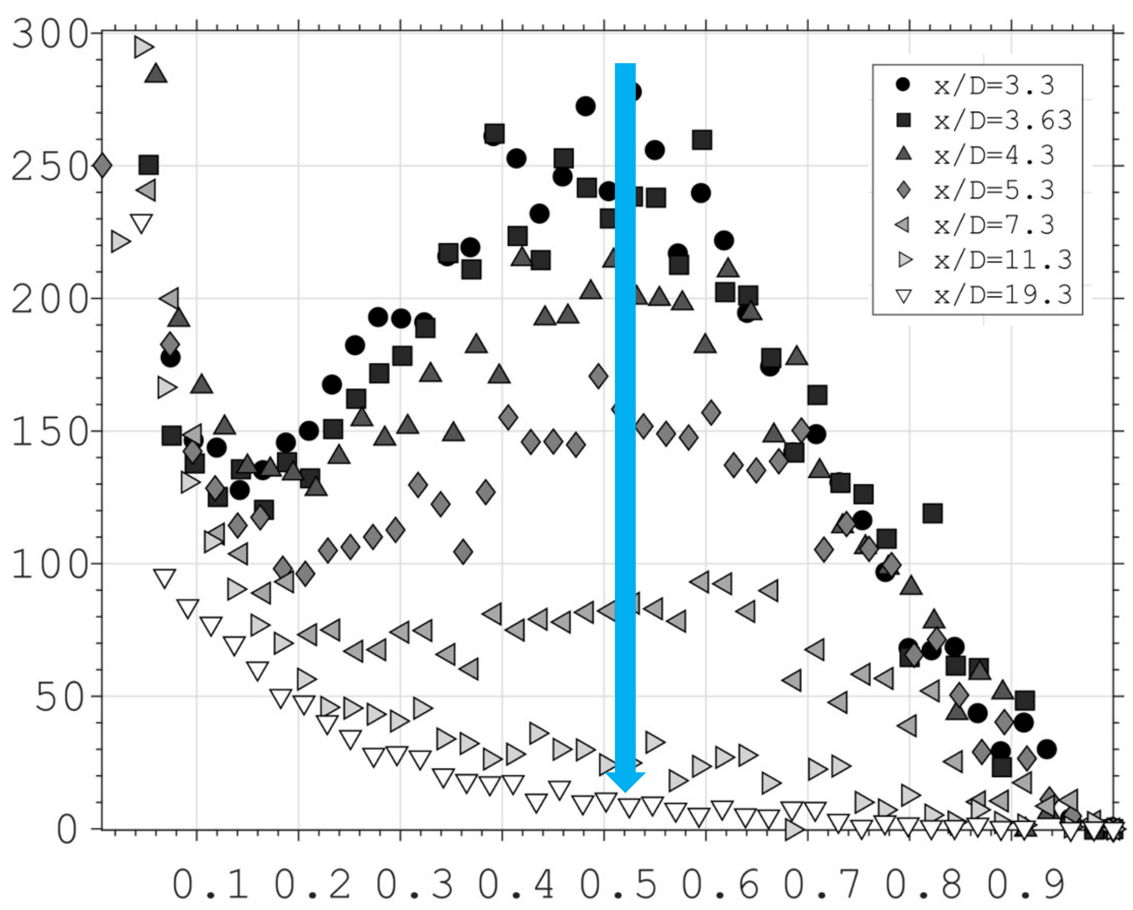

y/R

Production collapses

2. Flow over a square bar

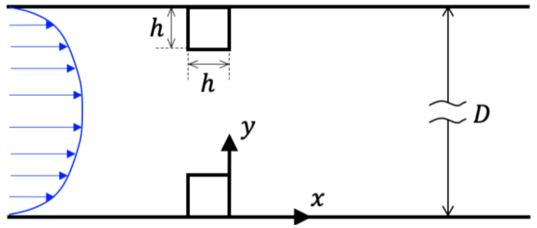

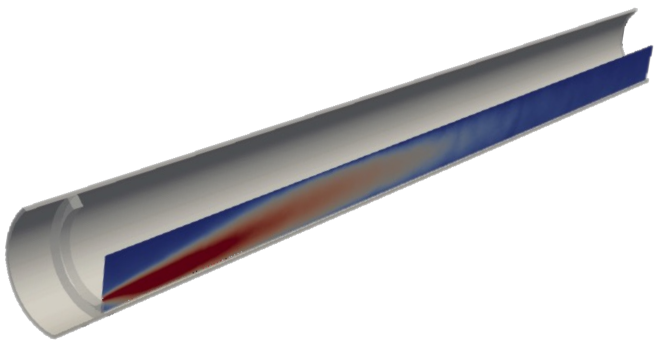

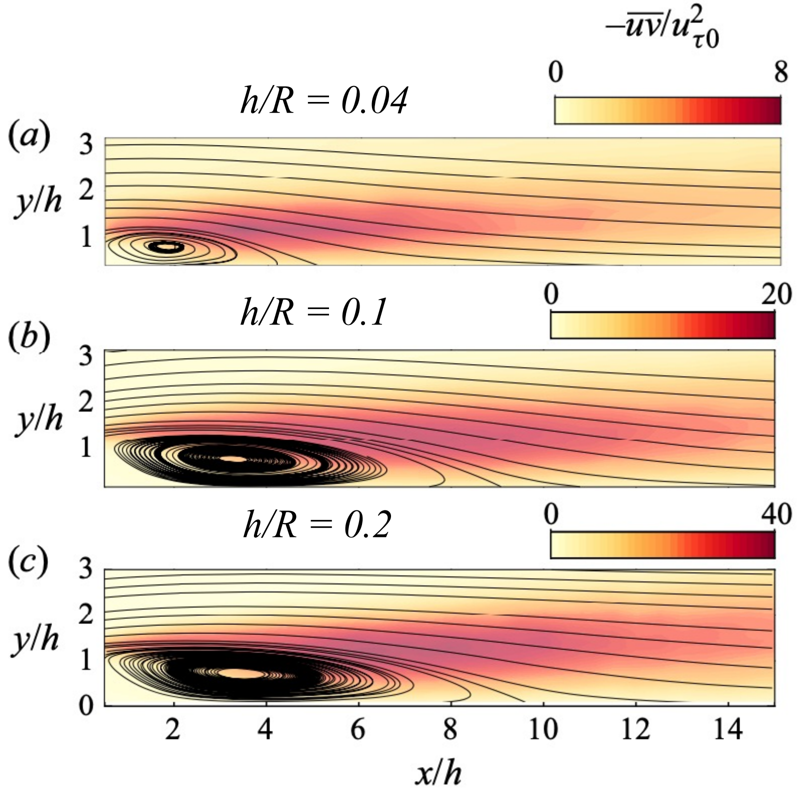

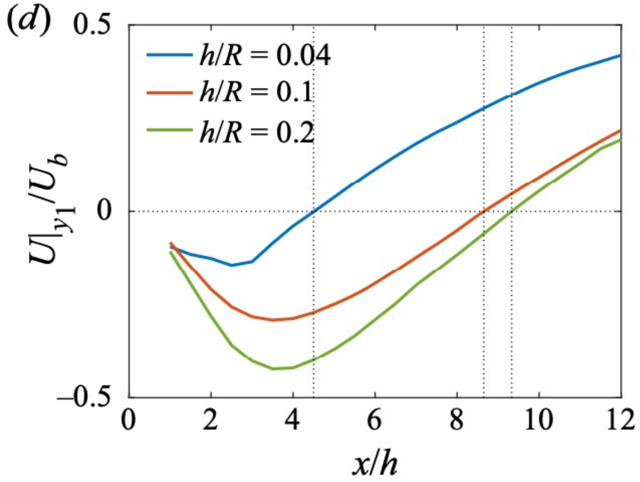

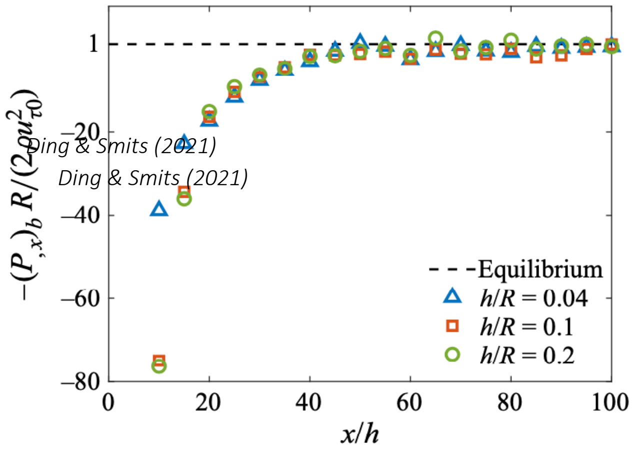

Ding & Smits (2021)

Flow over a square bar response

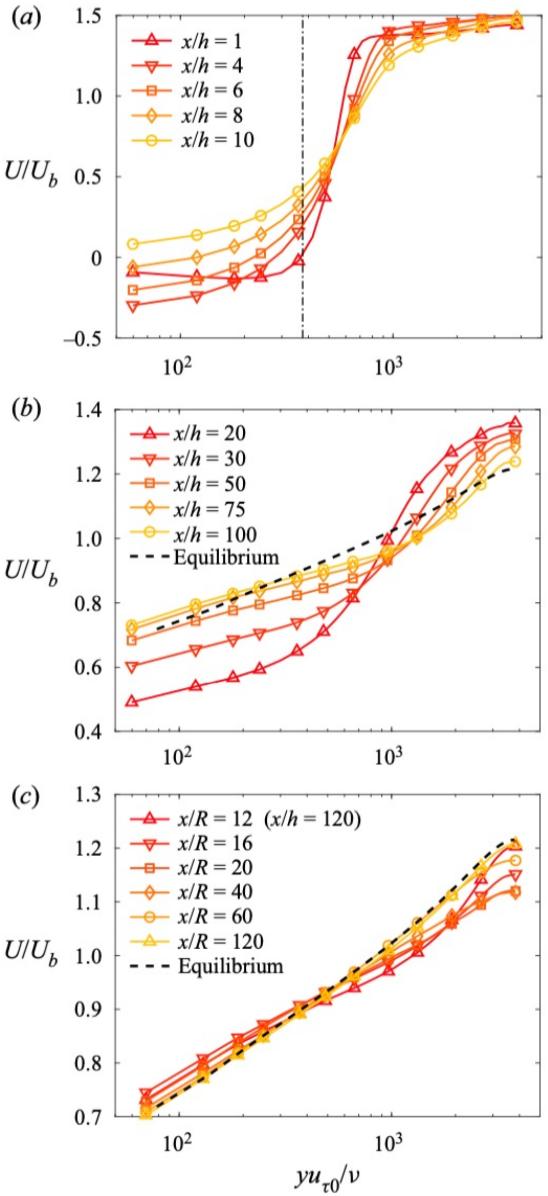

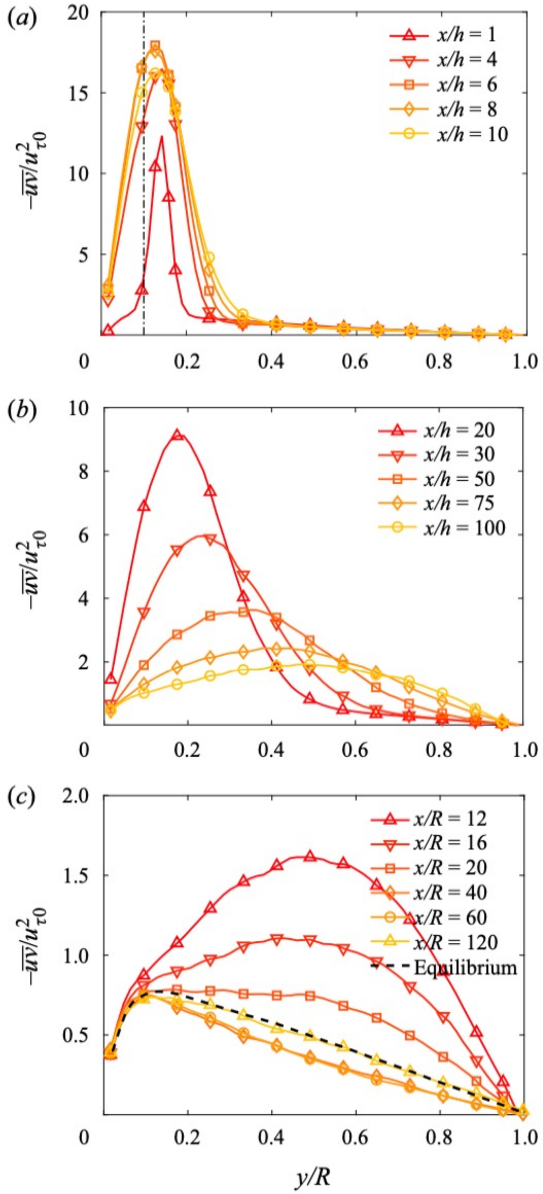

- Mean flow near wall recovers by x/h ≈ 100
- Mean flow in outer region recovers by x/R ≈ 120 (x/h = 1200)
- Shear stress near wall recovers by x/R ≈ 20 (x/h = 1200)
- Shear stress in outer region overshoots recovery before approaching equilibrium state by x/R ≈ 120 (x/h = 1200)

h/R = 0.1

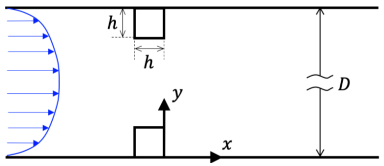

General Reynolds shear stress response

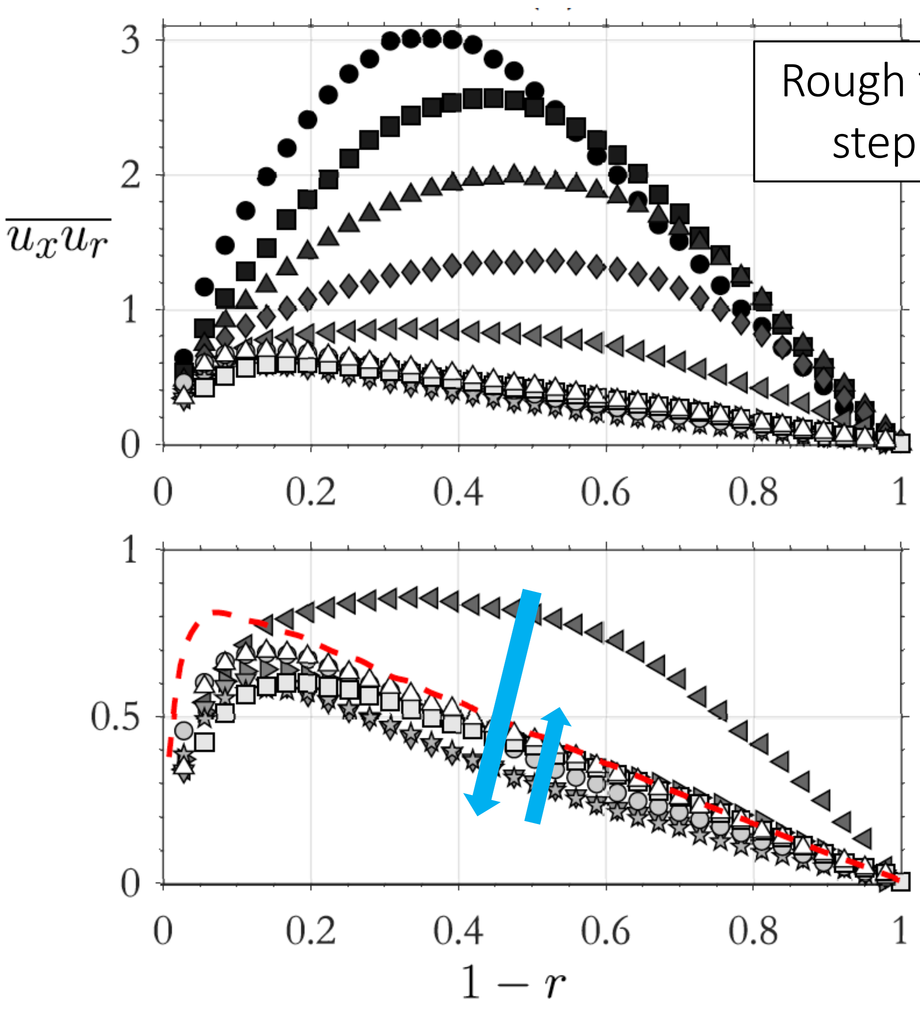

Rough to smooth step change

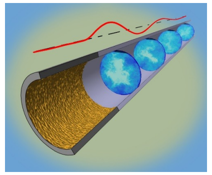

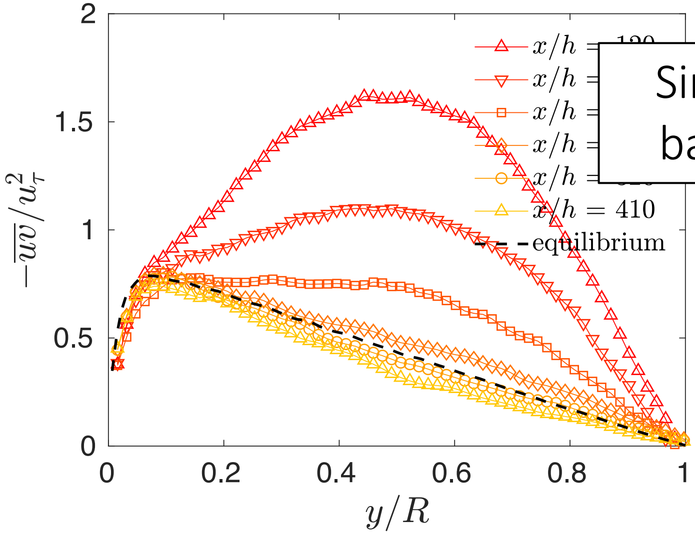

Single square bar h/R = 0.1

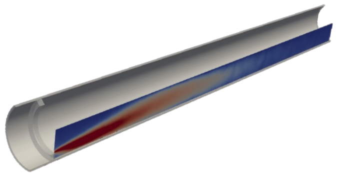

Overshoot before recovery far downstream (x/R > 100)

General Reynolds shear stress response

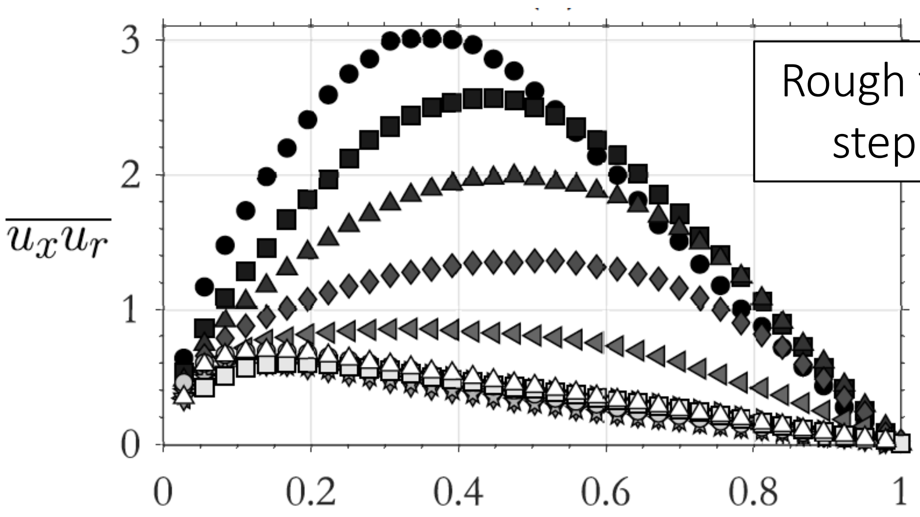

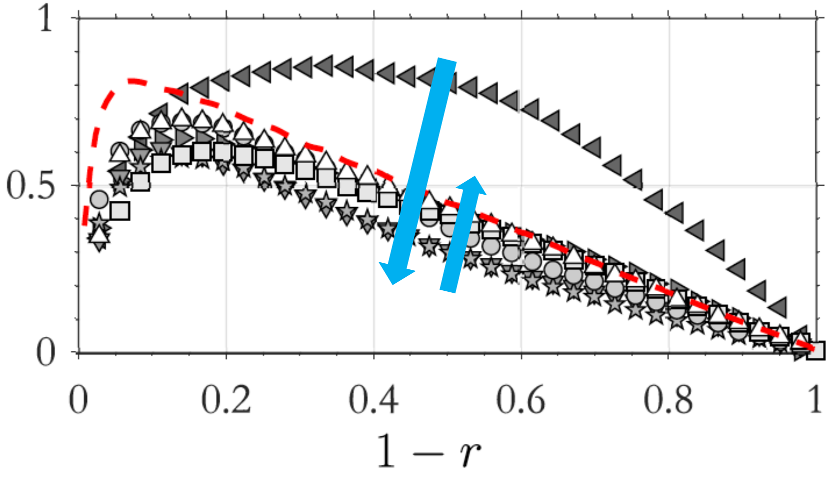

Rough to smooth step change

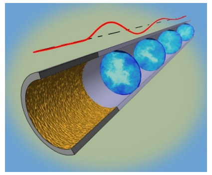

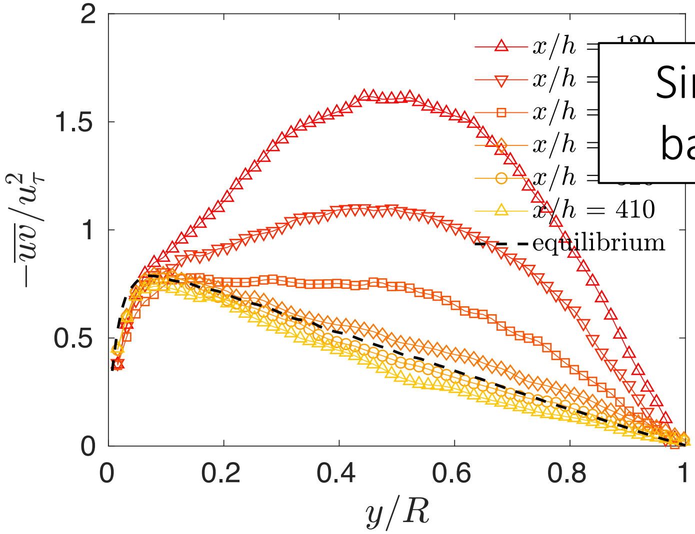

Single square bar h/R = 0.1

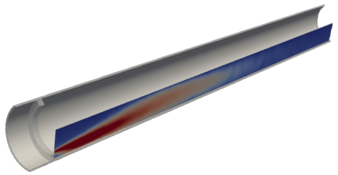

Short region of concave curvature

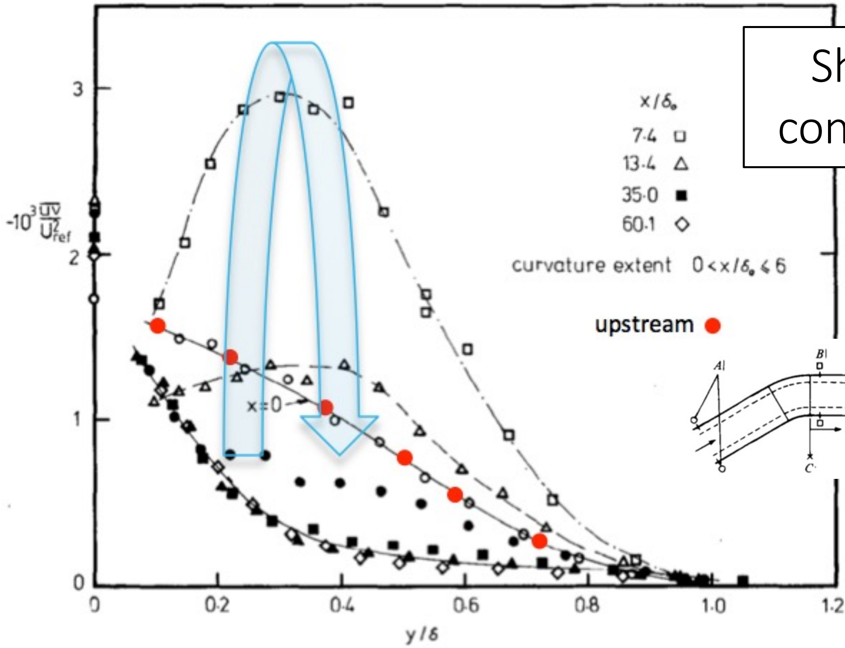

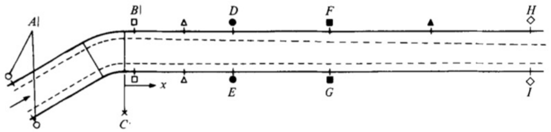

Smits, Young & Bradshaw (1979)

Another example of stress overshoot

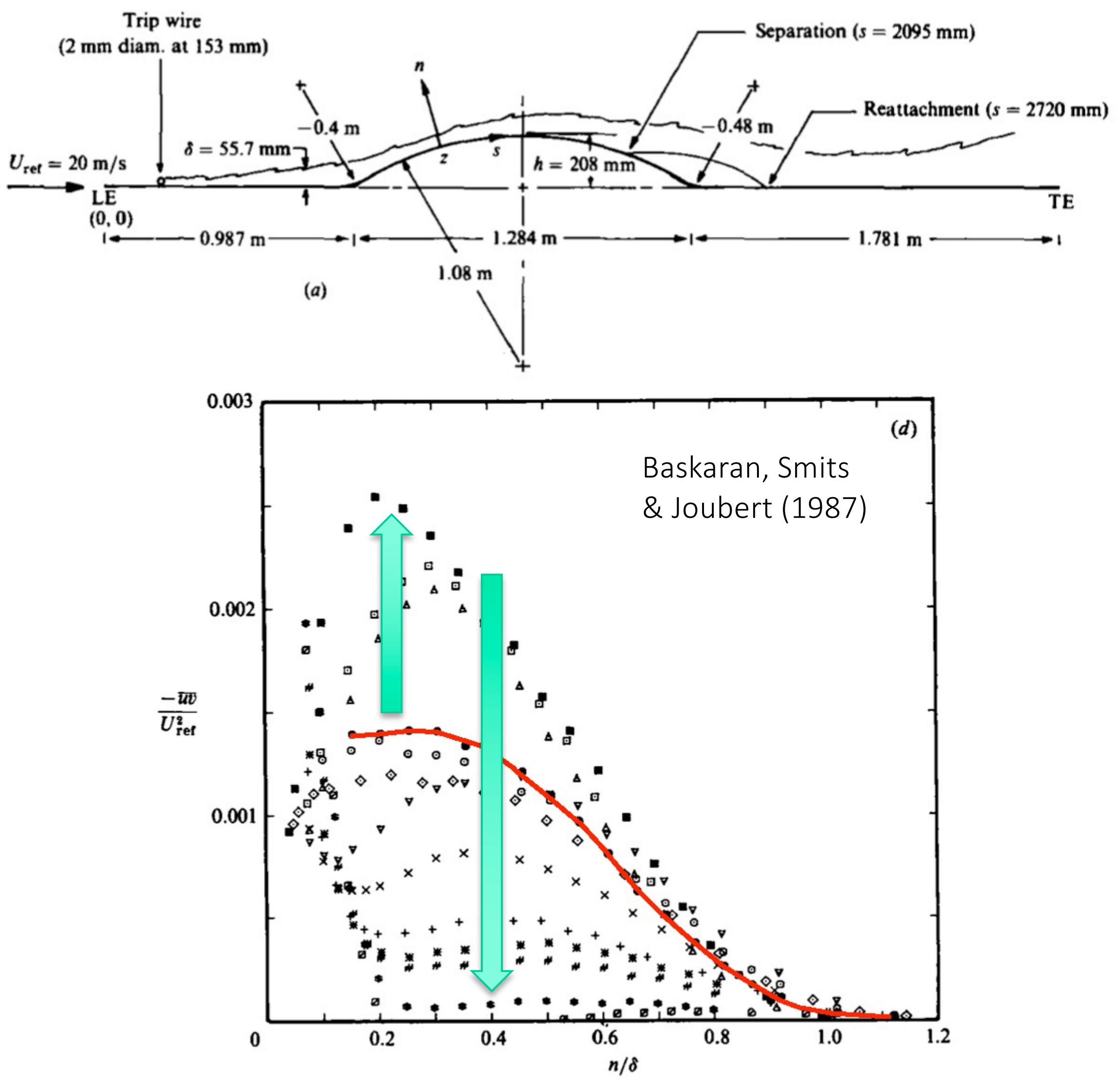

Short region of concave curvature followed by prolonged convex curvature and adverse pressure gradient

- Shear stress amplified by concave curvature, then collapses in outer region over convex curvature prior to separation

- Slow recovery from upstream disturbances (sometimes very slow)
- Successive pressure gradients do not add linearly

A model for non-monotonic recovery

$$\frac{\mathrm{D}U_x}{\mathrm{D}t} = -\frac{\partial P}{\partial x} - \frac{1}{r}\frac{\partial r\tau}{\partial r}$$

Remove P

$$\frac{\mathrm{D}}{\mathrm{D}t}\left(\frac{\partial U_x}{\partial r}\right) - \frac{U_r}{r}\frac{\partial U_x}{\partial r} = \frac{\tau}{r^2} - \frac{1}{r}\frac{\partial \tau}{\partial r} - \frac{\partial^2 \tau}{\partial r^2}$$

$$\frac{\mathrm{D}\tau}{\mathrm{D}t} = -\overline{u_r^2}\frac{\partial U_x}{\partial r} + \overline{p\left(\frac{\partial u_x}{\partial r} + \frac{\partial u_r}{\partial x}\right)}$$

Governing Eqs.

- Model pressure strain with using Rotta (1951), Crow (1968)
- Introduce perturbations for U_x and $\overline{u_x^2}$
- Assume shape-preserving disturbances, e.g., $\Delta\tau(x,r) = g(x)f(r)$

$$X = \frac{\partial \Delta U_x}{\partial r}$$

Second-order response

$$\boxed{\begin{aligned}\ddot{\mathrm{X}} + \left\{C_r U'_{x,0} - \frac{C^F_{PS}}{2} C_{tot} U'_{x,0} + \frac{C^S_{PS}}{2\mathcal{L}}\left[K_0^{\frac{1}{2}} + \frac{1}{4}K_0^{-\frac{1}{2}} C_{tot}\tau_0\right]\right\}\frac{1}{U_{x,0}}\dot{\mathrm{X}} \\ + \left(\overline{u^2_{r,0}} - C^F_{PS}K_0\right)\left(\frac{f}{r^2} - \frac{f'}{r} - f''\right)\frac{1}{fU^2_{x,0}}\mathrm{X} = 0,\end{aligned}}$$

Van Buren et al. (2020), Ding et al. (2021)

A model for non-monotonic recovery

$$\frac{\mathrm{D}U_x}{\mathrm{D}t} = -\frac{\partial P}{\partial x} - \frac{1}{r}\frac{\partial r\tau}{\partial r}$$

Remove P

$$\frac{\mathrm{D}}{\mathrm{D}t}\left(\frac{\partial U_x}{\partial r}\right) - \frac{U_r}{r}\frac{\partial U_x}{\partial r} = \frac{\tau}{r^2} - \frac{1}{r}\frac{\partial \tau}{\partial r} - \frac{\partial^2 \tau}{\partial r^2}$$

$$\frac{\mathrm{D}\tau}{\mathrm{D}t} = -\overline{u_r^2}\frac{\partial U_x}{\partial r} + \overline{p\left(\frac{\partial u_x}{\partial r} + \frac{\partial u_r}{\partial x}\right)}$$

Governing Eqs.

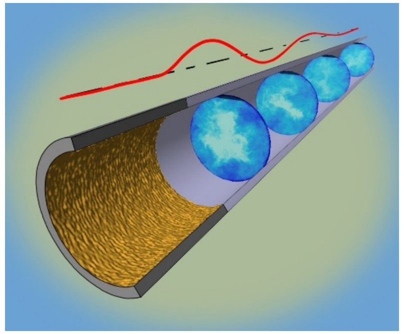

- Model pressure strain with using Rotta (1951), Crow (1968)
- Introduce perturbations for U_x and $\overline{u_x^2}$
- Assume shape-preserving disturbances, e.g., $\Delta\tau(x,r) = g(x)f(r)$

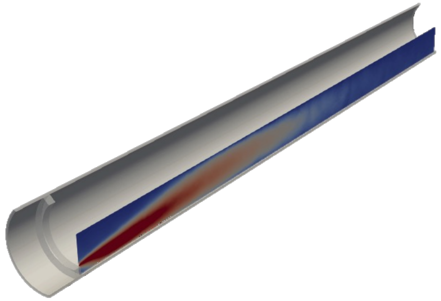

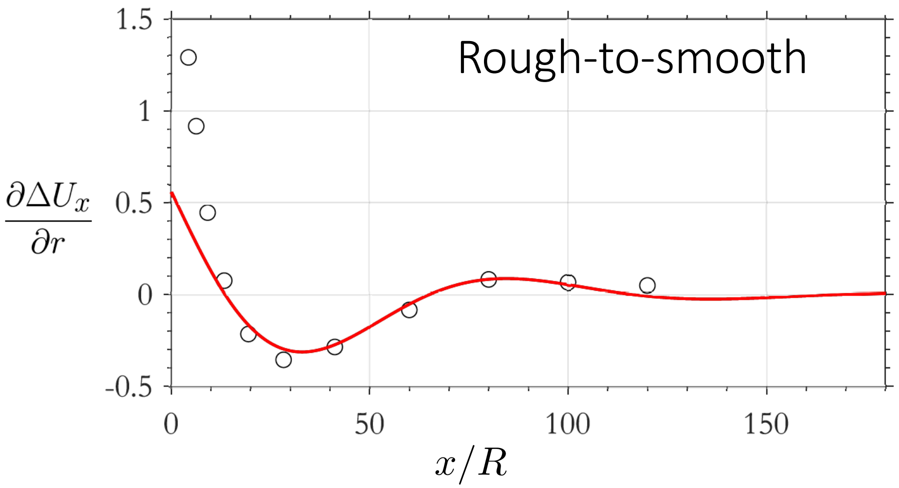

Square bar response

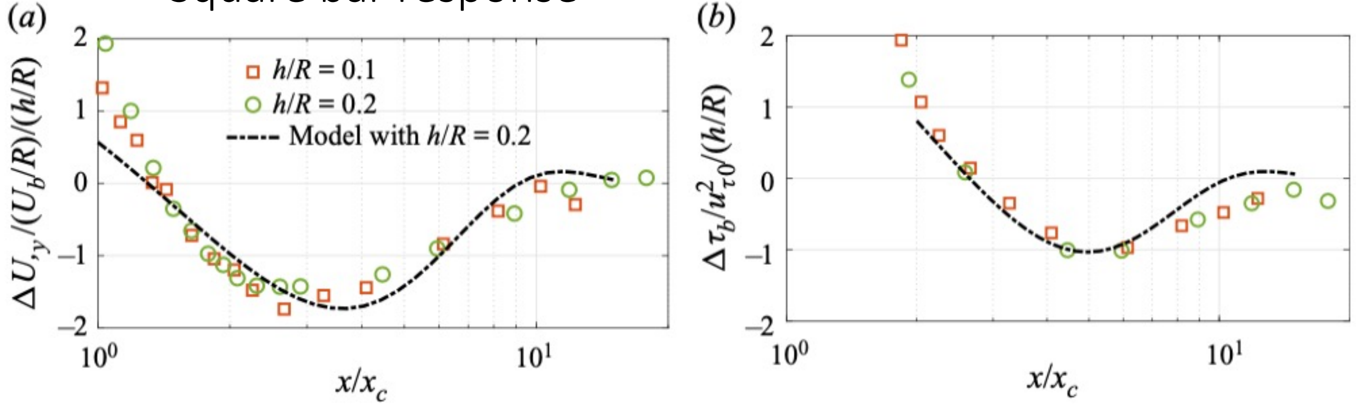

Van Buren et al. (2020), Ding et al. (2021)

Opportunities for flow control?

- Perturbed flows are very slow to recover
- Typically exhibit a second-order response
- Overshoots are associated with production “trapping”
- Can these observations be used in flow control?

3. POD inspired turbulence control in pipes

- The use of a varying spanwise Reynolds stress may be used to enhance (increase mixing) or suppress (reduce losses) specific turbulence structures
- Target the most energetic POD mode (m=3, 15.5%)

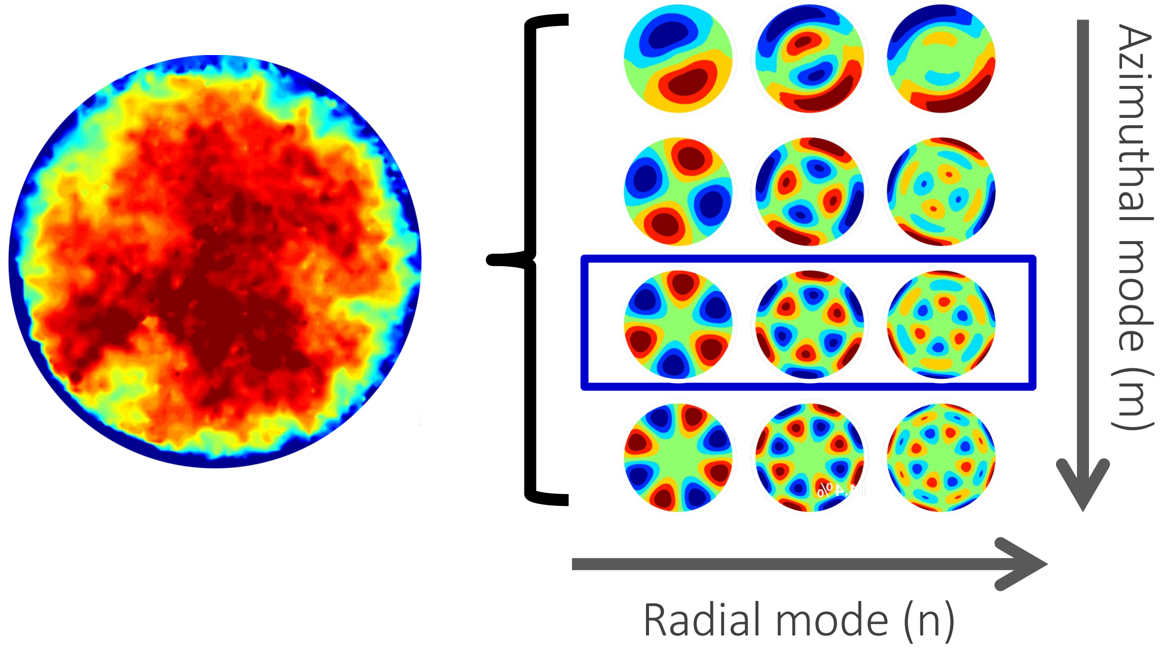

Van Buren, T., Hellström, L. H. O., Marusic, I.. and Smits, A. J., "Turbulent pipe flow response to wall changes targeting specific azimuthal modes," TSFP-10, Chicago IL, July 2017.

Experimental setup

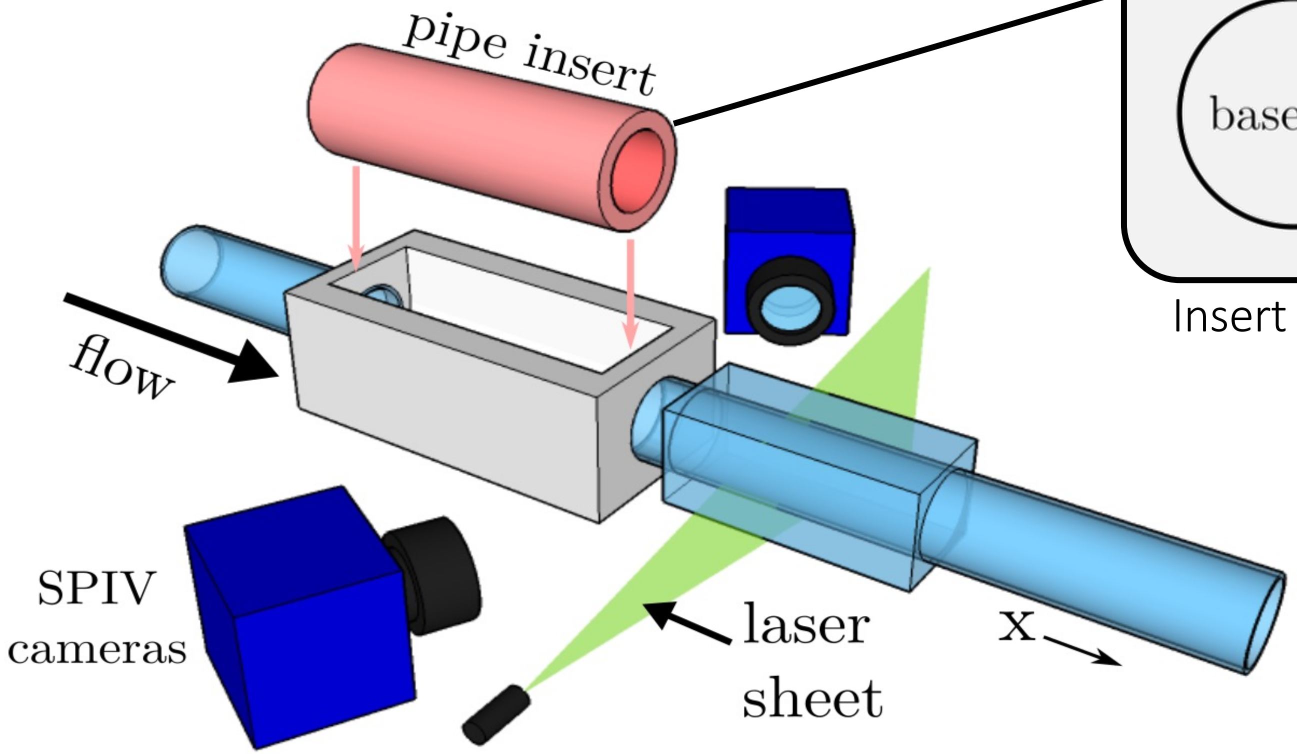

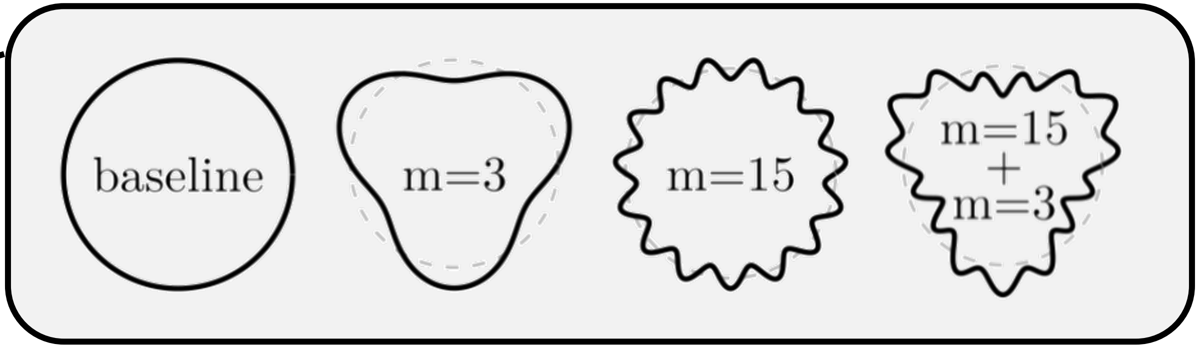

Insert cross sections

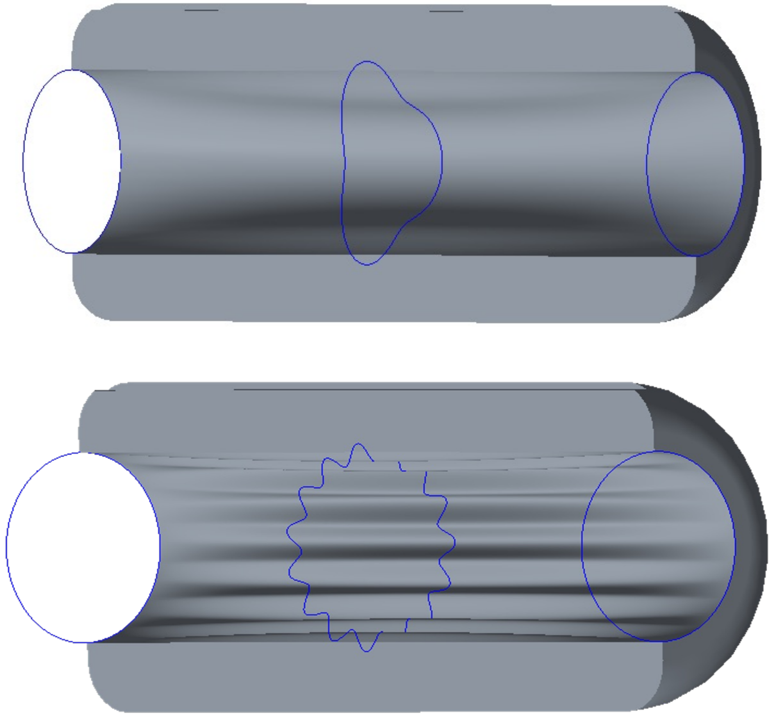

Re_D = 158,600
Re_τ = 3,486

Gradual streamwise changes

Streamwise development: mean velocity

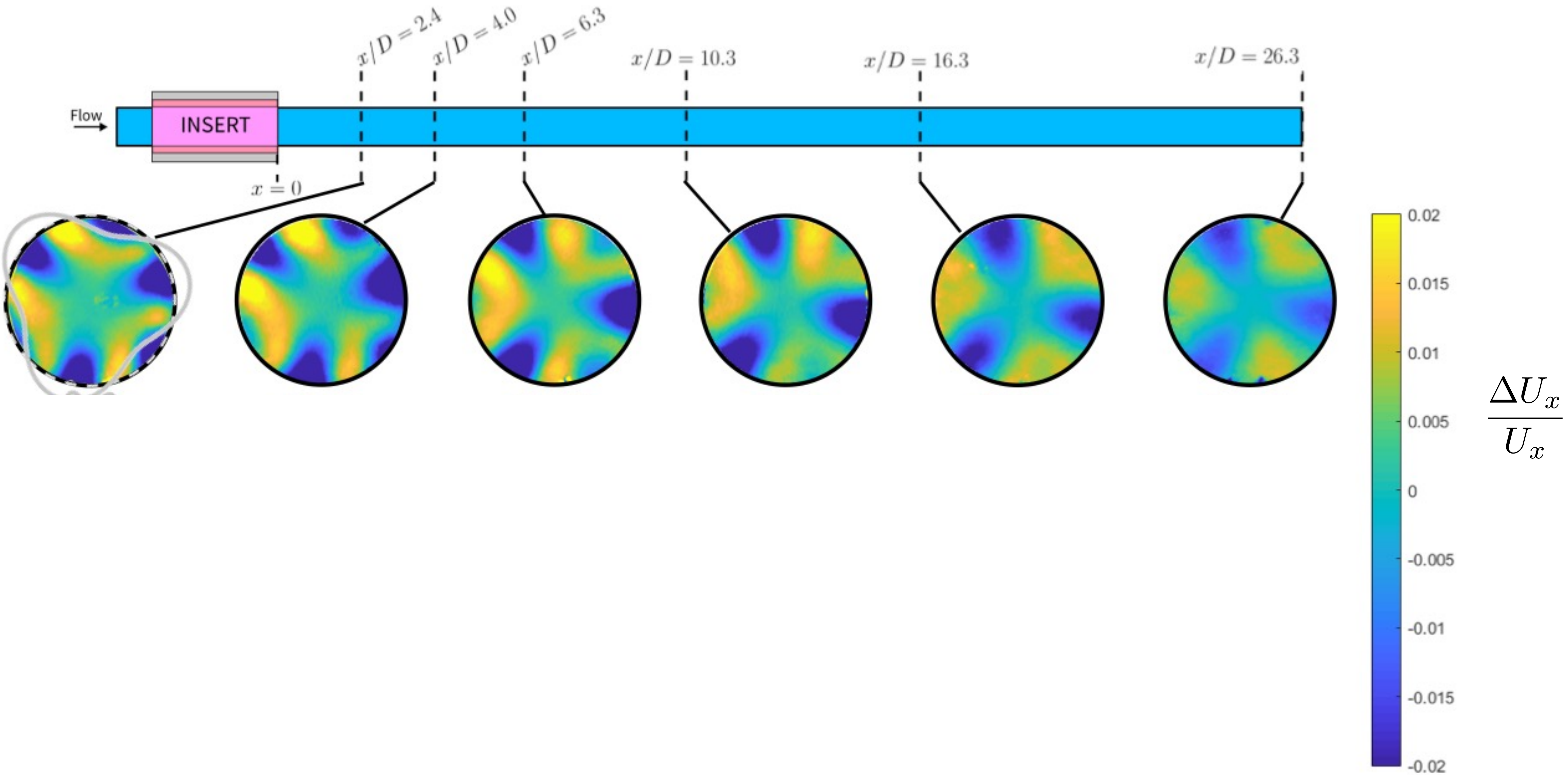

Streamwise development: mean velocity

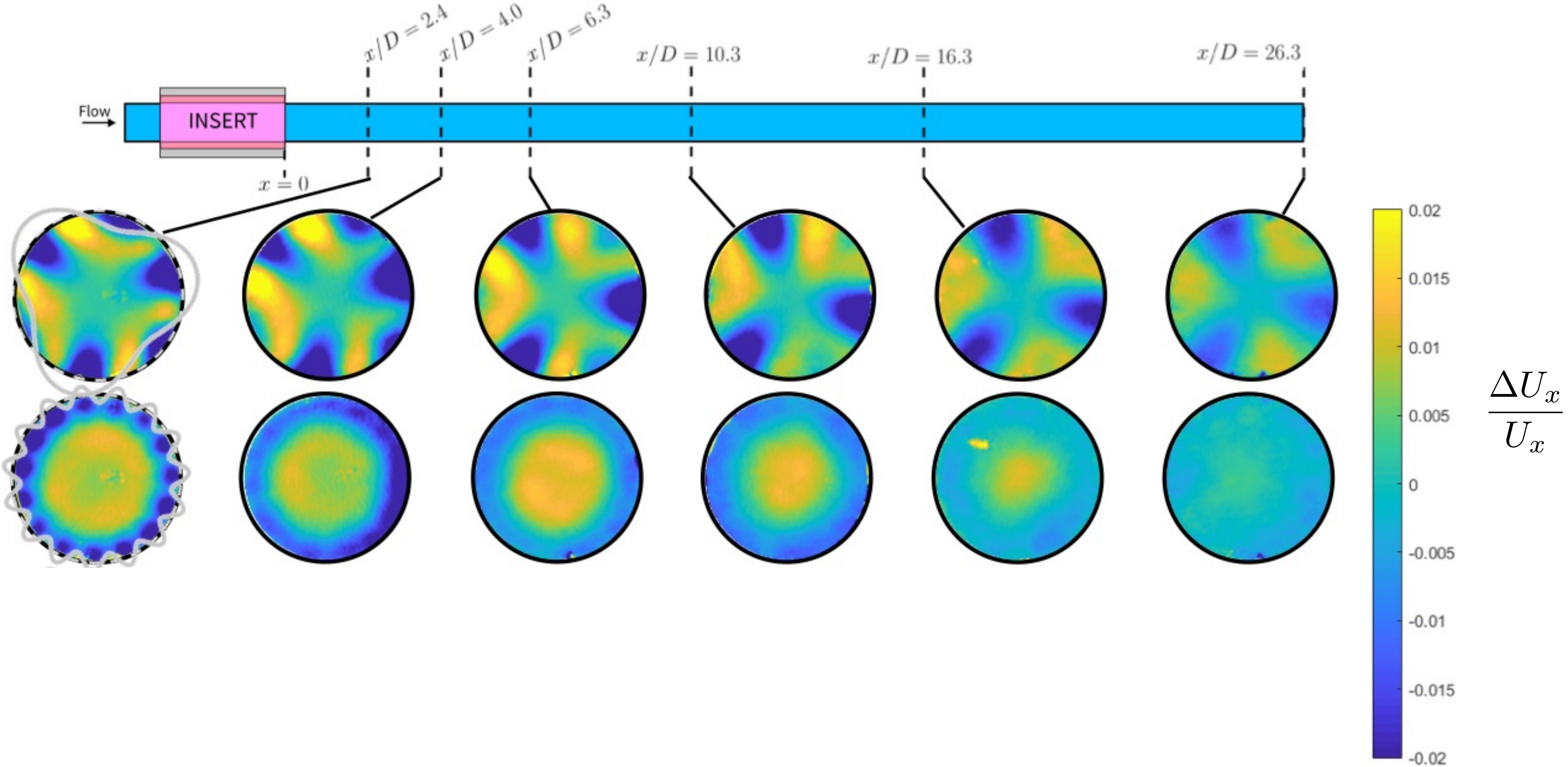

Streamwise development: mean velocity

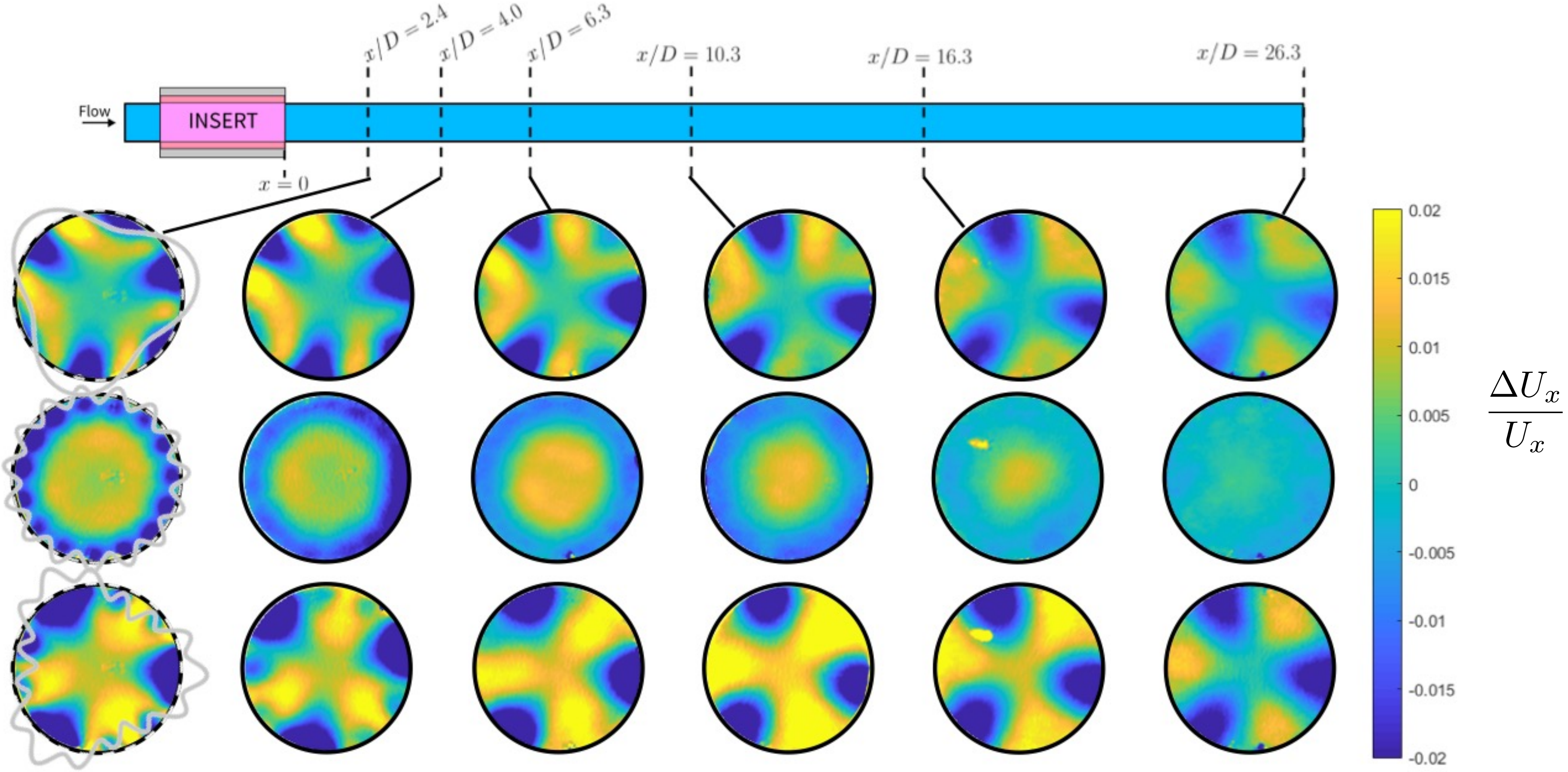

Streamwise development: TKE

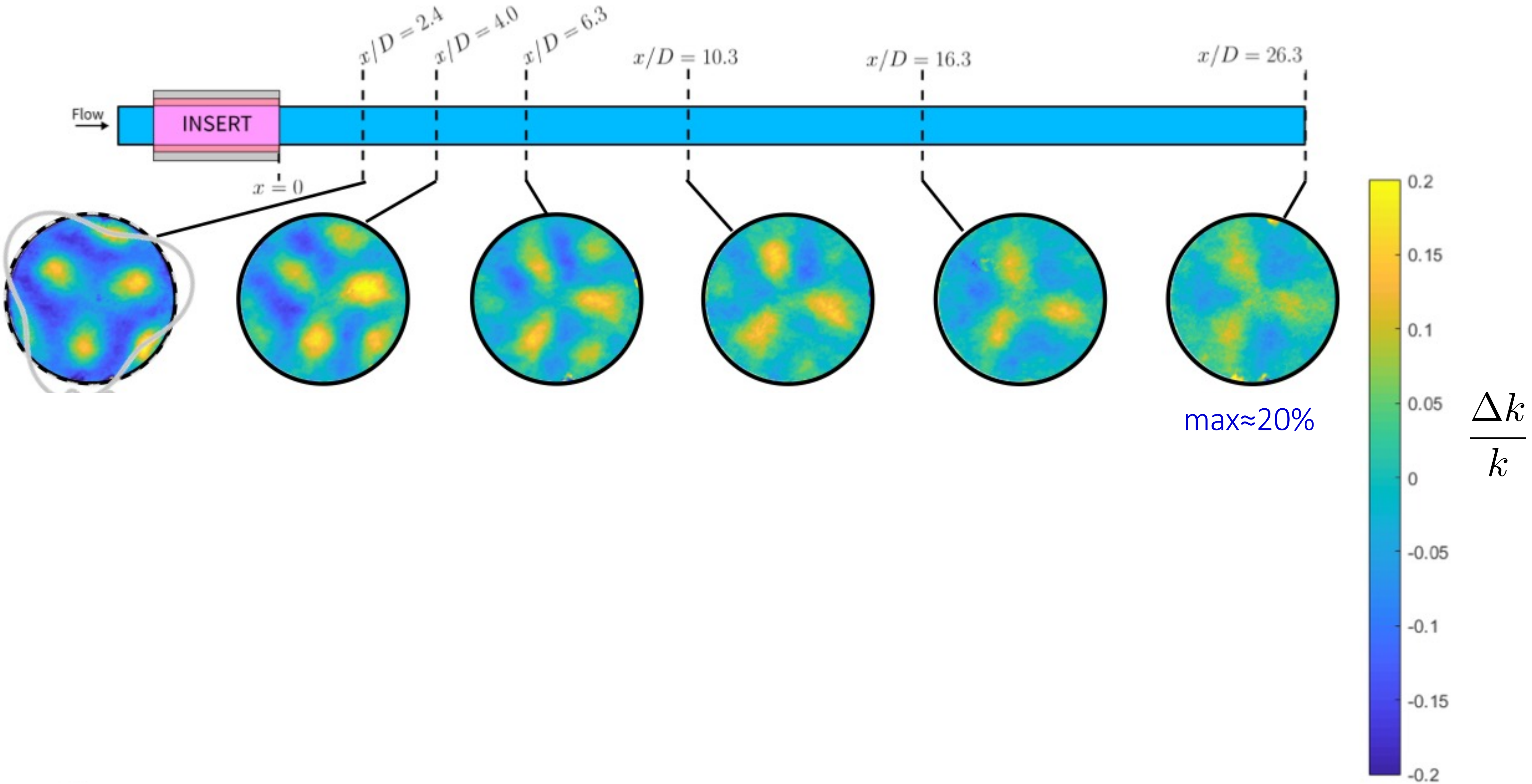

Streamwise development: TKE

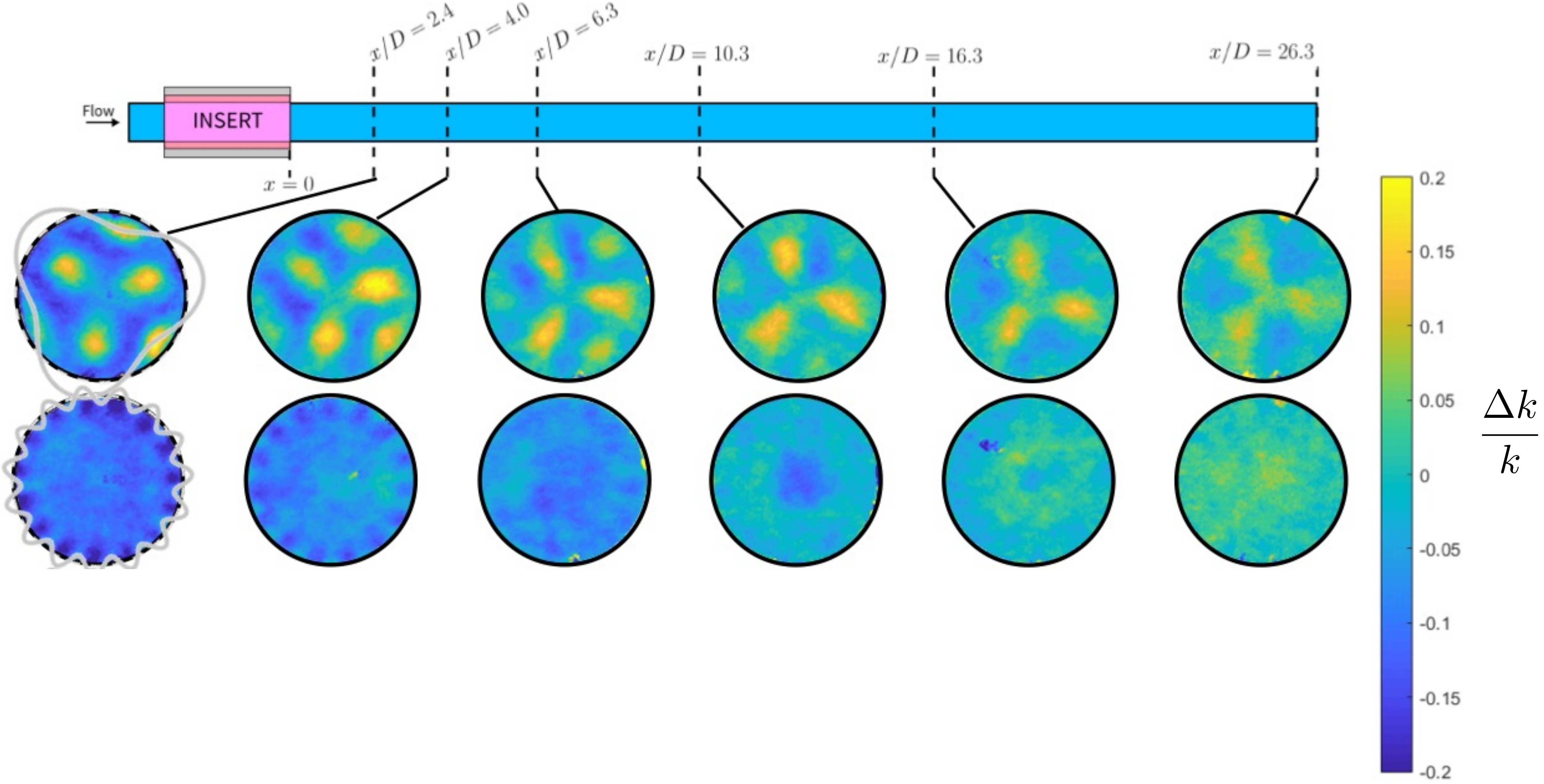

Streamwise development: TKE

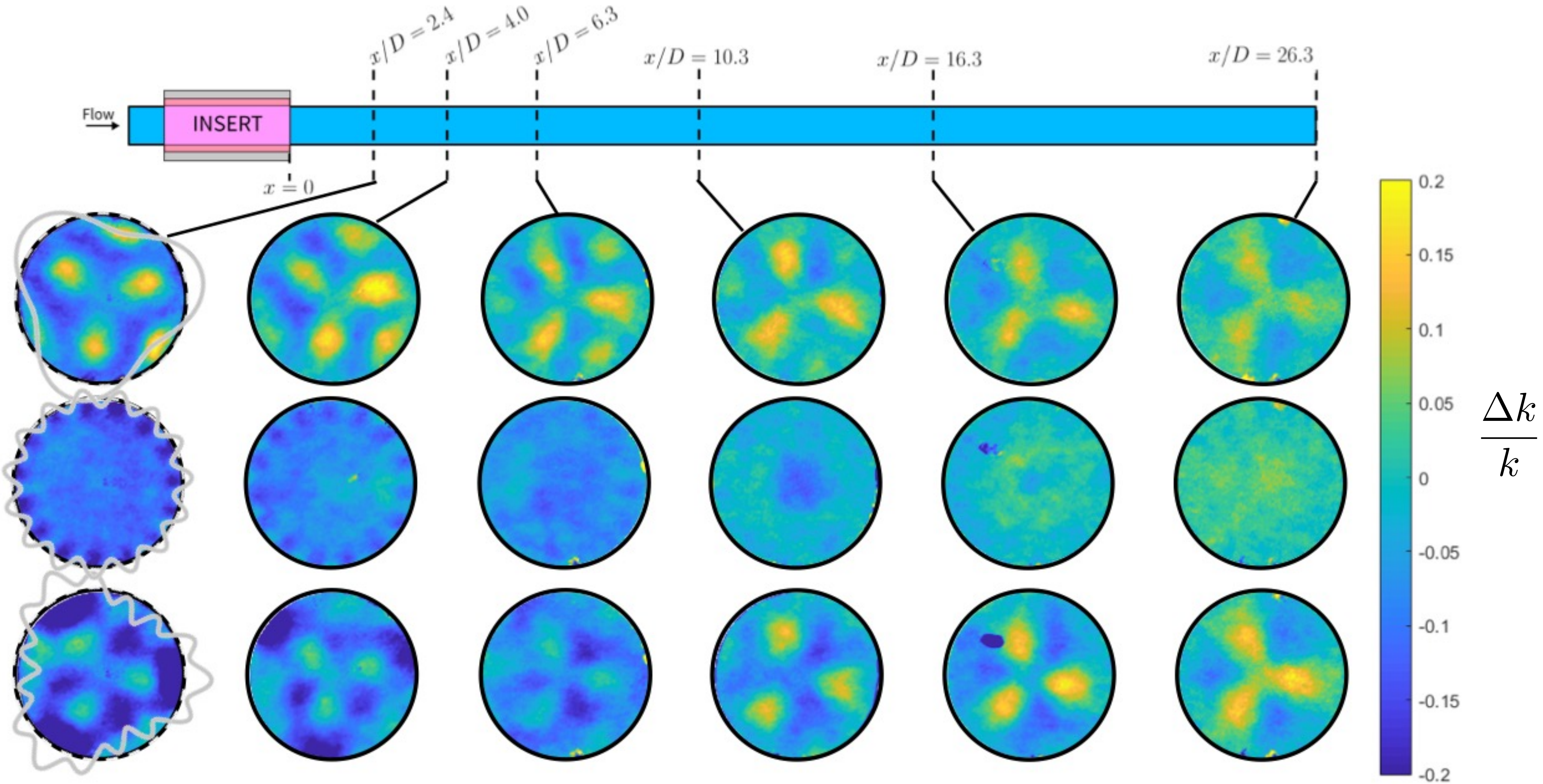

Observations

Able to create specific flow “shapes” in the mean statistics

Very little impact on mean for relatively large impact on the turbulence

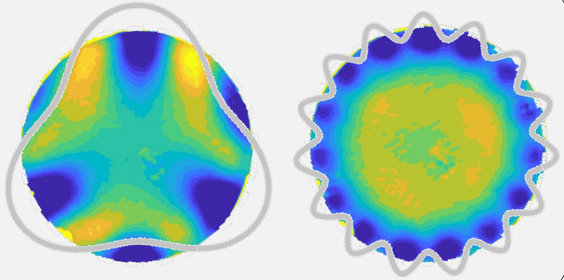

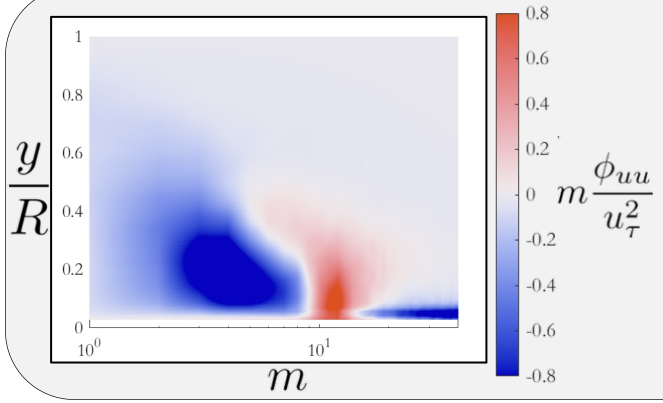

No single spikes in modes, more clouds of impact in the targeted region

Inserts act more like barriers to modes above or below the target

Inserts have long lasting impact, 30D downstream there is still 20% change in turbulence from equilibrium

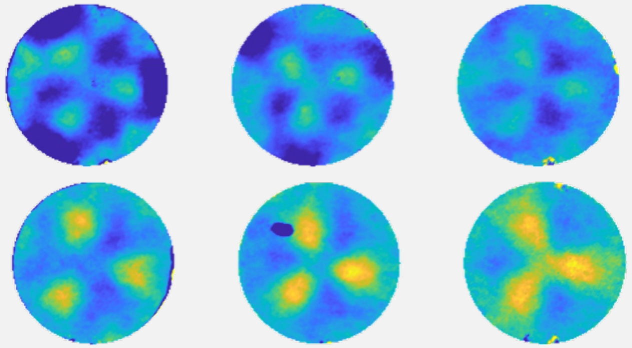

4. Active flow control by transverse wall oscillation

- A promising approach to drag reduction is transverse wall oscillation

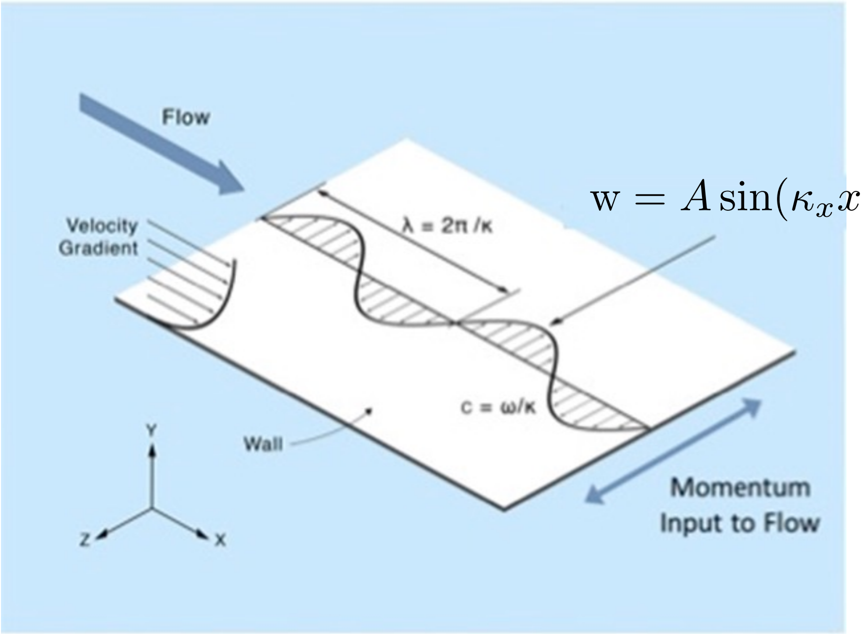

$$\mathrm{w} = A\sin(\kappa_x x - \omega t)$$

$$A^+ = \frac{\omega d}{u_\tau}, \qquad T^+_{osc} = \frac{2\pi}{\omega^+} = \frac{2\pi u_\tau^2}{\omega \nu}, \qquad \kappa_x^+ = \frac{\kappa_x \nu}{u_\tau}$$

4. Active flow control by transverse wall oscillation

- A promising approach to drag reduction is transverse wall oscillation

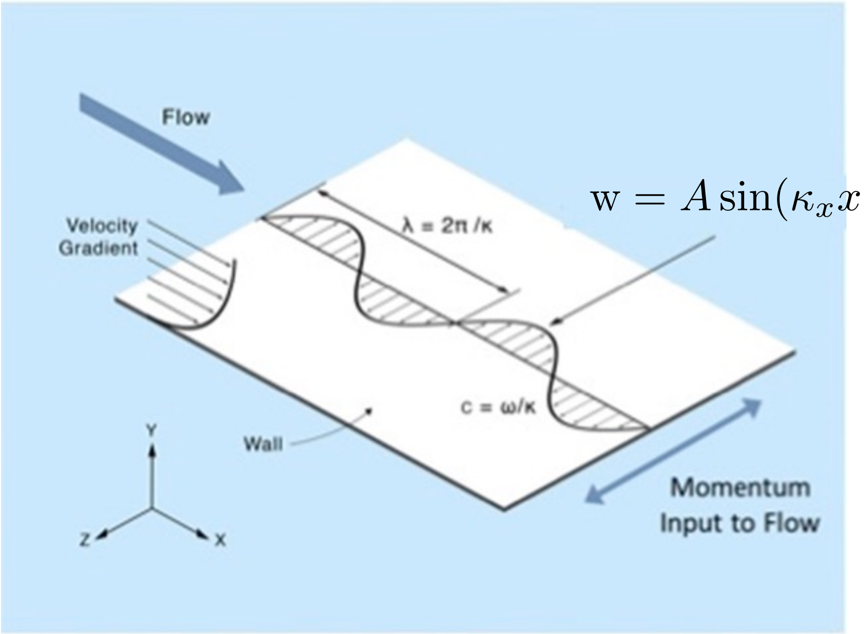

$$\mathrm{w} = A\sin(\kappa_x x - \omega t)$$

$$A^+ = \frac{\omega d}{u_\tau}, \qquad T^+_{osc} = \frac{2\pi}{\omega^+} = \frac{2\pi u_\tau^2}{\omega\nu}, \qquad \kappa_x^+ = \frac{\kappa_x \nu}{u_\tau}$$

- Gatti and Quadrio (2016, etc.) mapped actuation parameter space for low Re_τ (<1000) using DNS

$$DR_{max} = 39\% \quad (Re_\tau = 1000)$$

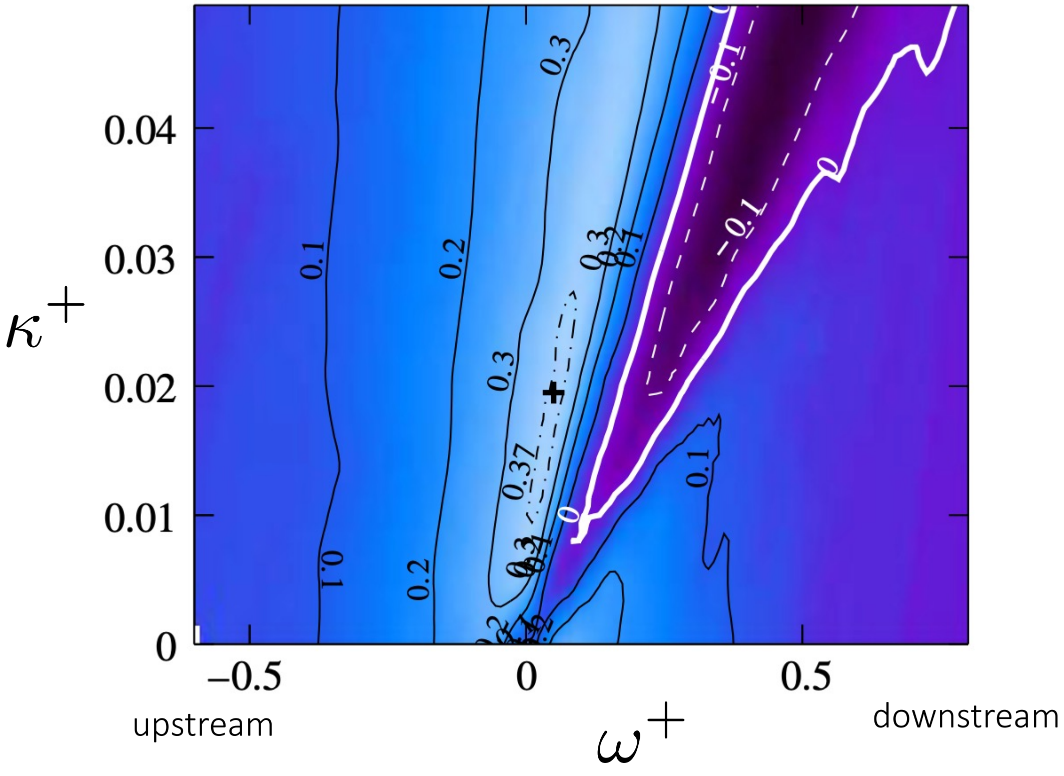

Reynolds number dependence

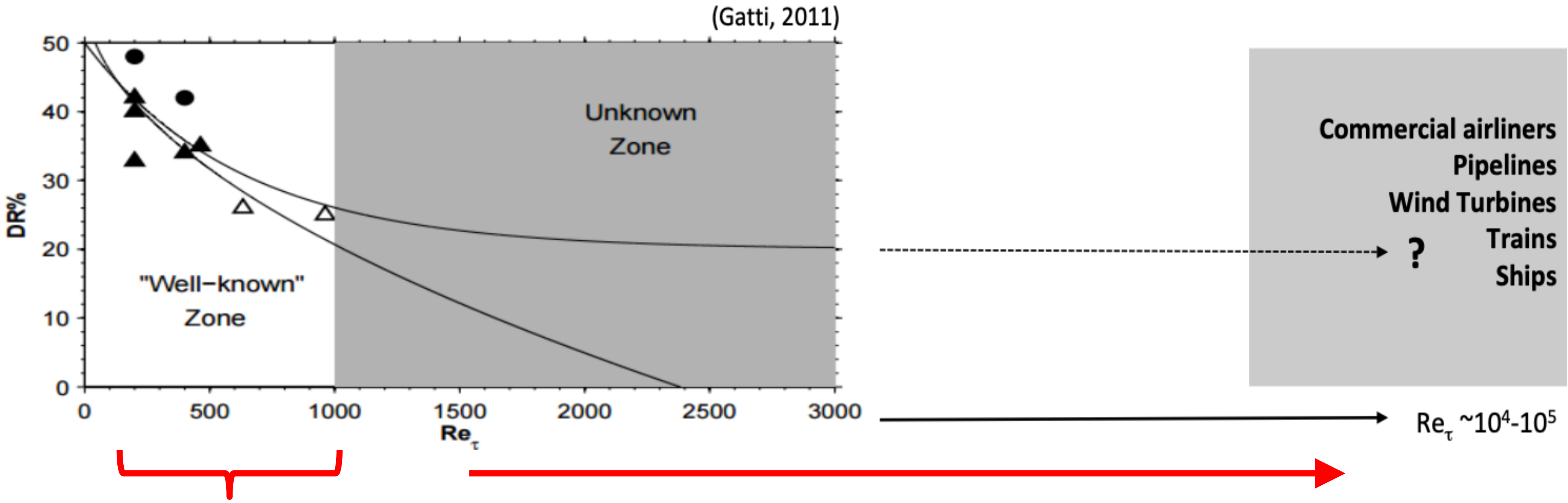

Small scales dominate drag

Large scales emerge and become increasingly important

Can we use wall oscillation to get meaningful drag reduction at high Reynolds number?

Transverse wall oscillation experiment

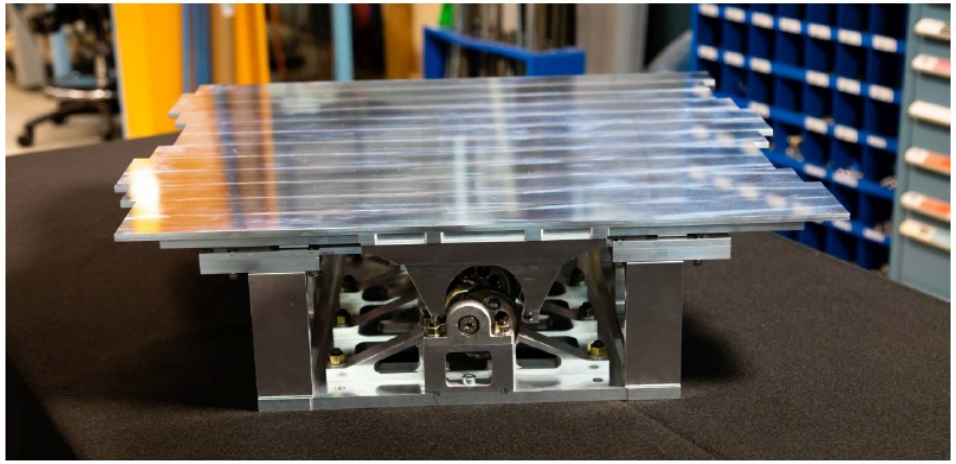

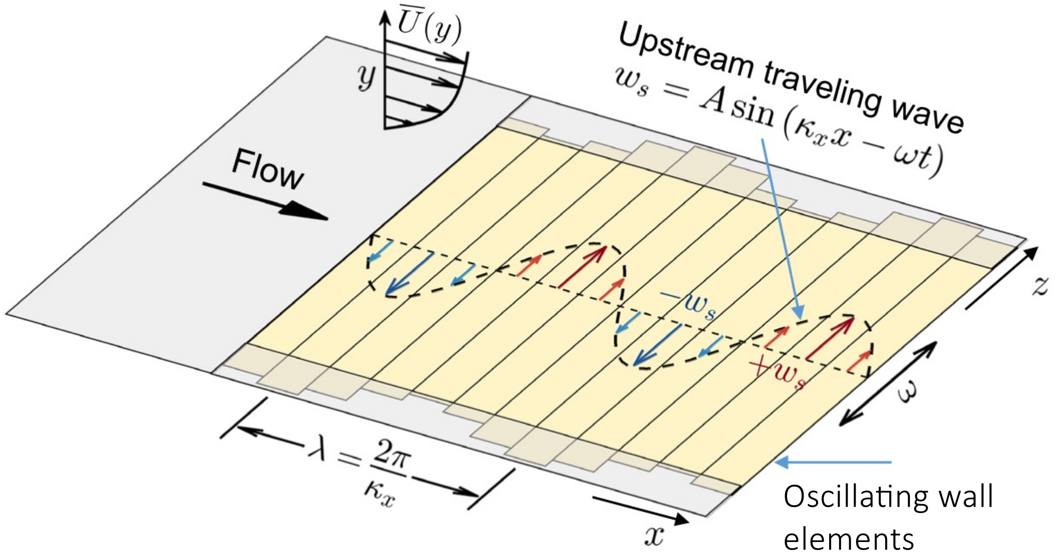

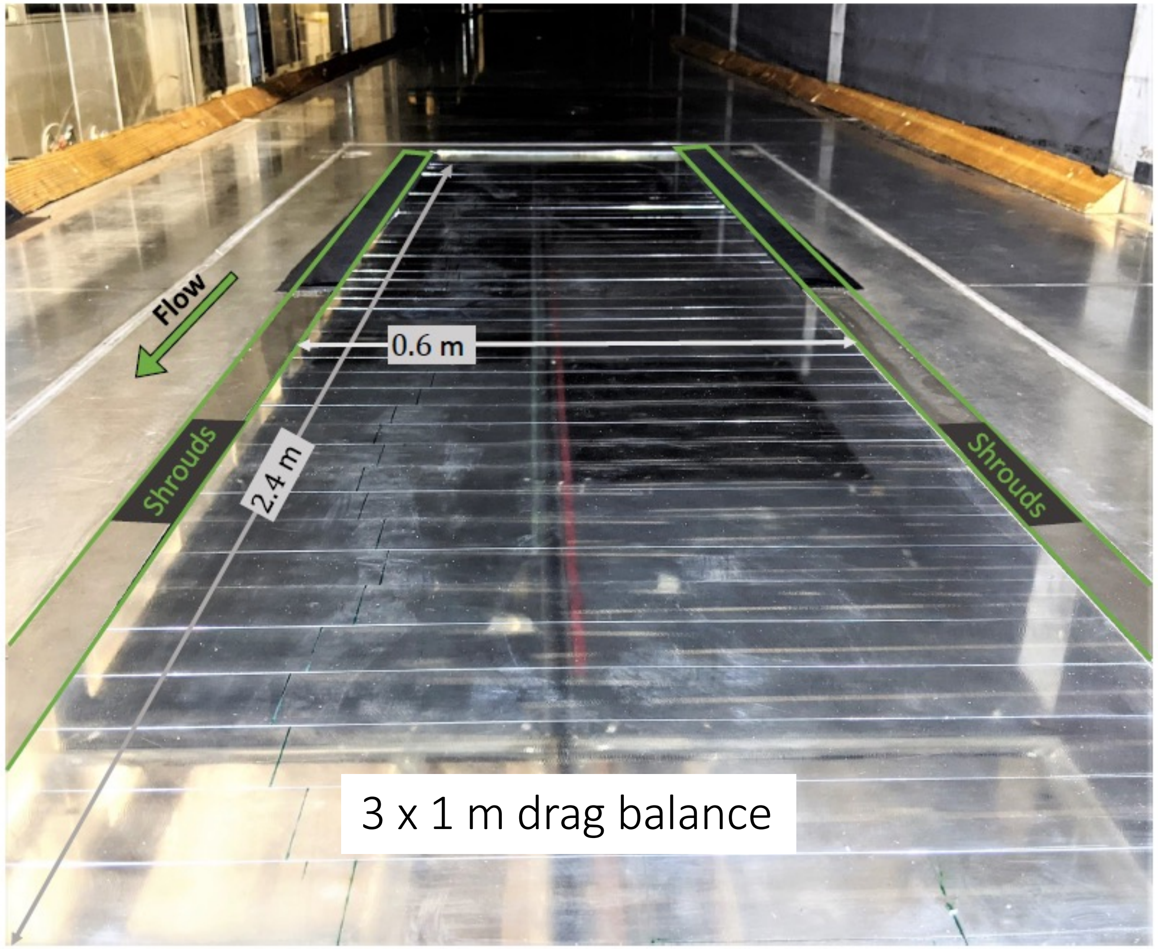

Melbourne wind tunnel at x = 21m

Marusic, Chandran, Rouhi, Fu, Wine, Holloway, Chung, Smits, Nature Communications, 2021

Used only upstream traveling wave (up to 25 Hz)

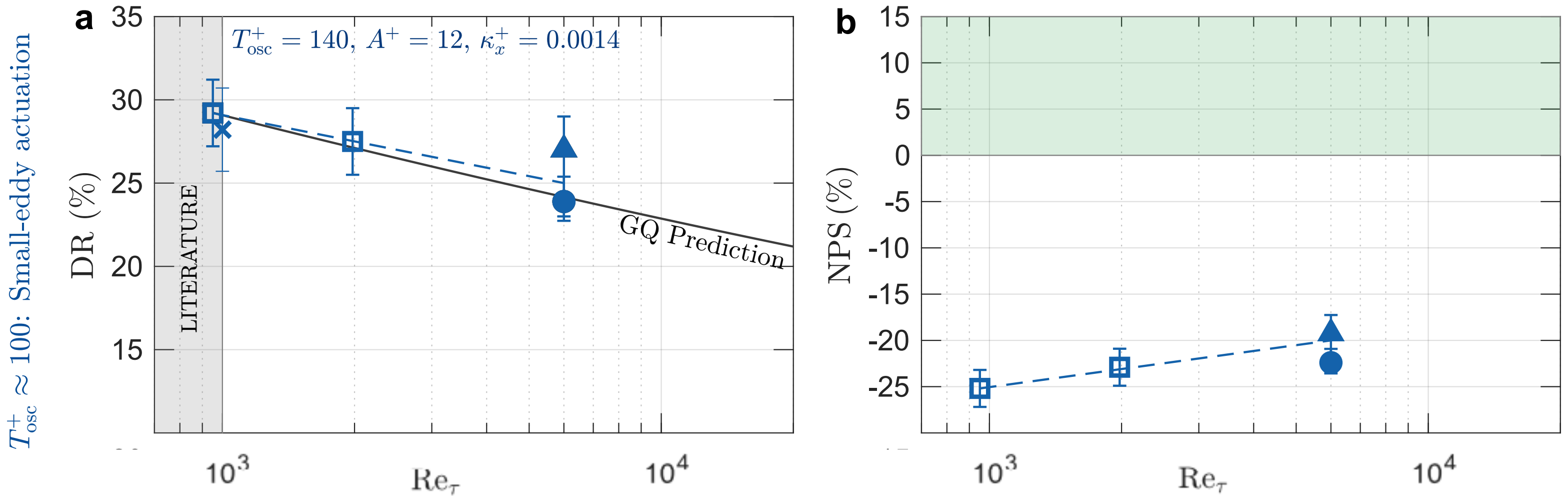

T+ ≈ 100

NPS = relative change in the total power cost between an oscillating wall and its stationary counterpart for an idealized actuator

“Inner-scale actuation”

Our experiments and LES follow Gatti & Quadrio (2016) prediction:
DR decreases with Reynolds number

<u>NPS is not possible</u>

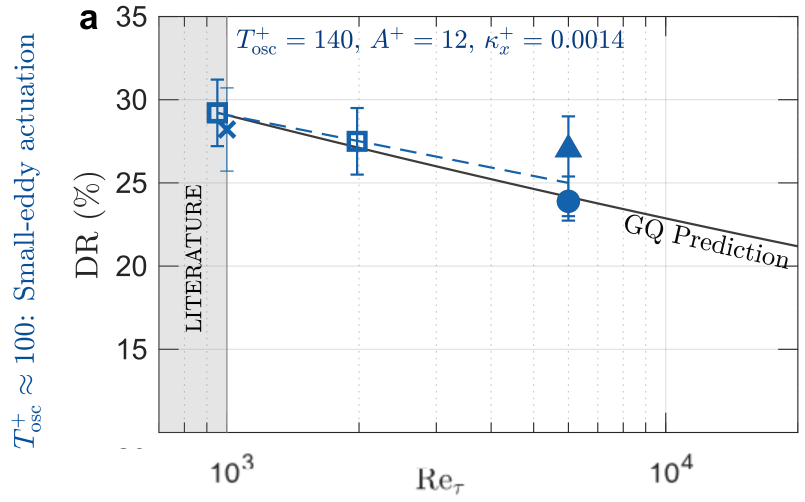

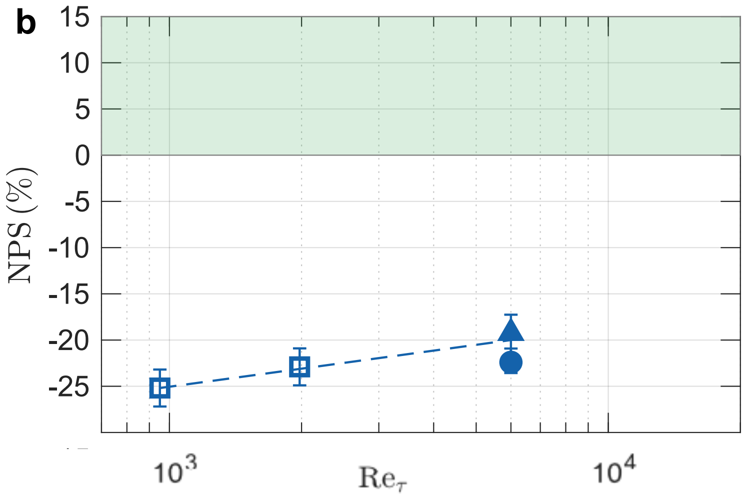

“Inner-scale actuation”

Our experiments and LES follow Gatti & Quadrio (2016) prediction:
DR decreases with Reynolds number

NPS is not possible

T+ ≈ 100

NPS = relative change in the total power cost between an oscillating wall and its stationary counterpart for an idealized actuator

T+ > 350

“Outer-scale actuation”

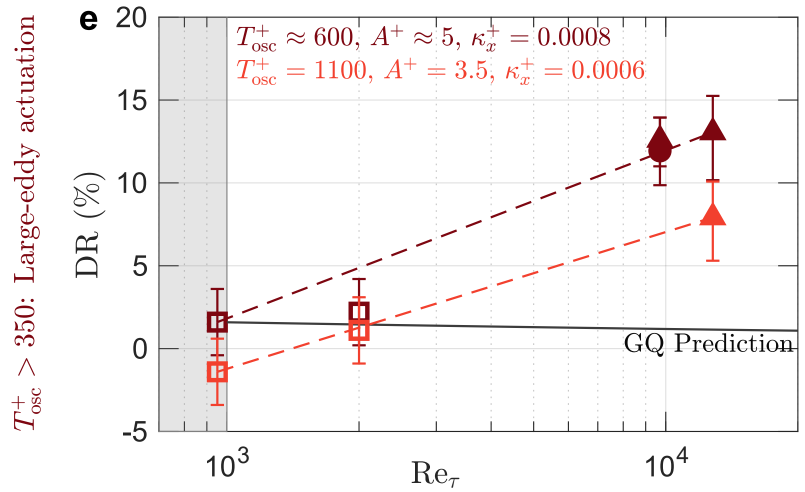

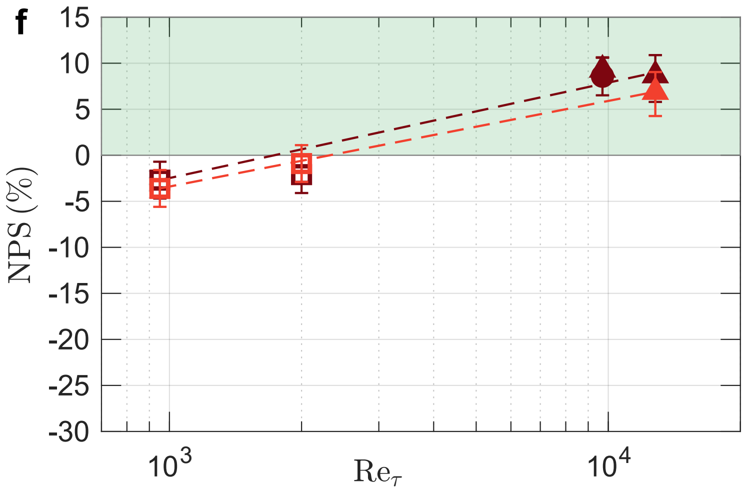

Our experiments and LES do not follow Gatti & Quadrio (2016) prediction:
DR increases with Reynolds number

NPS is possible

An energy-efficient pathway to turbulent drag reduction

Effects on wall stress

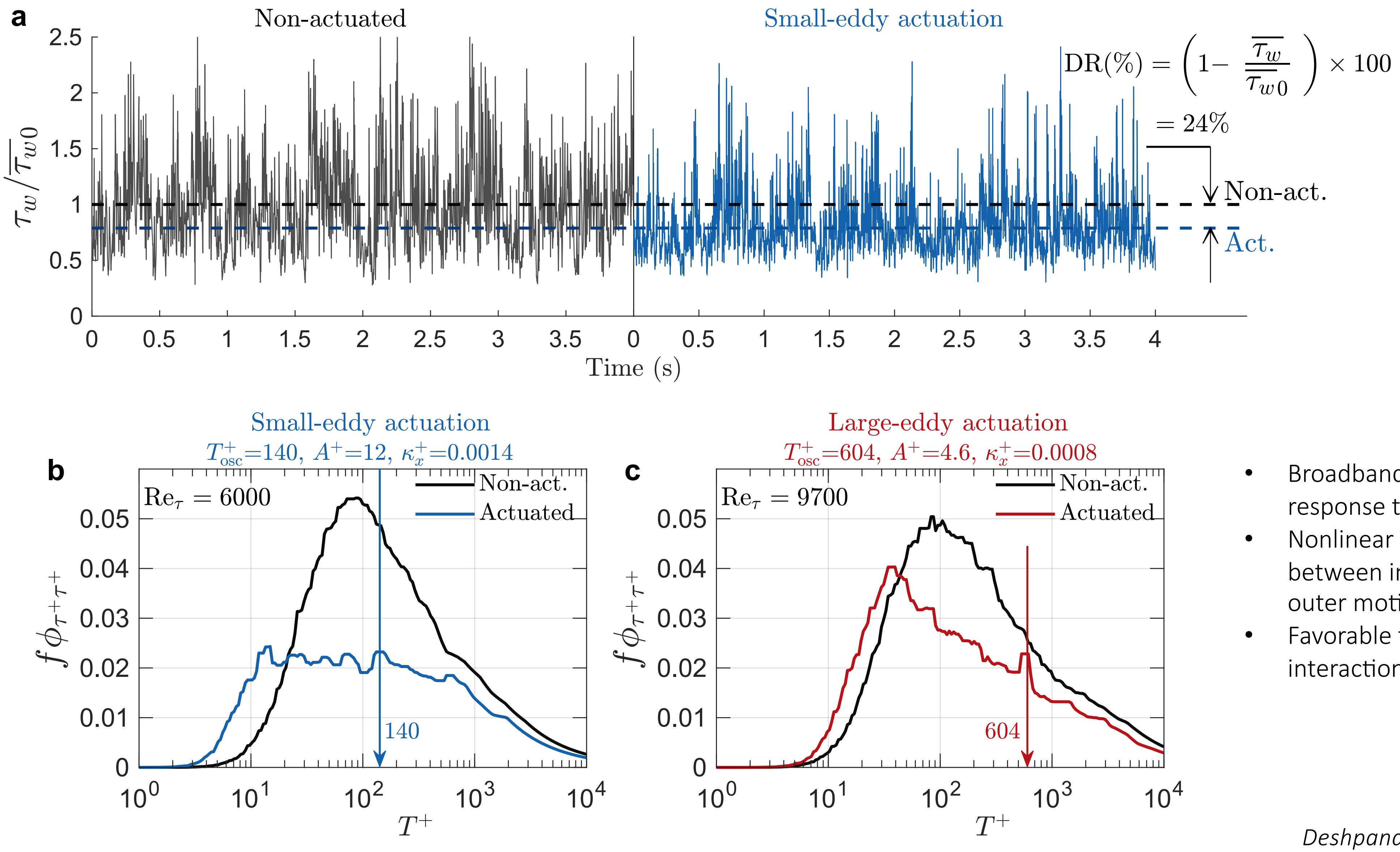

Pre-multiplied shear stress spectra

τ'_w

- Broadband frequency response to forcing
- Nonlinear interactions between inner and outer motions
- Favorable triadic interactions

Deshpande et al. 2023

5. Flow control using liquid-infused surfaces

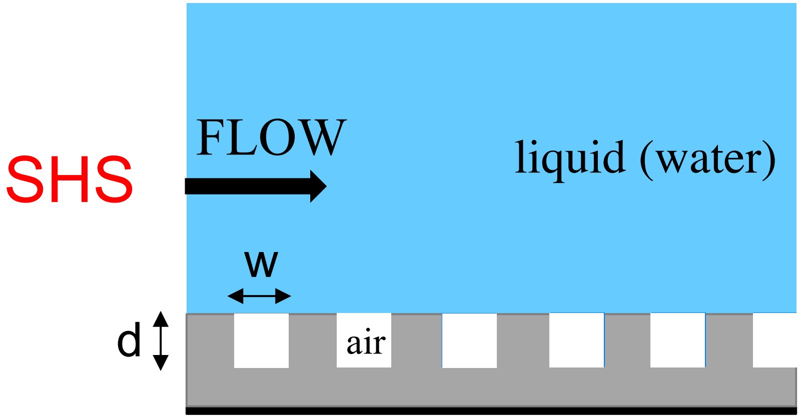

"LOTUS LEAF"

SHS: Superhydrophobic surface

air/water interface

5. Flow control using liquid-infused surfaces

SHS

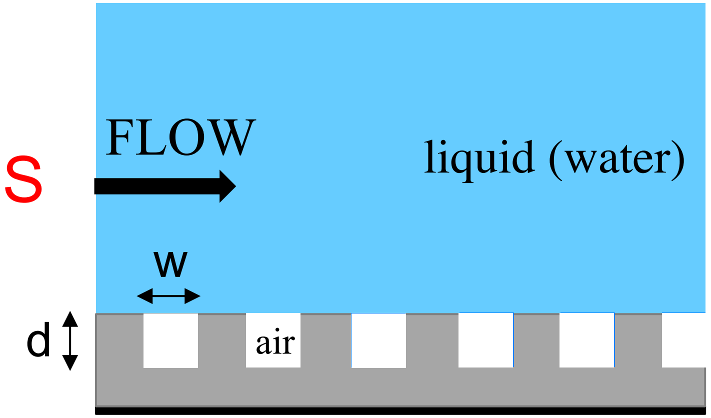

"LOTUS LEAF"

SHS: Superhydrophobic surface

air/water interface

SLIPS

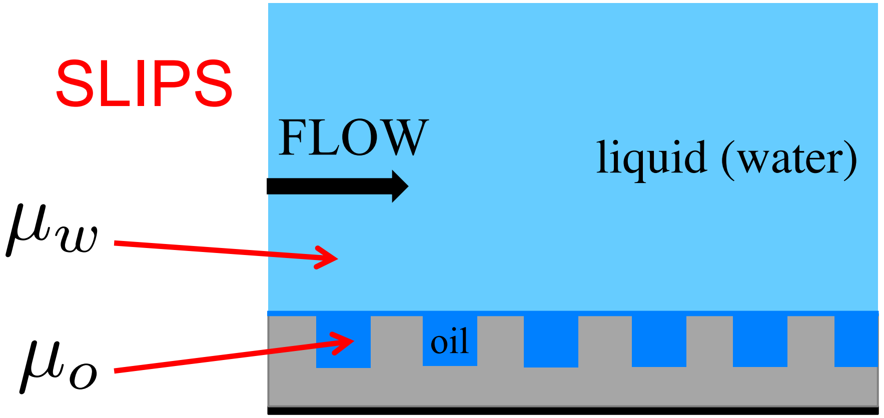

"PITCHER PLANT"

SLIPS: Slippery Liquid-Infused Porous Surface

oil/water interface

$$N = \frac{\mu_w}{\mu_o}$$

$N = O(1)$ for SLIPS drag reduction

$N = 50$ for SHS

Turbulent Taylor-Couette experiments

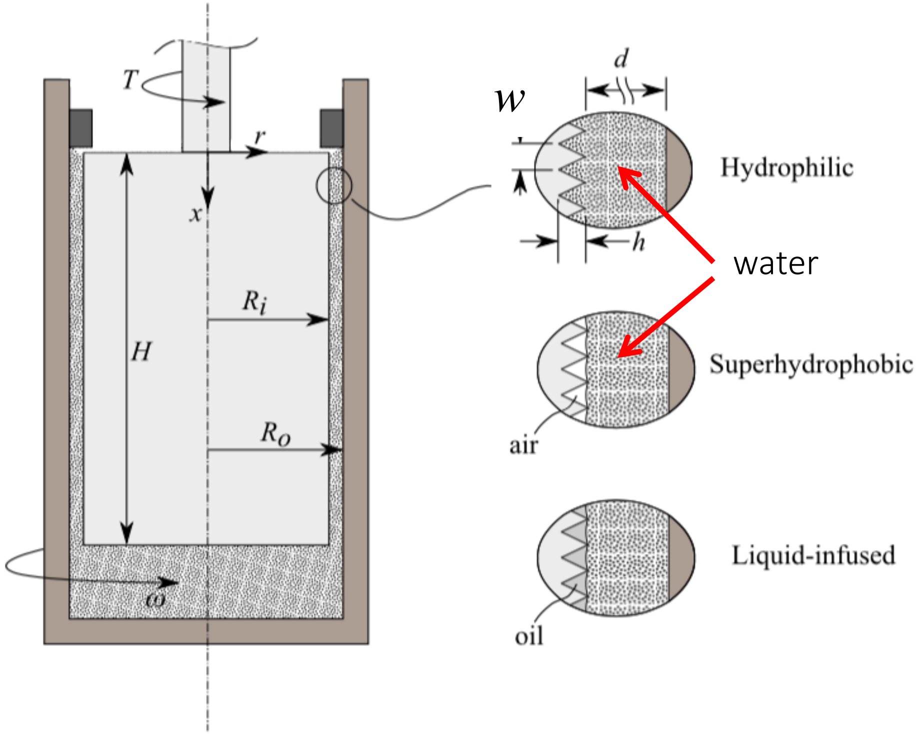

(a)

Taylor-Couette experiments on grooved surfaces

106 μm pitch

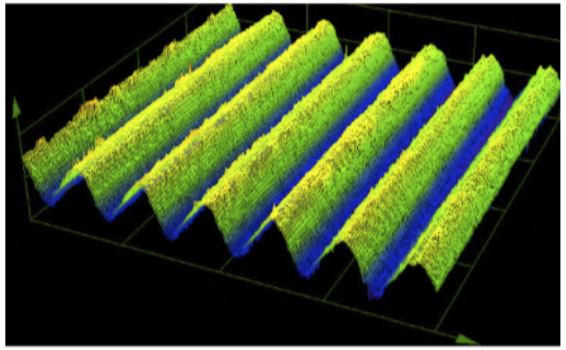

(b)

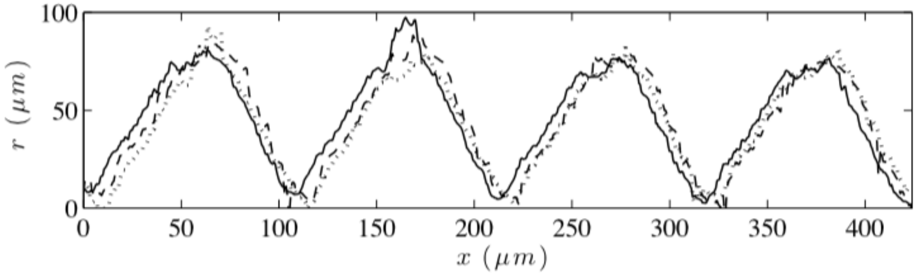

(c)

w = 106 μm (width)

Rosenberg, Van Buren, Fu & Smits (2016)

Drag measurements

	Impregnating fluid	Surface functionalization	μ_w/μ_o	
◇	Dupont Krytox GPL-101	fluorinated	0.033	◇
△	3M Fluorinert FC-3283	fluorinated	0.66	△
☆	Heptane	OTS	2.7	☆
□	Air	fluorinated	50 (SHS)	□

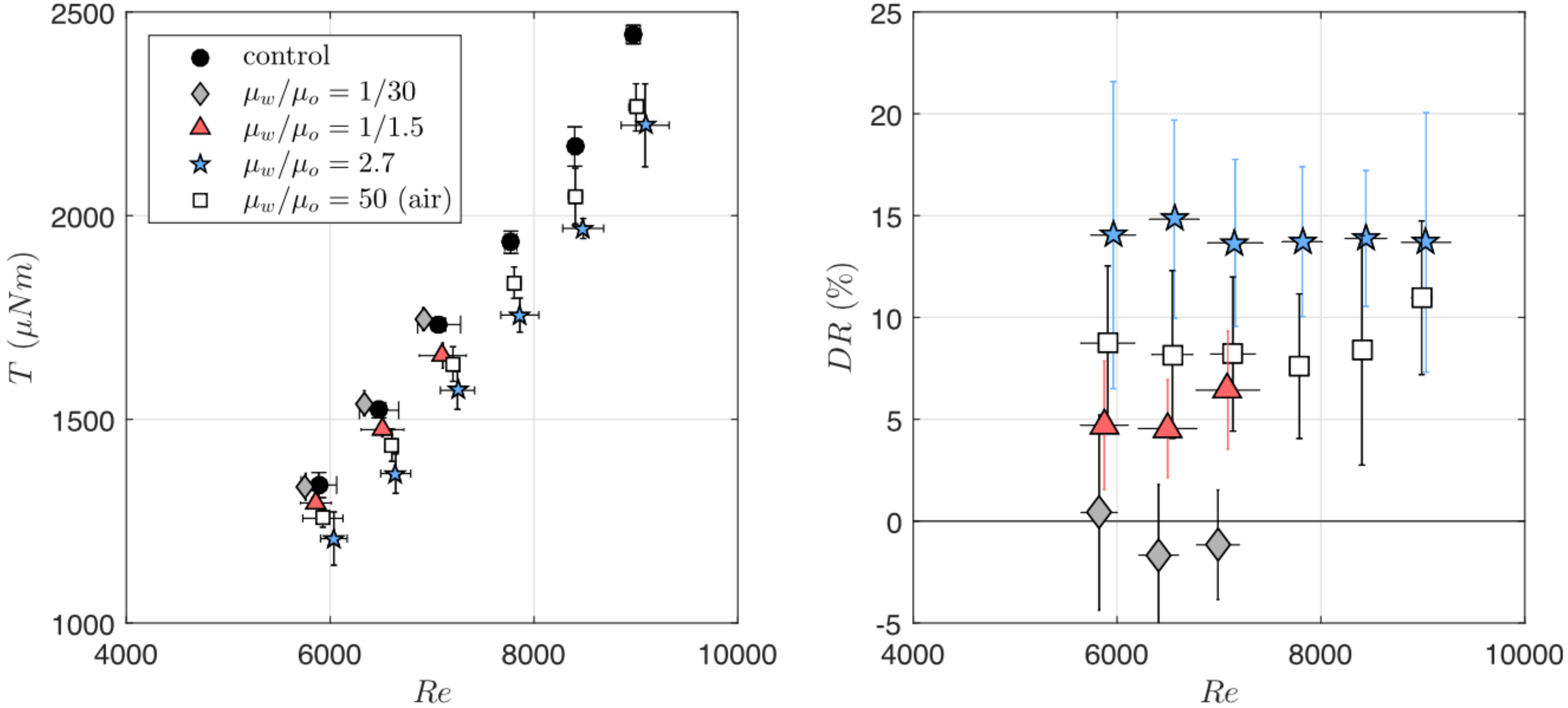

Rosenberg, Van Buren, Fu & Smits (2016)

Drag measurements

	Impregnating fluid	Surface functionalization	μ_w/μ_o
●			
◇	Dupont Krytox GPL-101	fluorinated	0.033
△	3M Fluorinert FC-3283	fluorinated	0.66
☆	Heptane	OTS	2.7
□	Air	fluorinated	50 (SHS)

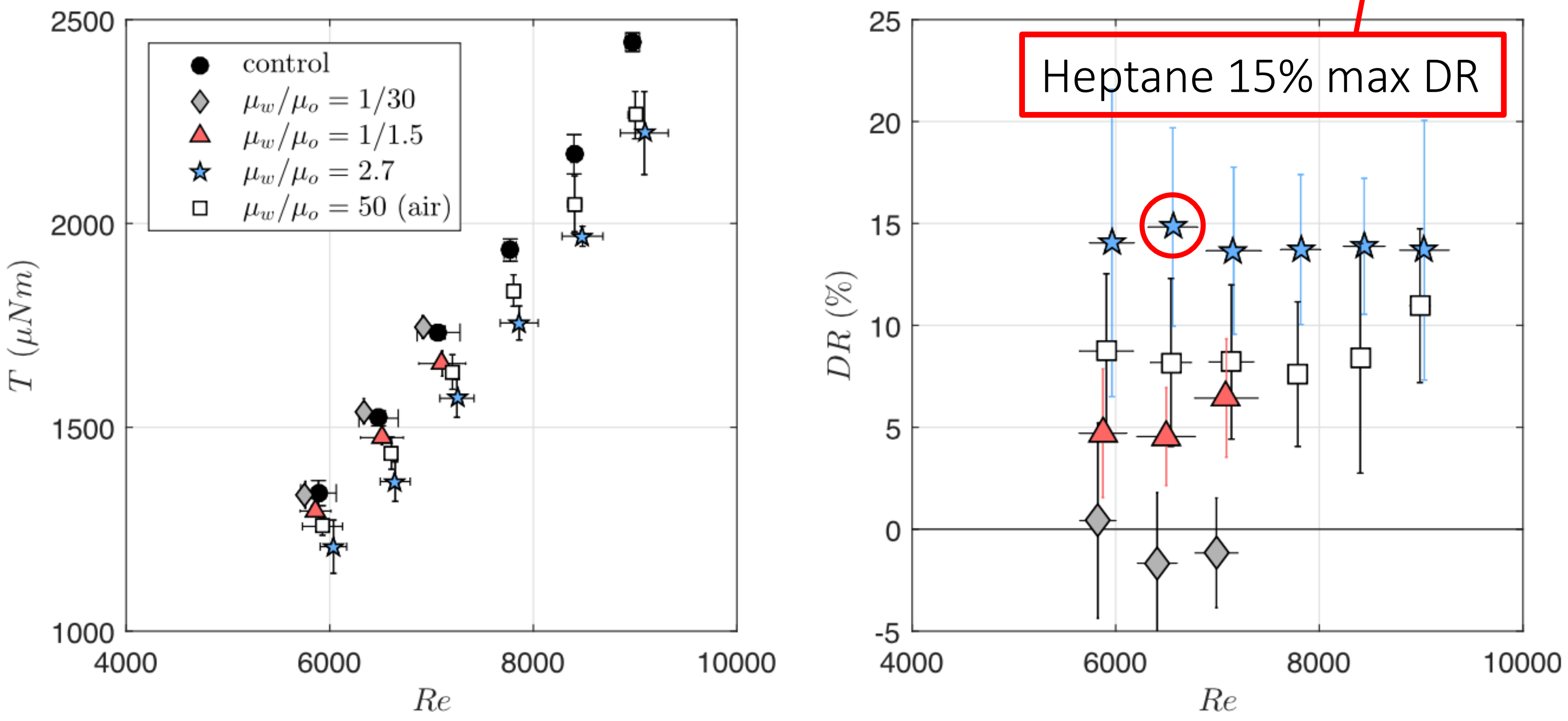

Can we do better?

1. Try other alkanes

Impregnating fluid	Surface functionalization	μ_w/μ_o
Hexane	OTS	3
Heptane	OTS	2.3
Octane	OTS	1.8
Decane	OTS	1.1
Undecane	OTS	0.8
Dodecane	OTS	0.6
Air	fluorinated	50 (SHS)

2. Try larger groove sizes

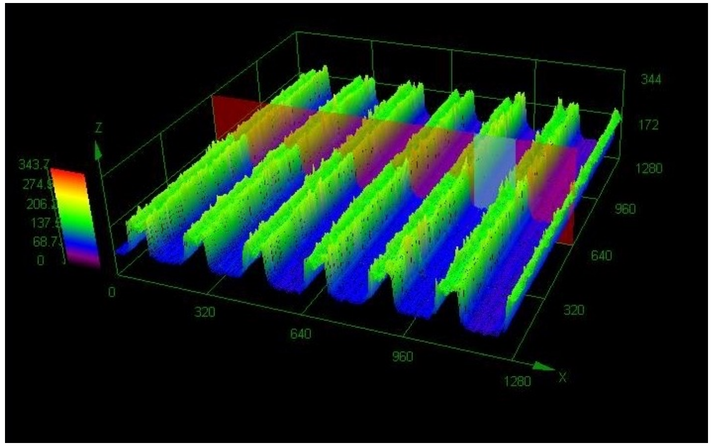

Confocal microscope measurement

$$w = \boxed{100,}\ 200,\ 400,\ 800\ \mu m$$

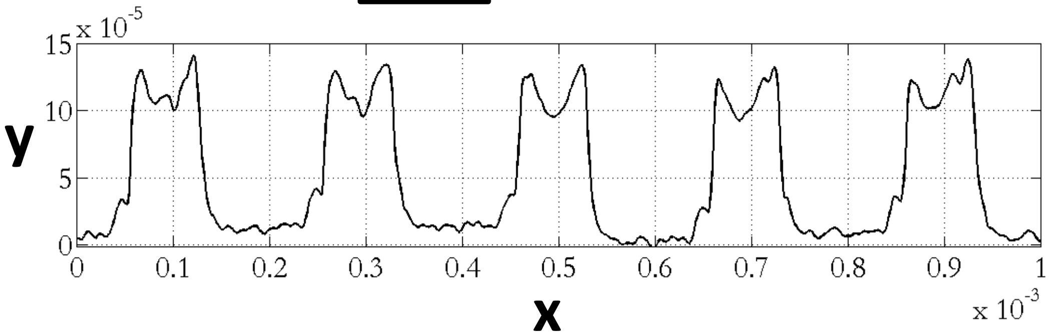

Torque data

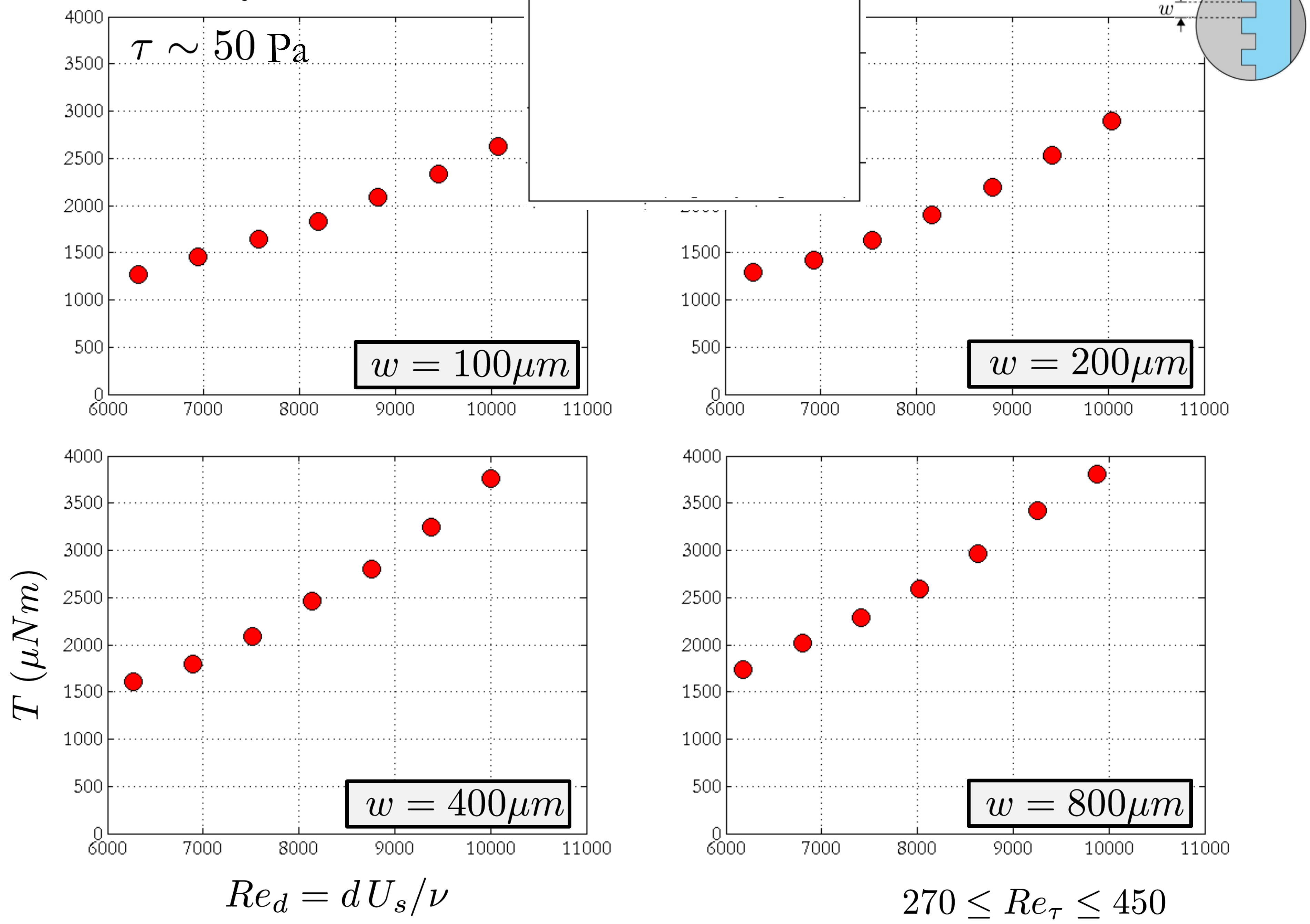

N=1 (Baseline)
$\tau \sim 50$ Pa
$w = 100\mu m$
$w = 200\mu m$
$w = 400\mu m$
$w = 800\mu m$
$T\ (\mu Nm)$
$Re_d = dU_s/\nu$
$270 \leq Re_\tau \leq 450$
d
w

Torque data

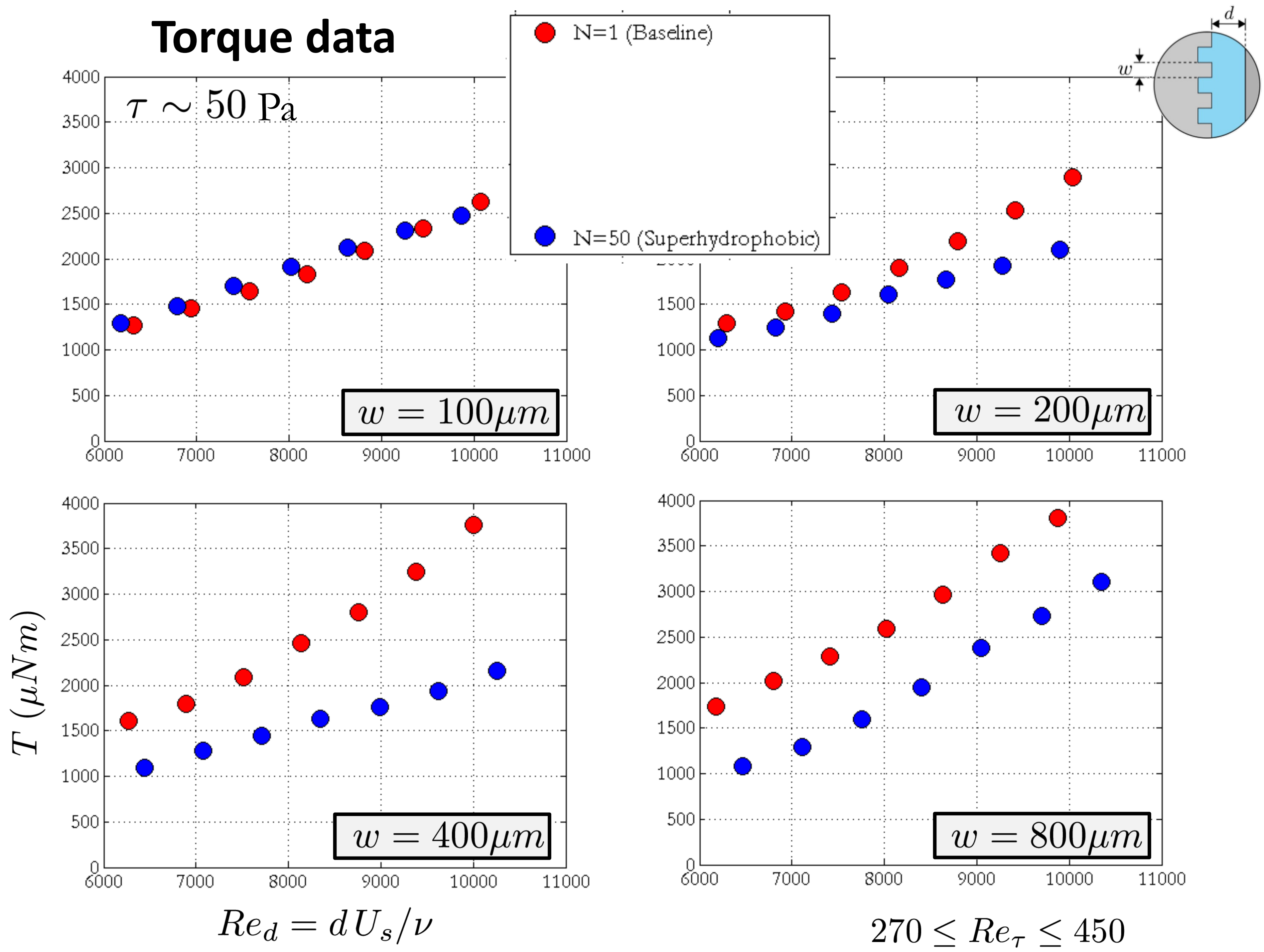

$\tau \sim 50$ Pa
N=1 (Baseline)
N=50 (Superhydrophobic)
d
w
$w = 100\mu m$
$w = 200\mu m$
$w = 400\mu m$
$w = 800\mu m$
T (μNm)
$Re_d = dU_s/\nu$
$270 \leq Re_\tau \leq 450$

Torque data

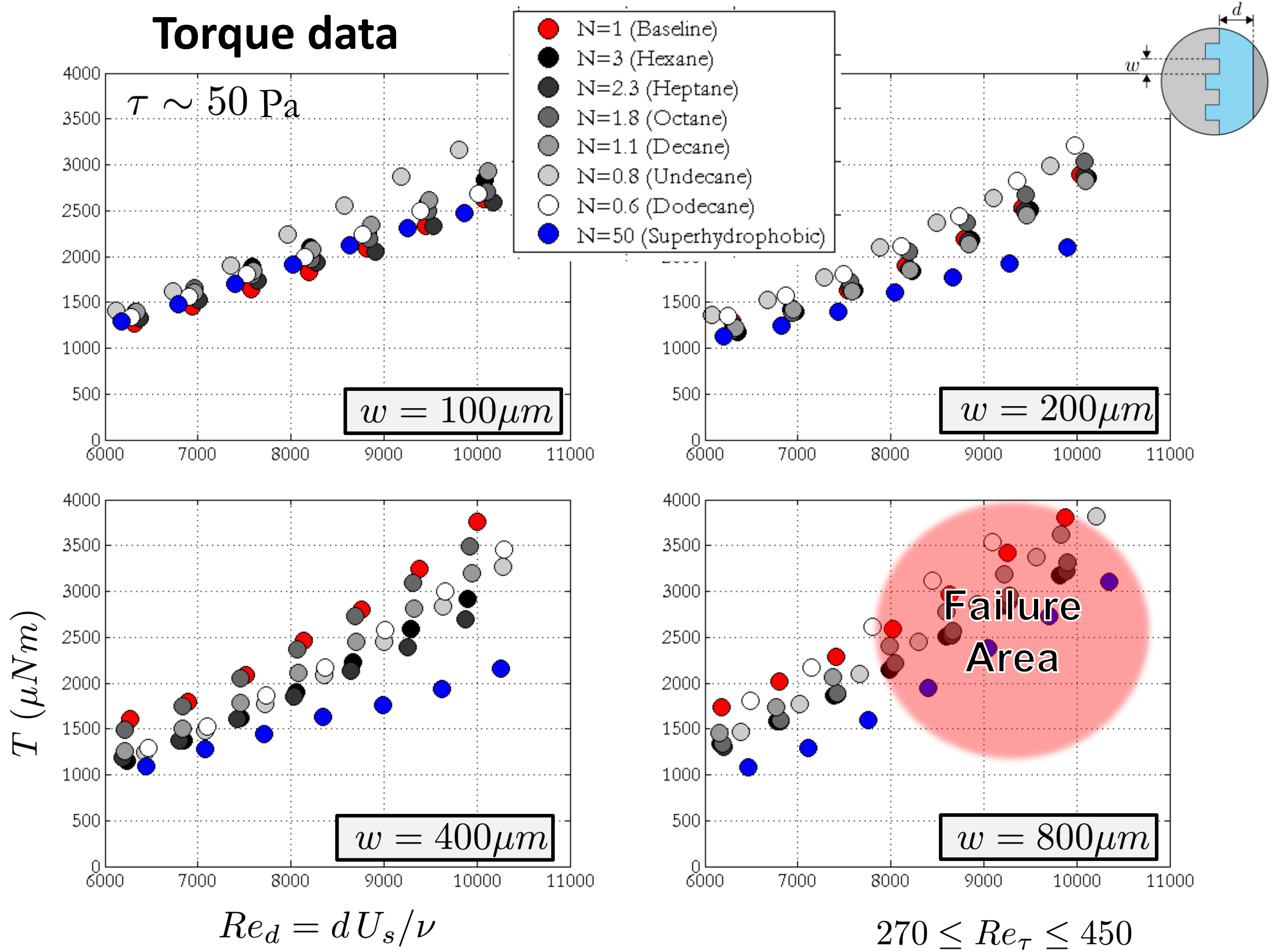

$\tau \sim 50$ Pa
N=1 (Baseline)
N=3 (Hexane)
N=2.3 (Heptane)
N=1.8 (Octane)
N=1.1 (Decane)
N=0.8 (Undecane)
N=0.6 (Dodecane)
N=50 (Superhydrophobic)
d
w
$w = 100\mu m$
$w = 200\mu m$
$w = 400\mu m$
$w = 800\mu m$
Failure Area
$T\ (\mu Nm)$
$Re_d = dU_s/\nu$
$270 \leq Re_\tau \leq 450$

Drag reduction

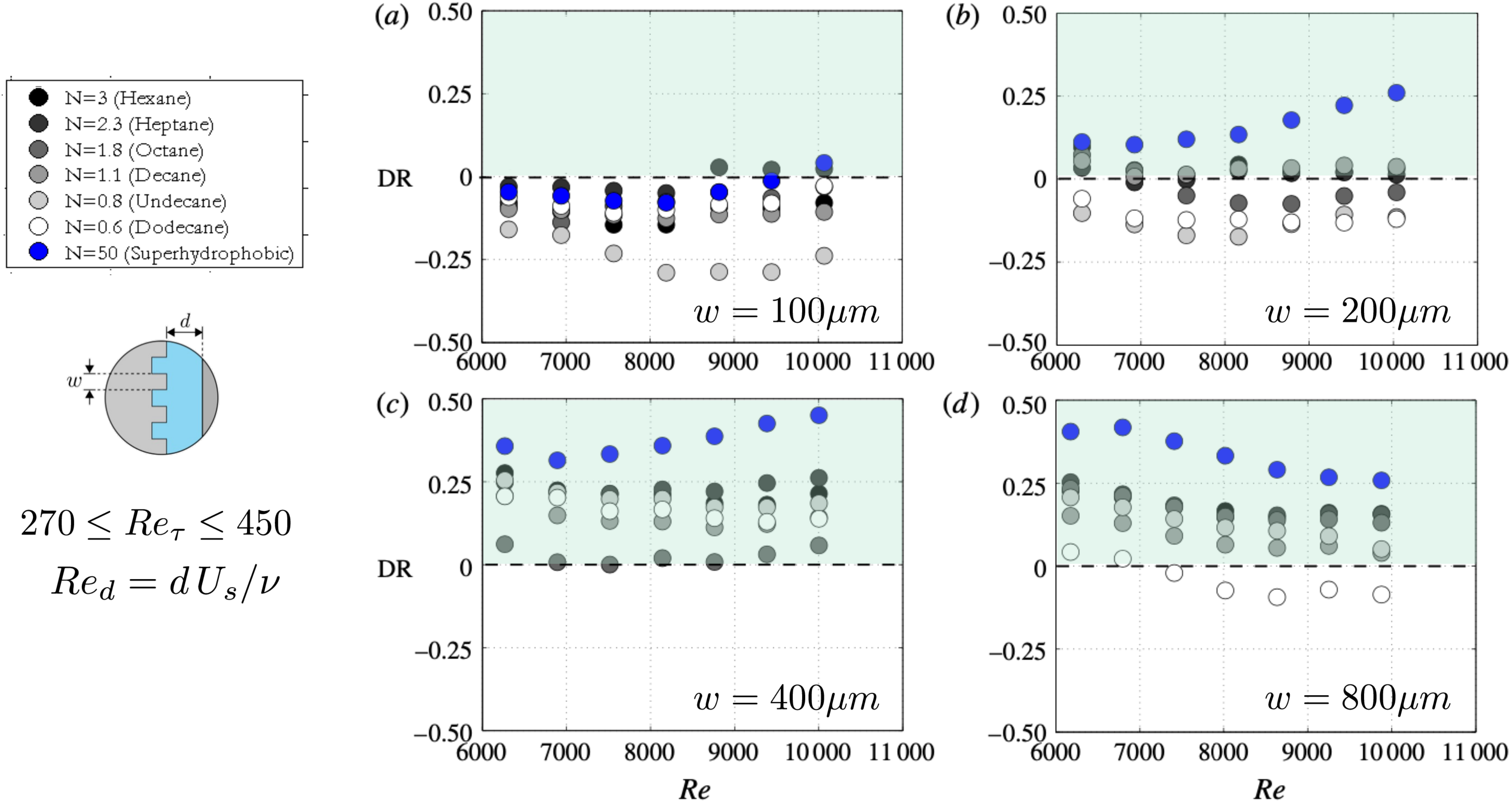

$$270 \leq Re_\tau \leq 450$$

$$Re_d = dU_s/\nu$$

Drag reduction

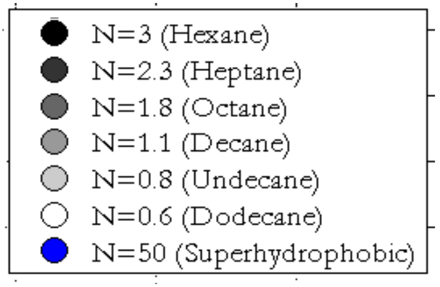

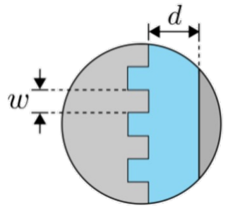

$$270 \leq Re_\tau \leq 450$$

$$Re_d = d\,U_s/\nu$$

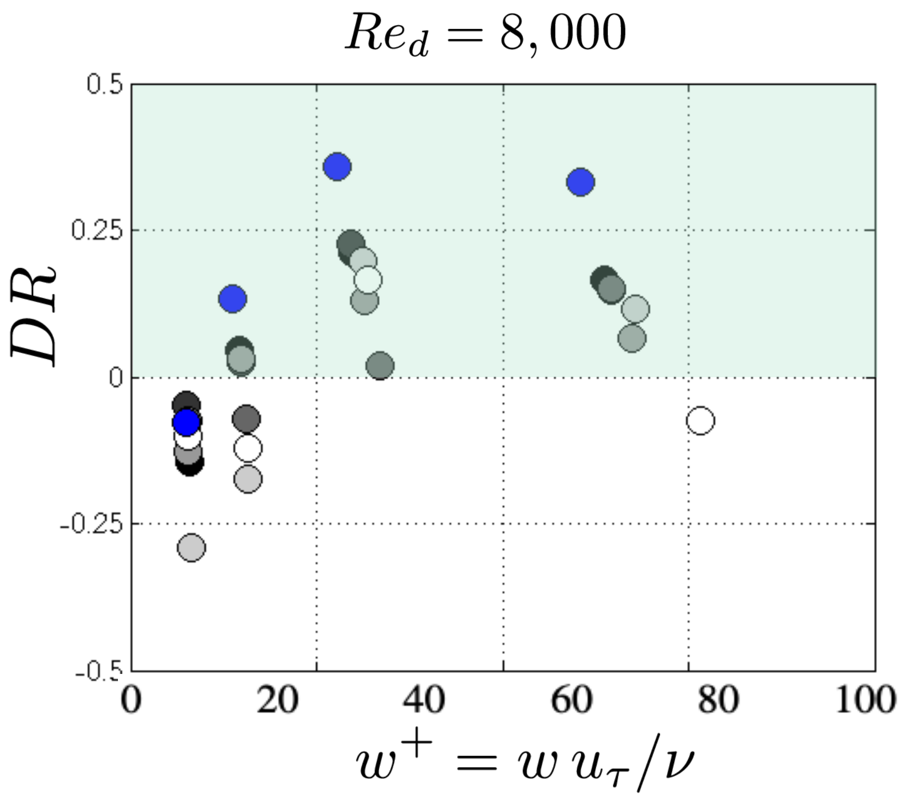

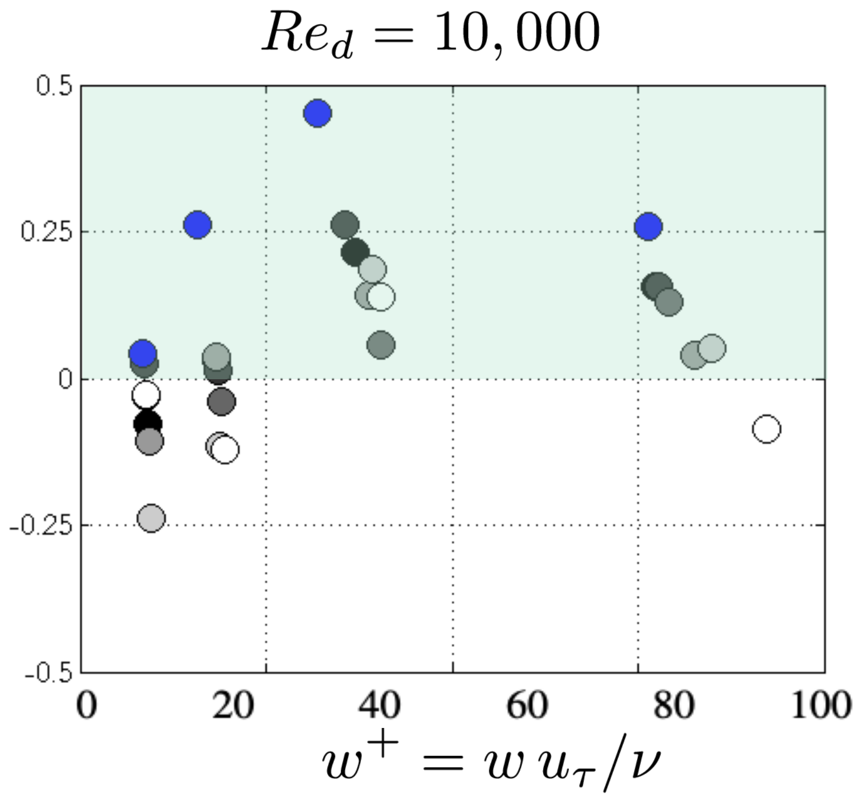

Drag reduction increases with Reynolds number
Drag reduction maximum near $w^+ = 35$

Summary on SLIPS drag reduction

- <u>Turbulent drag reduction:</u>
- Drag reduction up to 45% for air and 30% for liquids (hexane, heptane)
- Larger grooves successful at retaining air and liquid $(w < 800\,\mu m)$
- "Best" drag reduction occurs with $w^+ \approx 35$
- DNS (Leonardi) shows that drag reduction tied to damping of wall-normal velocity fluctuations
- DNS (Park et al. 2013) shows damping of near-wall vortical structures

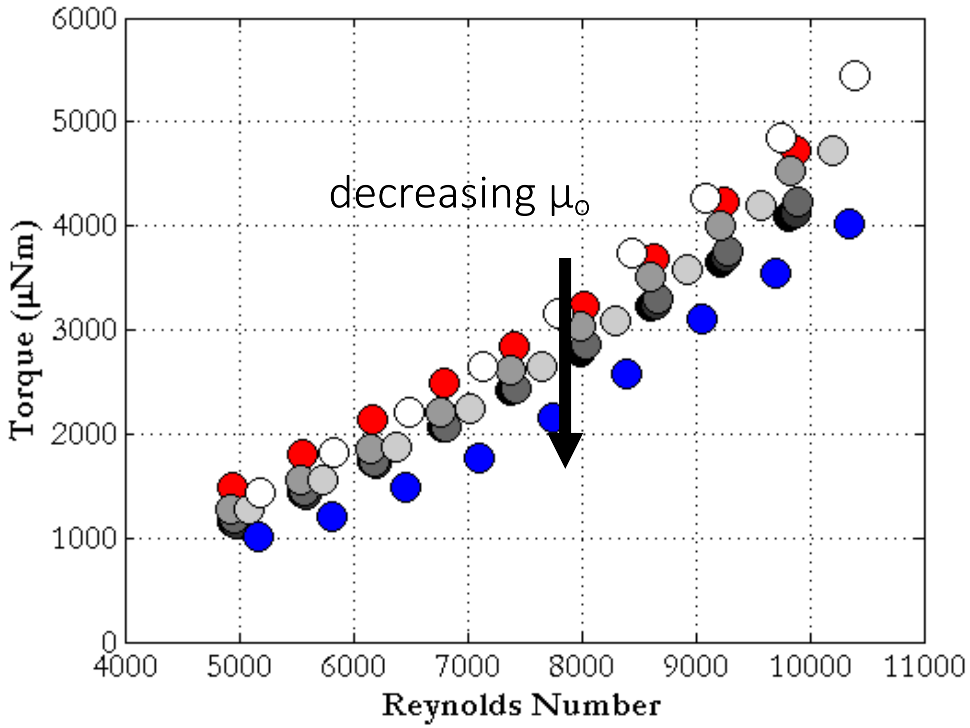

Overall summary

- The response of a turbulent flow to changes in surface roughness is very slow, and may lead to production trapping
  - Provides fundamental information on non-equilibrium turbulence response
  - Can be modeled using RANS equations
  - Suggest concepts for turbulence control
- Targeting energetic large-scale modes (surface modulations) lead to long-lasting modifications to turbulence structure, and demonstrate nonlinear interactions
  - Can be used to control turbulence
  - Provides fundamental information on non-equilibrium turbulence response
- Smart surfaces show promise for implementing drag reduction
  - More needs to be done – opportunities for future work

Questions?